Aus dem Institut für Virologie
des Fachbereichs Veterinärmedizin
der Freien Universität Berlin

THE UL36-ENCODED UBIQUITIN-SPECIFIC PROTEASE IN MAREK'S DISEASE VIRUS REPLICATION AND TUMOURIGENESIS

Inaugural-Dissertation
zur Erlangung des Grades eines
Ph.D. am Fachbereich
Veterinärmedizin
an der
Freien Universität Berlin

vorgelegt von
Inês Margarida Berenguer Veiga
Tierärztin
aus Lissabon, Portugal

Berlin 2012

Journal-Nr.:3622

Gedruckt mit Genehmigung des Fachbereichs Veterinärmedizin
der Freien Universität Berlin

Dekan:	Univ.-Prof. Dr. Jürgen Zentek
Erster Gutachter:	Univ.-Prof. Dr. Nikolaus Osterrieder
Zweiter Gutachter:	Prof. Dr. Keith Jarosinski
Dritter Gutachter:	Univ.-Prof. Dr. Hafez Mohamed Hafez

Deskriptoren (nach CAB-Thesaurus):
Marek´s disease, Mardivirus, Herpesviridae, tumours, replication, ubiquitin

Tag der Promotion: 17.04.2013

Bibliografische Information der *Deutschen Nationalbibliothek*
Die Deutsche Nationalbibliothek verzeichnet diese Publikation in der Deutschen Nationalbibliografie; detaillierte bibliografische Daten sind im Internet über <http://dnb.ddb.de> abrufbar.

ISBN: 978-3-86387-300-4
Zugl.: Berlin, Freie Univ., Diss., 2012
Dissertation, Freie Universität Berlin
D 188

Choriner Str. 85 - 10119 Berlin
verlag@menschundbuch.de – www.menschundbuch.de

“Navegadores antigos tinham uma frase gloriosa:
Navegar é preciso; viver não é preciso".

Fernando Pessoa, „Navegar é preciso“

(“Old sailors had a glorious sentence;
Sailing is necessary; living is not”)

1 Table of Contents

2 List of Abbreviations

aa	Amino acid
ab	Antibody
AMP	Ampicillin
APS	Ammonium persulfate
Atg8	Autofagy-related protein 8
BAC	Bacterial artificial chromosome
BSA	Albumin bovine fraction V
bZIP	Basic leucine zipper domain
C	Cysteine
C98A	Mutation of the cysteine to alanine in position 98
CAM	Chloramphenicol
CBD	Capsid binding domain
CCSC	C-capsid specific component
CECs	Chicken embryo cells
CEFs	Chicken embryo fibroblasts
CIP	Calf intestinal phosphatase
CKCs	Chicken kidney cells
co-int	Co-integrate clones
Cys	Cysteine
D	Asparagine
DMSO	Dimethyl sulfoxide
DNA	Deoxyribonucleic acid
DTT	Dithiothreitol
E1	Ubiquitin-activating enzyme
E1-Ub	Ubiquitin-activating enzyme coupled to ubiquitin (first high energy thiol intermediate)
E2	Ubiquitin-carrier protein

E2-Ub	Ubiquitin-carrier protein coupled to ubiquitin (second high energy thiol intermediate)
E3	Ubiquitin-protein ligase
E3-Ub	Ubiquitin-protein ligase coupled to ubiquitin (third high energy thiol intermediate)
EBV	Epstein-Barr virus
E. coli	Escherichia coli
EDTA	Ethylendiamine tetraacetic acid
eGFP	Enhanced green fluorescent protein
EHV-1	Equine herpesvirus 1
EHV-2	Equine herpesvirus 2
EHV-9	Equine herpesvirus 9
ELL-0	East Lansing cell line
FCS	Fetal calf serum
GaHV-1	Gallid herpesvirus 1
GaHV-2	Gallid herpesvirus 2
GaHV-3	Gallid herpesvirus 3
H	Histidine
h	Hour
HA	Hemaglutinin
HAUbVME	HA-tagged Ubiquitin-vinylmethyl esther
HBS	HEPES buffer saline
His	Histidine
HMWP	High molecular weight protein
HSV-1	Herpes simplex virus 1
HSV-2	Herpes simplex virus 2
htUSP	Herpesvirus tegument ubiquitin-specific protease
HVT	Herpesvirus of Turkeys
HCMV	Human cytomegalovirus

HHV-6	Human herpesvirus 6
HRP	Horseradish peroxidase
ICP1/2	Infected cell protein 1/2
ICP4	Infect cell protein 4
ICTV	International Committee on Taxonomy of Viruses
IE	Immediate early
IF	Immunofluorescence
IL8	Interleukin 8
ind	Independent
INM	Inner nuclear membrane
IRES	Internal ribosomal entry site
IRL	Internal repeat long
IRS	Internal repeat short
ISG15	Interferon-induced gene protein 15
K	Lysine
KANA	Kanamycin
Kb	Kilobases
kDa	Kilodaltons
KSHV	Kaposi’s sarcoma-associated herpesvirus
L	Leucine
LATs	Latency-associated transcripts
LCLs	Lymphoblastoid cell lines
link	linked
LL	Lymphoid leucosis
MCMV	Murine cytomegalovirus
MDV	Marek’s disease virus
MDV-1	MDV serotype 1
MDV-2	MDV serotype 2
MeHV1	Meleagridis herpesvirus 1

MEM	Minimum essential Medium Eagle
MHC I	Major histocompatibility Complex I
min	Minutes
MJDs	Machado-Joseph disease protein domains
MLV	Modified live virus
mMDV	Mild Marek's disease virus strain
MuHV-4	Murine herpesvirus 68 strain
NEDD8	Neural precursor cell –Expressed Developmentally down-regulated (gene) 8
NFDM	Non-fat dry milk
NLS	Nuclear localisation signal
O/N	Overnight
OD_{600}	Optical density, 600 nm wavelength
ONM	Outer nuclear membrane
ORF	Open reading frame
OTUs	Ovarian-tumour family
PBS	Phosphate saline buffer
PBST	Phosphate saline buffer with 0,1% Teen-20
PCR	Polymerase chain reaction
PDB	Protein database
PEI	Polyethylenimine
PFA	Paraformaldehyde
pKa	Acidity constant
p	Protein or plasmid
pi	Post-infection
P/S	Penicillin/streptomycin
pUL36	Protein encoded by UL36
PRV	Pseudorabies virus
Q	Glutamine

qPCR	Quantitative Real Time PCR
r	Recombinant
rev	Revertant
rpm	Rotations per minute
RR	Ribonucleotide reductase
RT	Room temperature
SBP	Streptavidin-binding peptide
SCMV	Simian cytomegalovirus
SDS	Sodium Dodecyl Sulphate
sec	Seconds
SynUSP	Synthetic ubiquitin-specific protease
SPF	Specific-pathogen-free
SUMO	Small ubiquitin-like Modifier
TAE	Tris-acetate-EDTA buffer
TAP	Tandem affinity purification
TEMED	N,N,N',N'-tetramethyl-ethane-1,2-diamine
Tm	Melting temperature
TMR	Telomeric repeat
TRL	Terminal repeat long
TRS	Terminal repeat short
Ub	Ubiquitin
UbLs	Ubiquitin-like proteins
UCHs	Ubiquitin COOH-terminal hydrolases
UL	Unique long
US	Unique short
USP	Ubiquitin-specific protease
UL31	Unique long region gene 31
UL34	Unique long region gene 34
UL36	Unique long region gene 36

v	Reconstituted virus
VZV	Varicella zoster virus
vvMDV	Very virulent Marek's disease virus
+vvMDV	Very virulent plus Marek's disease virus strain
vMDV	Virulent Marek's disease virus
VP1/2	Virion protein 1/2
vIL8	Viral interleukin 8
WB	Western blot
Y2H	Yeast-two hybrid

3 List of Figures

4 List of Tables

5 Prologue

Often times when someone says they are working with an avian virus, other than influenza, people think that such a study is neither interesting nor important. Most do not realise that poultry is one of the most common sources of animal protein worldwide, particularly in developing countries (146), and that the study of poultry pathogens will greatly improve the quality of life of developing nations. Also, it is not widely known that the poultry industry is one of the most industrialized animal production systems of our time, supported by multinational companies that generate breeds in order to obtain birds capable of high growth rates or egg production, as well as disease resistance.

Furthermore, chickens are often used as a model to study members of the *Aves* class. The chicken genome was the first avian genome unveiled by the International Chicken Genome Sequencing Consortium in 2004 (1). As direct descendants of therapod dinosaurs, chickens are known to present unique characteristics, such as the recently discovered non-hormonal dependent cellular sexual identity (27), heterogametic ZW females and homogametic ZZ males (42), and disease susceptibility that is often based on major histocompatibility class I (MHC I) molecules and haplotypes (83). This last characteristic has been utilized to develop breeds resistant to some diseases, such as Marek's disease virus (MDV).

The history of MDV and its stepwise co-evolution with the industrialization of poultry production in the past century, which shall be described later, is an excellent example of how human intervention can strongly influence the host-virus balance (33). A better understanding of MDV's replication cycle and the genes important for this process are paramount for the development of new control strategies.

Several virulence-related genes of MDV have been identified to date. Among them a deubiquitinase (DUB), which is a member of the family of ubiquitin-specific proteases (USP). The herpesviral USP was first discovered in herpes simplex virus 1 (HSV-1) (75) and was afterwards shown to be highly conserved in all herpesviruses. A mutation of the enzyme's putative active site in MDV resulted in significant impairment of tumourigenesis (66). This initial finding was the basis of this dissertation that focuses on the role of USP in MDV pathogenesis, specifically during both viral replication and virus-induced tumourigenesis.

6 Introduction

6.1 Herpesviruses

6.1.1 Classification, morphology and evolution

Herpesviruses are extremely widespread in nature, have been identified in more than 200 vertebrates (122) and in one invertebrate species so far (35), and were once organised within the family *Herpesviridae* (33, 34, 122). In 2009, the International Committee on Taxonomy of Viruses (ICTV) reorganised herpesvirus taxonomy by forming three families comprised within the new *Herpesvirales* order (34): the *Herpesviridae* family, which includes mammalian, avian and reptile viruses; the *Alloherpesviridae* family, composed of fish and frog herpesviruses; and the *Malacoherpesviridae* family, with a single virus identified so far that infects oysters.

It is believed that the herpesvirus ancestor existed prior to the first vertebrates, sharing the typical morphology we still observe today in all herpesviruses (33). It is the characteristic structure of the virion (Figure 1) that brings this very diverse group of viruses together under the *Herpesvirales* order, more so than the genetic makeup of its members (34, 122).

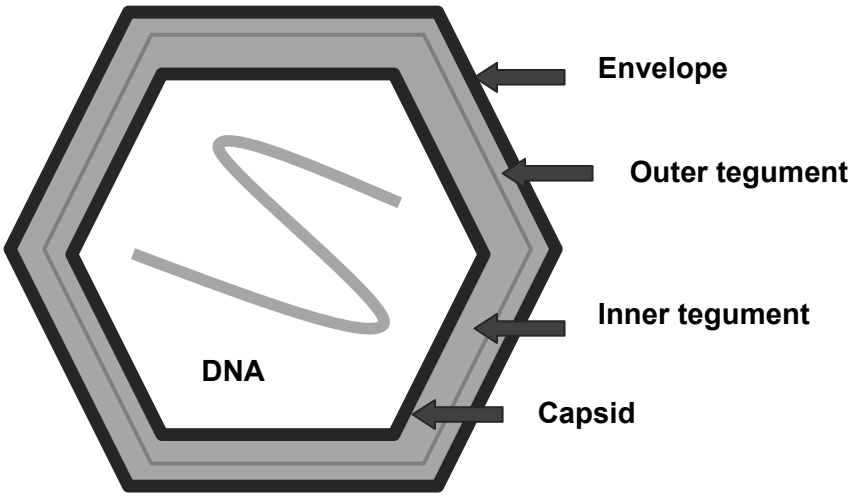

Figure 1. Schematic representation of typical herpesvirus morphology.

Each herpes virion contains a linear, double-stranded DNA genome of between approximately 108 and 290 kilobase pairs (Kb) within a T=16 icosahedral capsid. The capsid

is coated by the two-layered tegument, a proteinaceous matrix of variable thickness, which is in turn surrounded by a lipid envelope obtained by viral budding from cellular membranes (34, 122).

The *Herpesviridae* family is divided into three subfamilies, the *Alpha-*, *Beta-* and *Gammaherpesvirinae,* originally based on the biological properties of their members. Following sequencing of the complete genomes of many members of the subfamilies and reorganization based on their characteristics, their classifications by and large remained, although some viruses were allocated to other genera and subfamilies, such as MDV, which was originally thought to belong to the gammaherpesviruses due to its tumourigenic properties, but was later found to present typical alphaherpesvirus features (23, 116). It is thought that herpesviruses co-evolved with their hosts from reptilian to avian and mammalian herpesviruses, respectively (122); however, opinions diverge regarding the direction this evolution took: some authors believe that avian alphaherpesviruses diverged from their counterparts in mammals (33), while others contend that the exact opposite is true (74).

6.1.2 Biological characteristics

Herpesviruses share a remarkable number of biological characteristics, even without presenting striking genomic identities (122).

First, all herpesvirus species identified so far encode in their genome a large array of enzymes involved in crucial steps during viral replication such as nucleic acid metabolism (e.g. thymidine kinase), DNA synthesis (DNA polymerases, helicases) and protein processing (protein kinases). The enzymatic set encoded by each virus is quite distinct and none of the proteins conserved between members of the three subfamilies are herpesvirus-specific, which is intriguing when their common origin is taken into consideration. It is thought that transposition of viral and cellular DNA and recombination-based acquisition of big portions of cellular DNA played a role in this process (122, 135, 141). One example of gene “kidnapping” from the host is the presence of a homolog of chicken interleukin 8 (IL-8) in the MDV genome, which was named viral interleukin 8 (vIL-8) (90, 118). The gene that is the closest to being considered herpesvirus-specific is the putative pUL15 ATPase subunit of the terminase, the complex that allows packaging of viral DNA into capsids through the ring-like dodecameric complex of the portal protein located in one of the 12 capsid vertices. This gene is present in all herpesviruses and quite similar to a gene encoded by T4-like bacteriophages from the *Myoviridae* family (34, 101, 104). Two hypotheses have been put forward to explain

this phenomenon: either horizontal gene transfer between a herpesvirus ancestor and a T4-like bacteriophage occurred many millions of years ago or both viruses have a common origin. The latter is based on the fact that both are double-stranded DNA viruses with an icosahedral capsid (33).

Second, virion formation seems to be very similar for the various herpesvirus families and subfamilies, as suggested by their morphology (101). Synthesis of viral DNA and capsid assembly takes place in the nucleus, whereas final virion maturation occurs in the cytoplasm (122). After replication, viral DNA enters the capsid through the portal protein complex (24, 38). Several viral-encoded proteins are involved in the formation of the nucleocapsids, and some cellular-encoded proteins, such as actin and annexin, can be identified together with viral DNA within the capsid (161). For capsid liberation from the nucleus, the "envelopment/de-envelopment" model is currently accepted, although other models have been proposed (86, 100). This model proposes that an intermediate envelope is formed upon budding of the capsid through the inner nuclear membrane (INM), followed by fusion of this intermediate envelope with the outer nuclear membrane (ONM). A complex formed by two proteins, pUL31 and pUL34, is essential for this stage of viral development (101). Viral egress from the cell is still poorly understood (101). Virus replication ultimately leads to destruction of the infected cell (122).

Third, all herpesviruses studied so far retain the ability to establish and maintain latency in their natural hosts, a process that is still poorly understood. The latent state is characterised by the failure to produce viral progeny, a feature that distinguishes it from a chronic infection, and by the expression of a limited number of genes (122). The cell type in which latency is established varies between herpesviruses. Many alphaherpesviruses, including the human representatives HSV-1 and varicella zoster virus (VZV) establish latency in sensory ganglia, while MDV maintains latency in lymphocytes (122).

It is believed that herpesviruses have co-evolved with their hosts for millions of years (33), which may explain their marked host specificity. However, there are some exceptions to this rule. One of the best-known examples of this is the transmission of pseudorabies virus (PRV), whose natural host is the pig, to domestic carnivores such as cats and dogs, causing a rare but fatal disease (32). Also, the recently identified equine herpesvirus 9 (EHV-9), originally found in Thompson gazelles (13, 48) and subsequently characterised as an equine virus due to its similarities to equine herpesvirus 1 (EHV-1), has since then been implicated in infections of Grevy's zebras and polar bears in captivity (41), being also recently found to recombine with EHV-1 and cause fatal disease in polar bears kept in zoos (58). Also,

humans can be infected by herpesvirus B from macaques which causes often fatal encephalitis (65).

Herpesviruses can vary greatly regarding other characteristics (122). While some are highly cell-destructive and able to infect a wide range of cells (e.g., HSV-1), others are highly cell-specific, like Epstein Barr virus (EBV) or human herpesvirus 6 (HHV-6), which only infect B-lymphocytes. Additionally, some herpesviruses, like human cytomegalovirus (HCMV), have long replication cycles, which takes around one week to induce infected cell lysis, while others like HSV-1, can induce the same effect in less than one day (144). Therefore, symptoms associated with herpesvirus infections also differ greatly. It is well known that one and the same animal species can harbour a number of several herpesviruses. For example, eight human herpesviruses have been so far identified; these viruses contribute to a wide range of diseases that range from mononucleosis, induced by EBV, to gingivostomatitis and genital herpes induced by HSV-1 and herpes simplex virus 2 (HSV-2) (157). Another example is the nine equine herpesviruses that have so far been identified in *Equids*. While EHV-1 infections lead to abortion and neurological symptoms, equine herpesvirus 2 (EHV-2) can cause keratoconjunctivitis and respiratory tract disease, besides contributing to immunosuppression (44).

6.2 Marek's disease virus

Previously called MDV serotype 1 (MDV-1), the virus responsible for MD is now classified as gallid herpesvirus type 2 (GaHV-2) (34). However, the term MDV is still used regularly in the literature to avoid confusion and will be used throughout this thesis as well, instead of GaHV-2. MDV belongs to the *Mardivirus* genus, together with other avian herpesviruses (34) including the non-oncogenic gallid herpesvirus type 3 (GaHV-3), previously known as MDV serotype 2 (MDV-2), and meleagrid herpesvirus 1 (MeHV-1), also commonly referred to as herpesvirus of turkeys (HVT). The latter two viruses, due to their antigenic similarity with MDV, have been widely used as vaccines against MD. In spite of having collinear sequences, these viruses clearly do not represent serotypes, but individual and distinct species, with significant differences both in base composition and genome size (115), which have undergone parallel evolution for millions of years. Gallid herpesvirus 1 (GaHV-1), the causative agent of infectious laryngotracheitis (ILT) in chickens, which presents more significant differences both in terms of genomic makeup and pathogenesis (88), belongs to the *Iltovirus* genus (34).

6.2.1 MDV structure and characteristics

Once classified as a member of the *Gammaherpesvirinae* due to its clinical presentation and lymphotropic properties (8, 116, 120, 137), MDV is now classified as a member of the *Alphaherpesvirinae* subfamily, presenting the typical class E genome morphology depicted in Figure 2. The MDV genome is composed of two unique regions, one long (UL) and one short (US), which each are flanked by inverted terminal (TR_L and TR_S) and internal (IR_L and IR_S) repeats. The genome resembles that of HSV-1, the prototype virus of this subfamily (115).

Figure 2. Genome of MDV.

The MDV genome is approximately 180 kbp in size and it is predicted to encode more than 100 proteins, whose expression varies throughout replication cycle. In addition to proteins, there are also other genetic elements encoded in the MDV genome, such as telomere-like sequences called telomeric repeats (TMRs) located at the terminal ends of the MDV genome (137) and viral telomerase RNA (vTR) (45). The TMRs facilitate viral genome integration into host telomeres, a process involved in the establishment of latency, reactivation and lymphoma formation (36, 37) and vTR is important for telomere stability in transformed cells (76, 77).

The MDV virion presents as a hexagonal nucleocapsid of 100 to 125 nm in diameter, whereas enveloped particles have a size of around 150-160 nm in infected cells; enveloped virions released from the feather follicle are around 200-400 nm (137).

6.2.2 Historic hallmarks

The first description of MD was made in Hungary by Jozef Marek, an eminent clinician from the Budapest Veterinary School and contemporary of Aladar Aujeszky, who first identified PRV in swine. In his seminal 1907 paper, Dr. Marek described the occurrence of polyneuritis in four chickens (107, 116, 120, 137). Later, the disease was linked to the formation of visceral lymphomas, after a series of experiments performed by Pappenheimer between 1926 and 1929, which led the author to formulate a hypothesis that visceral tumours and polyneuritis could, in fact, be caused by the same agent (116, 123). However, due to the

great number of avian pathogens that induce tumour formation (43), particularly retrovirus-induced avian leukosis (120) that has a similar clinical presentation (43), MD remained indistinguishable from other diseases for many decades. Until 1960, several denominations had been used to describe either one or both diseases such as neuritis, neurolymphomatosis gallinarum (from the times of Pappenheimer) and also range paralysis (137). During the first Conference of the World Veterinary Poultry Association led by Biggs and Campbell, the names Marek´s disease and lymphoid leukosis (LL) were officially proposed to better distinguish the two different conditions (123).

The new classification was validated after studies performed by Biggs and Payne in 1964, in which they compared the two conditions in poultry, which were sensitive to each disease, and concluded that they varied in median latent period, distribution, frequency, and cytology of the induced tumours (123). Shortly afterwards, MDV was successfully isolated both in England and in the USA and defined as a strongly cell-associated virus (120, 137). Finally, in the later part of the 1960's, experiments performed at Cornell University by Calnek and colleagues and Witter and colleagues at the USDA – Avian Disease and Oncology Laboratory (ADOL) in East Lansing, MI, identified infectious cell-free virus being produced by the disruption of feather-follicle associated epithelial cells (123). This led a better understanding of both aetiology and pathogenesis of MD.

The intensification of poultry industry led to an increase of MDV virulence that resulted in serious outbreaks of MD in the 1960s (107), condemnation of a significant number of carcasses and 30-60% mortality of pullets and layers (137). Identification of the causative agent was key for the preparation of vaccines, first using attenuated MDV strains like HPRS-16 (26, 109, 120), and then the closely related HVT (109, 114, 159). The vaccines effectively controlled these initial outbreaks until the end of the 1970's, when new outbreaks by more virulent MDV strains led to the development of bivalent vaccines, containing both HVT and GaHV-3 strains (e.g. SB-1) (109). The vaccines were able to prevent further outbreaks until the end of the 1980's, when breaks in vaccine-induced protection began again. The introduction of the attenuated CVI988 vaccine strain, also known as the Rispens strain that was isolated in the Netherlands in the early 1970's has since then been adopted for MD control worldwide (107, 128, 129) and to date is considered the "gold standard" of MDV vaccination (116). However, there are some indications that it may, in the future, become insufficient to prevent new MDV outbreaks (137).

As it can be seen in Figure 3, the stepwise evolution of MDV throughout the 20th century gave origin to several MDV pathotypes: the mildly virulent MDV strains (mMDV), whose

representatives are strains CVI9888 and CU2; the virulent strains (vMDV), represented by the JM, GA and HPRS-16 strains, predominant in the 1960's; the very virulent MDV group (vvMDV), composed of strains such as Md5 and RB-1B, which first appeared in the 1970's; and the very virulent plus MDV group (vv+MDV), represented by strains like 648a, 652 (RK-1), and TK strain (133), which first appeared in the 1980's (158).

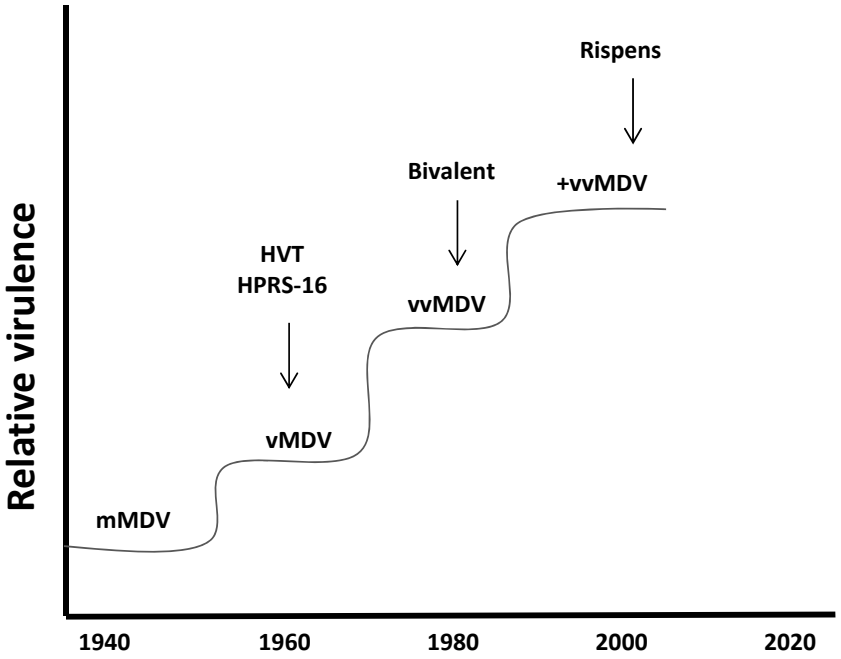

Figure 3. Stepwise evolution of MDV starting in the 1960s. The connection between vaccine introduction and increased virulence can be clearly observed. HVT stands for turkey herpesvirus, HPRS-16 is an attenuated MDV strain; the term bivalent for HVT and GaHV-3 (SB-1) vaccines and Rispens corresponds to the CVI988 strain of MDV. Figure adapted from Witter, 1997 (158).

Today, MDV is a highly transmissible disease, which is distributed worldwide and associated with neurological symptoms and visceral tumour formation. It is estimated to be responsible for annual losses of $US 1-2 billion to the poultry industry (107, 109) as the vaccines, even if effective against the development of disease, do not induce sterilizing immunity. While always facing the possibility of a new outbreak, the poultry industry continues to develop new vaccines, both protective against more MDV virulent strains and cell-free, if possible, which would result in lower costs of vaccine production. Still, MDV is one of the few tumourigenic conditions in any species that can be effectively treated by vaccines (137). Since the introduction of vaccination with modified live virus (MLV) vaccines in the 1960's, the incidence of MD has been reduced by more than 99% (116).

MDV is also an accepted model organism to understand basic principles of viral-induced human disease. While sharing some characteristics with VZV, namely its highly cell-

associated nature and entry into, dissemination throughout, and egress from the host, it also provides a well-defined small animal model for virus-induced lymphomagenesis (116).

6.2.3 The MDV replication cycle

MDV replication is unusually complex (8) and still not completely understood. Viral transmission between several different cell types within an infected host is required. The currently accepted replication cycle described in Figure 4, known as the Cornell Model, comprises four phases: an early cytolytic phase from 2-7 days post-infection (pi), a latent phase from roughly 7-10 days pi onwards, a reactive cytolytic and immunosuppressive phase, from 18 days pi onwards, and a proliferative phase, from 28 days pi onwards (8, 19, 20).

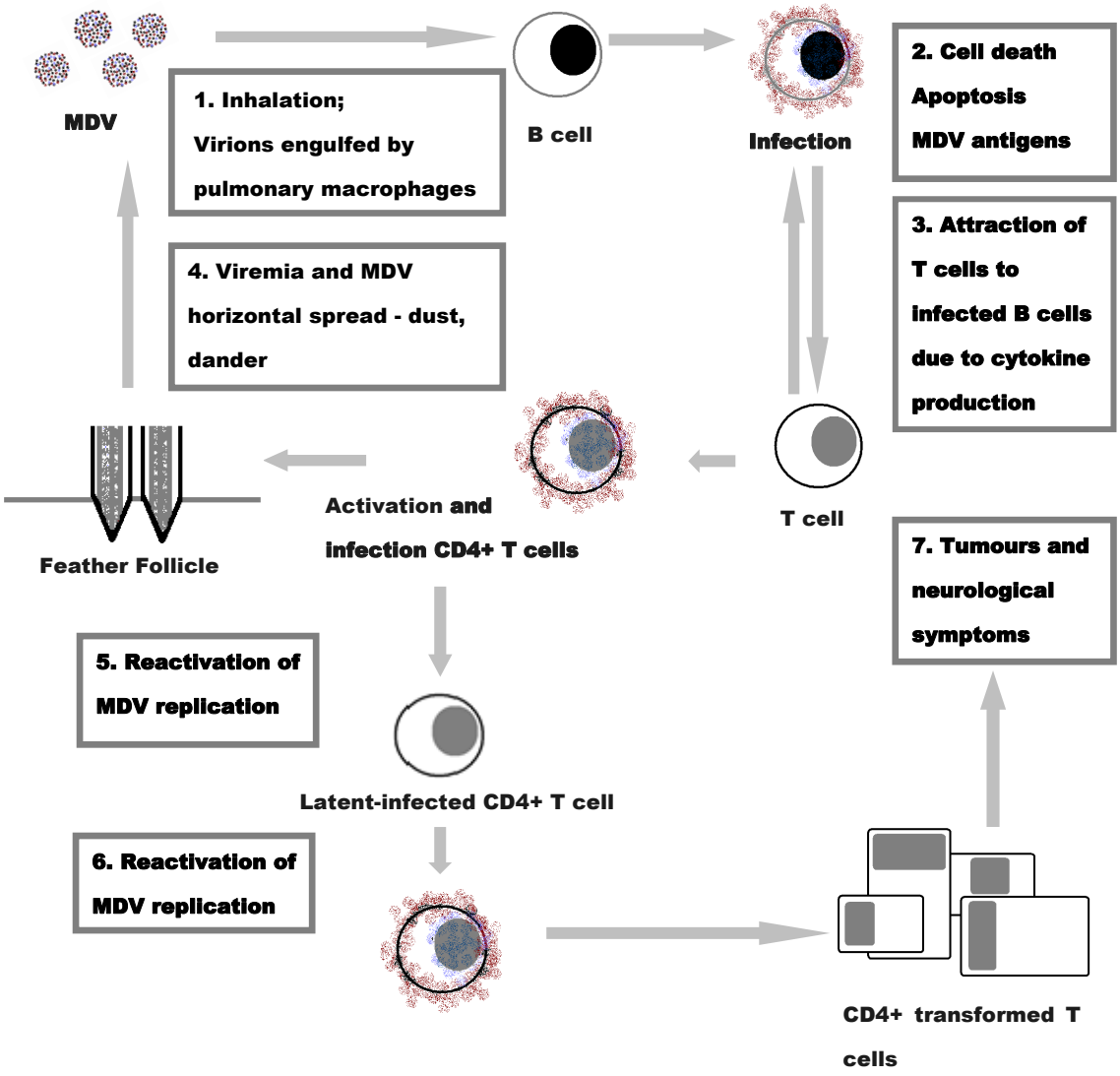

.

Figure 4. Schematic depiction of the MDV replication cycle.

During natural infection, infectious virus present in the environment is believed to enter naïve hosts through the respiratory tract, even if other entry routes cannot be ruled out. The virus is then engulfed by pulmonary macrophages or dendritic cells and carried to lymphoid organs, where it infects B cells. Infected B cells undergo apoptosis and release cytokines that attract and activate T cells. Activated T cells are the preferred cell type that MDV then infects. The latent phase follows approximately one week into the infection (120); the duration of this poorly understood stage is highly dependent on the strain of virus and chicken line (8, 107, 137). In genetically resistant birds, the virus usually does not reactivate and remains latent in lymphocytes (120, 137). Mostly CD4+ T, but also B and CD8+ T cells can be latently infected with MDV (137). This process is dependent not only on the previously mentioned TMRs (36, 37, 77), but also on down-regulation of immediate early genes such as infected cell protein 4 (ICP4) transcripts and up-regulation of latency-associated transcripts (LATs) (137). Essential for dissemination of MDV through the population, the release of infectious cell-free virus through feather follicle cell desquamation starts around 2 weeks pi, an occurrence that is maximal from 3 to 5 weeks pi and maintained for the lifetime of the infected host (137). Latent MDV reactivates during this stage, and neurological symptoms and visceral tumour formation can be observed. All these occurrences ultimately lead to death of the affected animals.

6.2.4 Clinical presentation

The clinical presentation of MD depends not only on the viral strain and chicken line, but also on environmental factors (107, 137). Although chickens are the main host of MDV, other varieties of poultry, such as quail, turkey, and pheasant, can also be affected (107, 137).

Originally, MD symptoms included sporadic and chronic polyneuritis; however, starting in the 1960's, the classical form of MD emerged characterized by nonspecific symptoms such as anorexia, weight loss due to inability to reach food and water (137), and various forms of neurological impairment. The so-called "ballerina" position is a common MD symptom, when the animal has one leg stretched to the front and the other to the back (Figure 5B).

Lymphomas can be found upon necropsy in the muscular tissue and in visceral organs such as spleen, kidneys, the reproductive tract, proventriculum and liver (Figure 5). Disease progression has accelerated since the 1960's (107). Now, a peracute presentation can be found in the field (137), which is characterised by sudden death of the affected animals,

sometimes without presenting either neurological symptoms (fowl paralysis and persistent neurological disease) or visceral tumours (116).

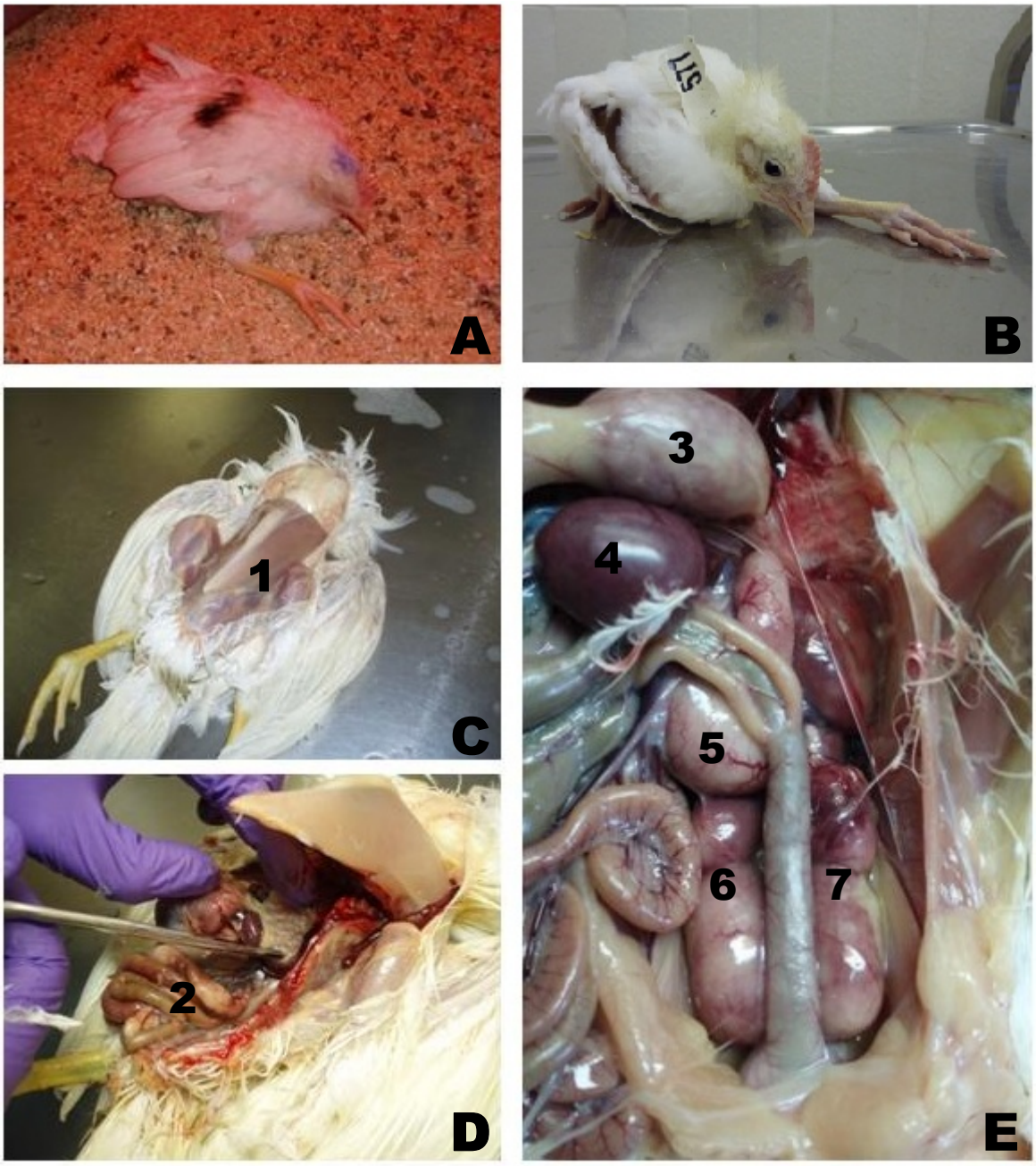

Figure 5. MD clinical signs and macroscopic lesions. Affected animals present nonspecific symptoms such as anorexia and depression or are unable to stand (A). The so-called "ballerina" position can be observed in (B). Typical findings upon necropsy include pronounced emaciation (C.1) and disseminated visceral lymphomas. The pictured animals had tumours in the intestines (D.2), proventiculum (E.3), spleen (E.4), reproductive organs (E.5), and kidneys (E.6 and E.7). Other organs such as heart and the breast muscles may also be affected.

Other manifestations associated with MDV lymphoproliferation include skin and ocular lesions (145), as well as degenerative and inflammatory lesions (137).

6.3 Herpesvirus large tegument proteins

6.3.1 Characterisation

The herpesviral tegument is a proteinaceous structure, which can vary in composition and symmetry (99), not only between different herpesviruses, but also at different stages of the replication cycle (112). From the 80 calculated open reading frames (ORFs) present in HSV-1, 39 are thought to encode for essential for viral morphogenesis (62). From these, 23 proteins have been identified as potential tegument proteins (91, 101), not all of which are essential for structure (130).

Large tegument proteins have been identified in all herpesviruses studied and are referred to as homologues of virion protein 1/2 (VP1/2) or infected cell protein 1/2 (ICP1/2) of HSV-1 (106). VP1/2 is encoded by the UL36 gene of HSV-1 and is the largest herpesvirus ORF (94). The protein was initially found to be part of the tegument of HSV-1 and HCMV (15, 52, 53) and in close association with the capsid in HSV-1 and simian cytomegalovirus (SCMV) (152, 154, 163).

Kinetic studies performed with HSV-1 (96, 97) identified VP1/2 as a late gene product produced from 8 to 9 h pi, which undergoes phosphorylation and can be found distributed diffusely in both the nucleus and cytoplasm. In addition, VP1/2 is found in purified nuclear B and C nucleocapsids as well as intact HSV-1 virions (17, 82). Additon of the inner tegument to capsids is thought to occur shortly after de-envelopment of the primary envelope and prior to the acquisition of the outer tegument (82). Around 100 to 150 copies of VP1/2 are predicted to be present within each HSV-1 virion (111).

A study of an HSV-1 temperature-sensitive mutant named tsB7, which has a mutation in the UL36 region (9), showed that VP1/2 is essential for virus replication. A partial HSV-1 UL36 deletion mutant named KΔUL36 (40) was able to produce DNA-filled capsids that accumulated in aggregates in the cytoplasm without being released, thus showing the essential role of VP1/2 in virus maturation and egress. Complete deletion of UL36 in HSV-1 led to the same observation, but without aggregation of capsids (130), as did deletion in PRV

(47, 82, 106). The presence of these aggregates was associated with the presence of 361 codons at the N terminus of the UL36 gene in the KΔUL36 mutant (5, 130).

Some well-conserved domains have been identified within the large tegument proteins of alphaherpesviruses (Figure 6). Besides the highly conserved USP that is described in detail below, a pUL37 interaction domain was identified in HSV-1 VP1/2 (102) and also for the PRV large tegument protein (81, 106). Also, a functional nuclear localisation signal (NLS) was identified at the N-terminus of HSV-1 (4), which is essential for viral propagation (3). In the PRV large tegument protein, three NLSs have been identified, one of which corresponds to the one first identified in HSV-1 (106). Interestingly, NLS1 and NLS2 were functional as shown by transient transfection assays, while NLS 3 was not. Moreover, the large tegument protein was not found in the nucleus of PRV-infected cells using specific antibodies (106). Apart from the interaction sites with other viral proteins, which have been identified in several viruses as shall be described, the basic leucine zipper domain (bZIP) and the late domain motifs PPKY and PSAP have been identified through bioinformatic analysis of the PRV large tegument protein without knowledge about their putative functions (14).

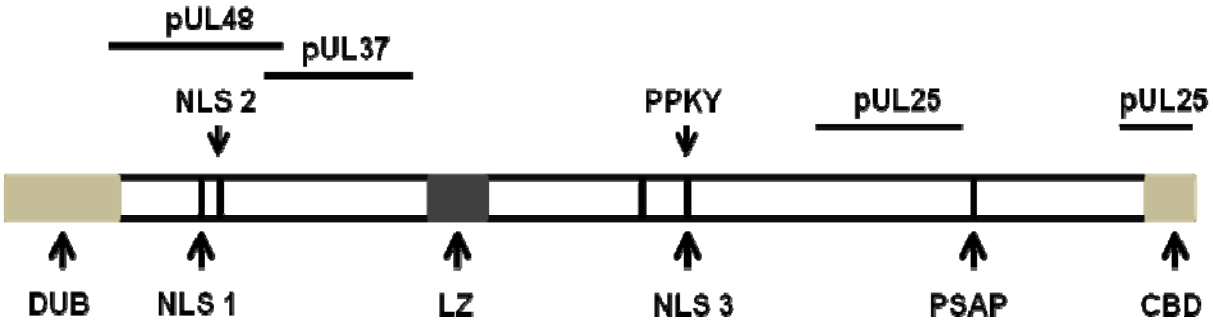

Figure 6. Schematic representation of an alphaherpesvirus large tegument protein. This scheme combines features as identified for HSV-1 and PRV VP1/2 and as documented in several references (3, 4, 14, 81, 106). CBD stands for capsid binding domain.

Isoforms of the herpesvirus large tegument protein exist, as was previously described for HSV-1 VP1/2, that was detected simultaneously in several cellular compartments (4). Also, a recent study in PRV identified a VP1/2 isoform in the nucleus that corresponds to the C-terminal portion of the protein and seems to play a crucial role throughout the final stages of virion maturation in the cytoplasm (87). However, herpesvirus large tegument proteins post-translational modification and cleavage is still poorly understood.

6.3.2 Function of large tegument proteins

Several functions have been attributed to the large herpesvirus tegument proteins. First, herpesvirus tegument proteins are thought to facilitate capsid transport along the cellular cytoskeleton within the cell. This is particularly important for neurotropic viruses, such as HSV-1 and PRV, which are transported over long distances along neuronal axons (2, 93, 101). Second, large tegument proteins play an essential role during docking of viral capsids to the nuclear pore, DNA release into the nucleus and virion assembly (30, 106, 130). The HSV-1 *tsBT* and ΔUL36 mutants both are unable to release viral DNA into the nucleus, even if the partial HSV-1 deletion mutant KΔUL36 is still able to produce DNA-filled capsids that accumulate in the cytoplasm (33). It is known that VP1/2 cleavage by a cysteine protease is necessary for DNA delivery into the nucleus in HSV-1 and it is thought that the VP1/2 N-terminal USP could actually be involved in the process, in spite of its late expression (72). Third, large tegument proteins are thought to act as flexible scaffolds to which other tegument proteins are added during virion transfer from the nucleus to the cytoplasm (21), a process recently described for PRV (87). Finally, virus maturation and egress has been shown to be highly impaired in the absence of large tegument proteins in both HSV-1 (40, 130) and PRV (15), suggesting its important role at this stage of viral replication.

6.3.3 Interactions of large tegument proteins

It is widely known that pUL37, a protein expressed by the UL37 ORF that is adjacent to UL36 in alphaherpesviruses, interacts with the UL36 large tegument protein. The UL36 and UL37 ORFs are highly conserved among herpesviruses and produce proteins located at the inner tegument layer surrounding the capsid (17, 99). Both proteins are likely added to the HSV-1, but not the PRV, nucleocapsid before it is transported to the cytoplasm (17, 82) (106). The complex formed by both proteins is crucial for outer tegument formation and virus egress as both were found to be present in tegument and envelope-only viral particles (L particles) during HSV-1 replication. Notably, detection of both pUL36 or pUL37 in L particles is dependant on the presence of one of these two proteins, even if L particles can be assembled in their absence (130). This finding indicates not only that these two proteins interact, but also that neither of the proteins are necessary for successful virion envelopment. As previously mentioned, a pUL37 interaction domain has been identified at the N-terminus of PRV and HSV-1 pUL36 (81) (78). In the latter, a single amino acid (aa) was found to be the determinant for interaction with pUL37 (78). Contrary to what has been observed in the absence of pUL36, HSV-1 pUL37-null mutants can still deliver viral DNA into the nucleus

(39), but virion release does not occur (130). PRV pUL37-null mutants remain viable, but impaired in their replication capacity (130).

Large tegument proteins are also important for the connecting the capsid/inner tegument and outer tegument/glycoprotein. It has been shown that large tegument proteins interact strongly not only with a component of the outer tegument layer, VP16, which is encoded by UL48 in HSV-1 (46, 82, 149, 153), but also with the major capsid (pUL19, VP5) in PRV (101). It is also known that the pUL25/pUL17 C-capsid specific component (CCSC), which is located in the virion apexes, interacts with the large tegument protein and is essential for its incorporation into the capsid (29, 82, 119). Recent work showed the presence of two important C-terminal domains in HSV-1 pUL25: one allows the recruitment of large tegument proteins into cytosolic capsids during assembly for secondary envelopment and the other was named capsid binding domain (CBD, Figure 6) and promotes their association with capsids during viral entry (138). All these interaction regions are described in Figure 6. It has been demonstrated for HSV-1 that interaction of large tegument proteins with each other is through the USP region (12).

6.4 The ubiquitin-proteasome pathway

Ubiquitin (Ub) is a key regulator of many physiological processes in eukaryotic cells (84, 126), such as protein degradation, cell-cycle control, stress response, DNA repair, immune responses, signal transduction, transcriptional regulation, endocytosis, and vesicle trafficking (59, 80, 140).

Ub is a highly conserved 76-residue polypeptide (22, 59, 73, 80, 103, 140) that usually forms stable isopeptide bonds with ε-amino groups of internal lysines (K) of substrate proteins. Exceptionally, Ub can also be found conjugated to the N-terminus of substrate proteins (55, 60). Ub itself encodes 7 lysine residues denominated as K6, K11, K27, K29, K33, K48, and K63 (73, 84, 103, 155). Addition of a single ubiquitin or monoubiquitination is an important regulatory signal required for down-regulation of plasma membrane proteins by targeting them to the lysosome (7, 60). Deregulation of Ub metabolism has been linked to serious diseases such as cancer (10) and neuromuscular disorders (31).

A subset of Ub-protein ligases (E3s) is capable of assembling polyubiquitin chains to lysine residues (84, 103), a process known as polyubiquitination. K48- and K63-linked polyubiquitin chains are the most studied. K48-linked ubiquitination targets proteins for degradation (25,

75), whereas K63-linked Ub chains are responsible for a variety of processes, including endocytosis of cell surface receptors and other basic cellular processes (60) including post-replication DNA repair (55). Subsequently, similar pathways requiring ubiquitination were identified that make use of so-called “Ub-like proteins (UbLs),” a group of modifiers including NEDD8, interferon-induced gene protein 15 (ISG15), small ubiquitin-like modifier (SUMO) and autophagy-related protein 8 (Atg 8) (51, 63, 79, 105). These molecules are not usually involved in protein degradation, but have been shown to interact with several E3s (51).

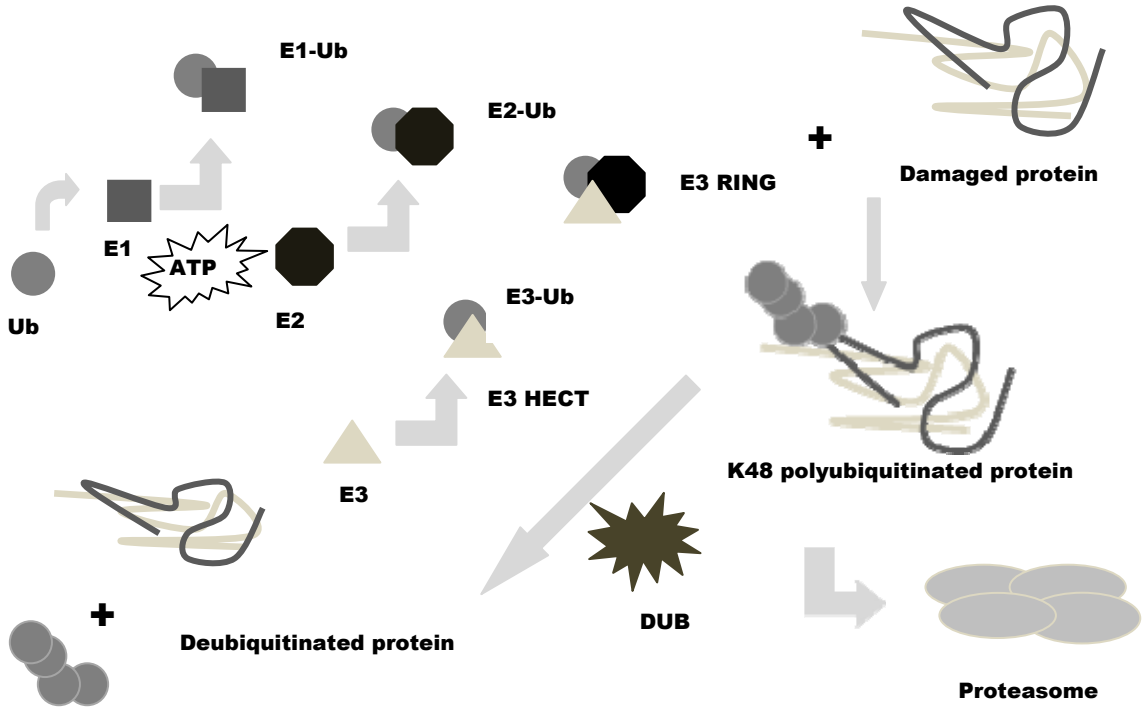

Figure 7. The ubiquitin-proteasome pathway. Free Ub is coupled to the Ub-activating enzyme (E1) and subsequently transported by Ub-carrier proteins (E2) to the Ub-protein ligases (E3). These will in turn link Ub to the protein in a chain-like fashion through K48 residues, thus marking it accessible for proteasomal degradation. This process can be reversed by deubiquitinases that remove the polyubiquitin chain from the marked protein.

The conjugation of the Ub molecule to the substrate protein for proteasomal degradation occurs in a complex three-step process (55, 60, 73, 75) that is summarized in Figure 7. It starts when a single Ub-activating enzyme (E1) activates Ub in an ATP-dependent fashion, creating a high-energy thiol intermediate (E1-Ub). This activated Ub is transferred to several dozens of Ub-carrier or Ub-conjugating enzymes (E2s) through the formation of an additional high-energy thiol ester intermediate (E2-Ub). This second Ub intermediate is then transferred to one of hundreds of E3s, either through the generation of a third thiol-Ub intermediate (E3-Ub) as is the case for the HECT (Homologous to the E6-AP Carboxy terminus) E3 enzymes,

or by direct transfer of E2 to the substrate protein in the case of RING (Really Interesting New Gene)-like E3 enzymes. This process repeats itself several times, until a polyubiquitin chain is formed.

The tagged substrate protein is then directed, in the case of K48 polyubiquitination, to the 26S proteasome complex for degradation (73). The proteasome complex is a large multicatalytic protease composed of a 19S regulatory particle, composed of six ATPase and 12 non-ATPase subunits (73), which is responsible for unfolding and recognition of tagged proteins. The 20S core particle, composed of seven α and seven β domains (73), converts ubiquitinated proteins into small peptides (55).

Several viruses and intracellular bacteria have developed strategies to control cellular ubiquitination by interfering with the ubiquitin-proteasome pathway (64, 140) at multiple levels such as cellular division, activation or suppression of the NF-κB, and destruction of MHC I molecules (49, 140).

6.5 Deubiquitinases

Ubiquitination can be reversed by deubiquitinases (DUB), enzymes that can release Ub from their covalent isopeptide bonds. Thus far, approximately 100 DUBs have been described to be encoded within the human genome (7, 10, 73, 75, 80, 84, 113). Besides their ability to rescue proteins from either proteasomal (cytoplasmatic proteins) or lysosomal degradation (internalised receptors) or to change protein location by manipulation of the chain size, DUBs can also contribute to Ub homeostasis by Ub recycling and by cleaving Ub chains transcribed from the four Ub-coding genes into single units (73, 84). It is thought that some DUBs present specificity for certain substrates and also for certain types of Ub chains (84).

Five classes of DUBs have so far been identified based in the characteristics of their catalytic domains; four cysteine proteases classes and one metalloprotease class (75, 84, 126):

Metalloproteases:

- JAMM/MPN+ motif proteases (JAB1/MPN/MOV34)

Cysteine proteases:

- Ubiquitin COOH-terminal hydrolases (UCHs)
- Machado-Joseph disease protein domain proteases or Josephins (MJDs)

- Ovarian tumour proteases (OTUs)
- Ubiquitin-specific proteases (USPs)

Cysteine proteases possess an enzymatically active diad or triad that is based on a histidine-cysteine-aspartic acid/asparagine combination: histidine lowers cysteine's acidity constant (pKa), thus allowing the disruption by cysteine of the isopeptide bond between substrate and Ub or between two Ub molecules. The third residue, aspartic acid/asparagine that is not always present, is believed to be responsible for the alignment and polarization of the catalytic histidine (84). The herpesvirus-encoded DUBs belong to the USP class.

6.5.1 Ubiquitin-specific proteases (USPs)

USPs are the most abundant DUBs, with around 55 members identified within the human genome so far (103). An active site of around 100 aa is characteristic of this class, usually embedded within non-catalytic domains that are important for USP-target interaction (103). Little sequence homology exists among the various USPs, apart from the catalytic core structure (103), which can be highly conserved (e.g. herpesvirus-encoded USPs) (75, 140). Its three-dimensional structure can be divided into three subdomains: the "palm", the "thumb" and the "fingers". The catalytic domain lies between the two first subdomains, while the fingers hold the distal Ub (84). Some USPs may undergo conformational changes following Ub binding in order to become catalytic.

6.5.1.1 Herpesvirus tegument USP (htUSPs)

In 2005, an active cysteine protease with deubiquitinating activity was identified, embedded within the N-terminus of the HSV-1 large tegument protein (pUL36). DUB activity was shown to be specific for K48 polyubiquitin chains (75), leading to the formation of a new family of DUBs of the USP group named herpesvirus tegument USPs (htUSPs) (140). The catalytic site (also called the cysteine box or cys box) is highly conserved among herpesviruses (Figure 8) (75, 140) and is expressed independently from VP1/2 from about 12 hs pi for HSV-1 (75).

In the case of the previously mentioned HSV-1 tsB7 mutant, a remarkable increase of ubiquitinated proteins during virus replication at non-permissive temperatures was described (5). DUB activity embedded in the large tegument protein was later confirmed for several members of each subfamily, including the alphaherpesviruses PRV (12) and MDV (55), the

betaherpesviruses HCMV, SCMV (154) and murine cytomegalovirus (MCMV) (139), and the gammaherpesviruses Kaposi's sarcoma-associated virus (KSHV) (47), EBV (139) and mouse herpesvirus strain 68 (MHV-68) (57). Due to differences between the nomenclature of the three subfamilies, USPs are encoded by homologous genes that have different names.

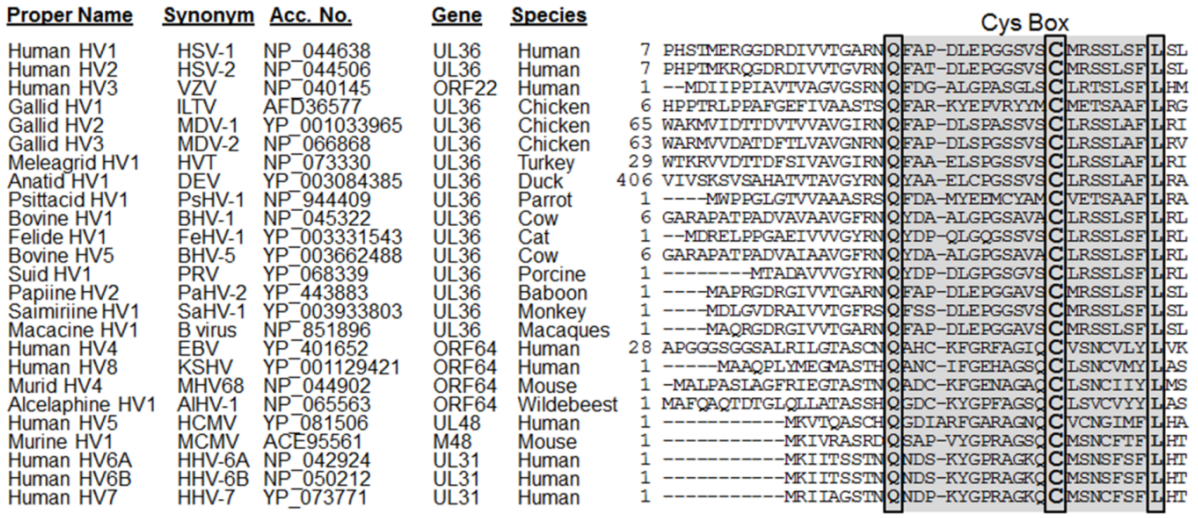

Figure 8. Comparison of the USP cysteine boxes of representative herpesviruses. In addition to the invariant active cysteine (C), glutamine (Q) and leucine (L) residues are present in every sequence. Aa encompassing the Cys box are shaded in light grey. Numbers before sequences represent the location of the first aa in the sequence within the UL36 protein. Whenever possible, sequences of reference strains for each virus were used. Figure courtesy of Dr. Keith Jarosinski.

The inactivation of the putative active site by mutation of the cysteine to an alanine in HSV-1 abolished enzymatic activity *in vitro* (75), but did not have any effect in terms of plaque sizes and growth kinetics (12). In contrast, inactivation of the putative active site led to impairment of viral replication *in vitro* in other herpesviruses. In some cases, *in vivo* activity of mutant viruses was also studied, where severe impairments in viral pathogenicity were observed; enzymatically inactive PRV USP was deficient in neuroinvasion using a mouse infection model (15) and intraperitoneal infection of C57/BL6 mice with a MHV-68 USP mutant presenting the same alteration was generally cleared by day 7 pi. These results clearly indicated an important role for htUSP in maintenance of persistent infection (56).

Epitope-tagged, Ub-based suicide probes like the HA-tagged Ub-vinylmethyl esther (HAUbVME) (140) were used both for detection of htUSPs and for crystallization of the N-terminal 232 aa of the MCMV large tegument protein, corresponding to the MCMV-encoded

M48 USP. MCMV USP was found to present a papain-like structure and to suffer minimal conformational alterations upon Ub binding (140) (
Figure 9).

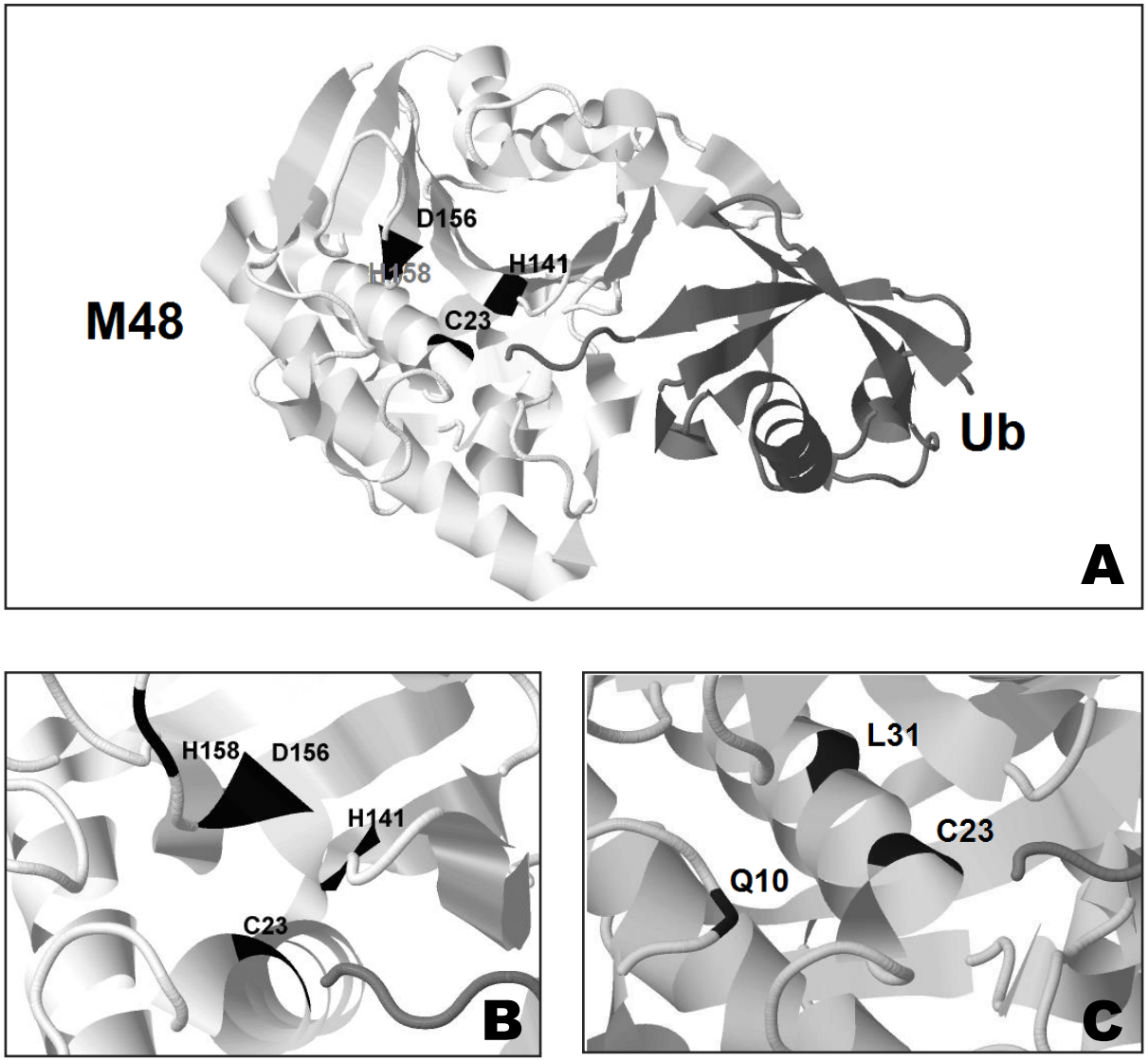

Figure 9. MCMV M48 USP crystal structure. (A) M48 USP structure, the only resolved htUSP structure solved and present in the protein database (PDB). Shown in file 2J7Q (140) is MCMV DUB while binding to an Ub molecule. (B) The residues that were identified as important for catalysis can be observed with higher resolution: cysteine in position 23 (C23), histidines in position 141 (H141) and 158 (H158); and asparagine in position 156 (D156). (C) shows the three highly conserved residues present in all htUSPs Cys boxes; in the case of M48, there is the previously described cysteine residue, glutamine in position 10 (Q10) and leucine in position 31 (L31). Figures were made using Jmol (www.jmol.org) (95) with the help of Dr. Dušan Kunec.

All studied htUSPs have specific activity for Ub chains and no activity towards Ub-like molecules like ISG15 (Interferon-induced Gene protein 15) or SUMO1 (Small Ubiquitin-like Modifier 1) (75, 139); however, specific activity for the Ub-like molecule NEDD8 (Neural

precursor cell -Expressed Developmentally Down-regulated 8) has been detected for EBV, KSHV, HSV-1 and MCMV-encoded USPs. This is not surprising due to the significant sequence homology between Ub and NEDD8 (50, 51).

Regarding USP activity, both HSV-1 USP and HCMV USP, originally thought to represent specific activity against K48 polyubiquitination chains (60, 125), were later found to also cleave K63 polyubiquitin chains. Due to some differences in the length of the constructs used, some groups found cleavage of K63 chains by HSV-1 USP to be slightly more efficient (64) or slightly less efficient (9) than K48 chain cleavage. The UL36 homologue BPLF1 encoded by EBV, KSHV ORF64-encoded USP and MCMV M48 cleave K48 and K63 polyubiquitin chains with varying efficiency. A 5-fold less efficient cleavage of K63 chains has been described for M48 (114).

Thus far, there is little information regarding *in vivo* substrates of htUSPs (12) and most of the known substrates were found for the gammaherpesviruses. BPLF1 from EBV interacts with viral-encoded ribonucleotide reductase (RR) (155). Additionally, this enzyme was described to act as a deneddylase, which interferes with the cullin-RING E3 ligase neddylation cycle (51) by inhibiting the binding of cullin-associated NEDD8-dissociated protein 1 (CAND1). This leads to cell cycle arrest in the S-phase that is favorable for viral replication (50, 51). Also, BPLF1 can deubiquitinate proliferating cell nuclear antigen (PCNA), which is essential for recruitment of specialized translesion polymerases following DNA damage (156). These studies indicate that the USP encoded by EBV is not only involved in multiple steps of virus replication, but can also eventually hinder DNA repair mechanisms. Studies performed with HSV-1-encoded USP and MCMV-M48 indicate that deneddylase activity and S-phase deregulation are common features of htUSPs (50, 51).

KSHV-encoded ORF64 protein has recently been found to inhibit RIG-I-mediated signalling upon infection, which could indicate a possibly protective function of this enzyme, since the RIG-I pathway leads to the production of the antiviral cytokine interferon α (IFN α) (134). It has been suggested that USPs may protect viral and cellular proteins from degradation by the proteasome (75, 84). The recent discovery of USP autocatalytic activity for stabilization of VP1/2 in HSV-1 (12) and of PRV large tegument protein (Huffmaster and Smith, personal communication) would support this hypothesis. Another hypothesis formulated upon discovery of htUSPs was that these enzymes may allow recycling of polyubiquitin chains for viral use of the Ub trafficking system (75).

As previously mentioned, the first htUSP to be discovered for HSV-1 was expressed independently from pUL36 from about 12 h pi. (75). A major question that remains is whether all USPs are expressed as separate transcriptional units, post-translationally cleaved from pUL36 or function in the context of pUL36. Both cleaved and non-cleaved forms seem to co-exist in HSV-1 and have both been shown to be active by using HAUbVME probes (154). In HCMV, the htUSP is encoded within its large tegument protein named high molecular weight protein (HMWP); again, both the non-cleaved and ~38 kDa catalytic fragment forms were found to bind the DUB probe. In the case of SCMV, however, only the uncleaved active form of the large tegument protein was found to bind the suicide probe (154). Also, a 325 aa N-terminal fragment of EBV BPLF1 transfected into HeLa cells and processed became catalytically active (50, 51), which may indicate that htUSPs can be expressed independently from the large tegument protein in most herpesviruses subfamilies.

6.5.1.1.1 MDV USP

Using sequence comparison with other herpesviruses large tegument proteins, the first 322 aa of the N-terminus of MDV large tegument protein pUL36 correspond to the USP sequence (66). Inactivation of the MDV DUB activity through mutation of the putative active site cysteine to an alanine at position 98 (C98A) led to virus that was slightly impaired in terms of *in vitro* viral replication, but severely impaired in its ability to cause tumours (66). Also, reversion of the mutation to its original sequence was found in some infected animals, which led to the suspicion that this enzyme plays an important role for the virus, as such a phenomenon is rarely observed when non-essential domains are mutated. Interestingly, MDV USP mRNA was shown to be present both during lytic infection of chicken cells and in lymphoblastoid cell lines (LCLs) that harbour the virus in its latent form. This region of the MDV genome is generally silent during latency. The findings show that USP expression occurs throughout the virus life cycle and may be important for maintenance during both lytic and latent infection (66).

6.6 Specific Aims of the Thesis

The initial findings described in the previous section were the basis for this thesis, during which we focused on further delineating the roles MDV USP played in viral replication and/or tumourigenesis. The first aim of this study was to identify MDV USP interacting proteins to better understand what makes this fragment of pUL36 so important for replication and/or tumourigenesis. Essentially, our goal was to determine whether MDV USP interacts with the MDV-encoded oncoprotein Meq or cell cycle regulators. For this purpose, tandem affinity purification (TAP) and immunofluorescence (IF) experiments where performed. Unfortunately, development of these systems was difficult and therefore shall only be briefly mentioned in the results section. In a near future, yeast two hybrid (Y2H) assays in collaboration with Professor Jürgen C. Haas and Clark Russell from the University of Edinburgh will hopefully contribute to the discovery of MDV USP substrates.

The second aim was to study the role of MDV USP in replication and tumourigenesis during virus infection. For this part of the project, several recombinants (r) MDV were generated using two-step Red recombination and the reconstituted viruses (v) were compared regarding their plaque sizes and growth kinetics. More specifically, we studied the replication ability of MDV mutants in the absence of the putative USP sequence or its cysteine active site, Cys box, and also whether defective viral phenotypes (both by cysteine to alanine mutation or complete removal of the USP portion) can be restored by ectopic expression of USP during virus infection.

Finally, rabbit anti-MDV USP and anti-MDV pUL36 antibodies developed, following peptide immunization, were analysed by western blot (WB) and IF analyses of infected and transfected cell lysates.

7 Material and Methods

7.1 Materials

All chemicals indicated below were used according to the manufacturer´s instructions. Buffers and media for cell and bacterial culture are indicated separately.

7.1.1 Chemicals, consumables and equipment

7.1.1.1 Chemicals

Name	Manufacturer
6-N--caproic-acid [Cat. No. A2504-1006]	Sigma-Aldrich, St Louis
Acetone ($(CH_3)_2CO$) [Cat. No. A160, 2500]	Applichem, Darmstadt
Acrylamide Rothiforese Gel 30 [Cat. No.3029.1]	Carl-Roth, Karlsruhe
Agar (agar bacteriological) [Cat. No. 2266.2]	Carl-Roth, Karlsruhe
Agarose- electrophoresis grade Seakem LE [Cat. No.500004]	Lonza, Rockland
Ampiciline Na-salt [Cat. No.K029.2]	Carl-Roth, Karlsruhe
Ammonium peroxodisulfate (APS) [Cat. No. 0.01201.011]	Merck, Darmstadt
Arabinose L (+) [Cat. No. A11921]	Alta Aesar, Karlsruhe
Bromephenol blue sodium salt [Cat. No. A3640,0025]	Applichem, Darmstadt
BSA (albumin bovine fraction V) [Cat. No. A6588.0100]	Applichem, Darmstadt
$CaCl_2$ (calcium chloride) dihidrat [Cat. No. T885,2]	Carl-Roth, Karlsruhe
CH_3COOH (acetic acid) [Cat. No. A3686, 2500]	Applichem, Darmstadt
Chloramphenicol [Cat. No. 3886.1]	Carl-Roth, Karlsruhe
Chloroform [Cat. No. 411 K3944831]	Merck, Darmstadt
Coomassie brilliant blue R250 [Cat. No. 17525]	Serva, Heidelberg
Desthiobiotin [Cat No. 2-1000-001]	IBA, Göttingen
Dimethyl sulfoxide (DMSO) [Cat. No. 1.02952.2500]	Merck, Darmstadt
dNTP Mix (10mM total) [Cat. No. BIO-39053]	Bioline, Luckenwalde
DTT (dithiothreitol) [Cat. No. 6908,3]	Carl-Roth, Karlsruhe
EDTA (ethylendiamine tetraacetic acid) [Cat. No. A2937, 1000]	Applichem, Darmstadt
Complete EDTA-free Protease Inhibitor Mix [Cat. No. 11873580001]	Roche Diagnostics,Mannheim
Ethanolamine [Cat. No. A2161,0100]	Applichem, Darmstadt

Ethidium bromide 1% [2218.2]	Carl-Roth, Karlsruhe
$EtOH_{den.}$ (ethanol 96%) [Cat. No.]	Applichem, Darmstadt
Glucose (α-D(+) glucose monohydrate) [Cat. No.303 K1468642]	Merck, Darmstadt
Glycerol [Cat. No. A2926,2500]	Applichem, Darmstadt
Glycine [Cat. No. 3908.2]	Carl-Roth, Karlsruhe
HEPES [Cat. No. A3724,0100]	Applichem, Darmstadt
HCl 37% (hydrochloric acid) [Cat. No. 4625.2]	Carl-Roth, Karlsruhe
Isopropyl alcohol (2-propanol) [Cat. No. A0892]	Applichem, Darmstadt
Kanamycin sulphate [Cat. No. T832.2]	Carl-Roth, Karlsruhe
KCH_3CO_2 (potassium acetate) [Cat. No. A4279,0100]	Applichem, Darmstadt
β-mercaptoethanol (2-mercaptoethanol) [Cat. No.28625]	Serva, Heidelberg
Methanol [Cat. No. A3493, 2500 PE]	Applichem, Darmstadt
$MgCl_2$ (magnesium chloride hexahydrate) [Cat. No. 5833.025]	Merck, Darmstadt
Milk powder non-fat dried- blotting grade [Cat. No. A0830,100]	Applichem, Darmstadt
NaCl (sodium chloride) [Cat. No. A3597,5000]	Applichem, Darmstadt
Na-desoxycholat (sodium desoxycholat) [Cat. No. B201759]	Alta Aesar, Karlsruhe
NaN_3 (sodium azide) [Cat. No. 8.22335.0250]	Merck, Darmstadt
NaOH (sodium hydroxide) [Cat. No. 1.06462]	Merck, Darmstadt
NP-40 (nonidet P-40) non-ionic detergent [Cat. No.18896-500]	Sigma- Aldrich, St Louis
Paraformaldehyde (PFA) [Cat. No. P6148]	Sigma- Aldrich, St Louis
Penicilin G potassium salt [Cat. No. A1837,0100]	Applichem, Darmstadt
Peptone/Tryptone [Cat. No. A2210,0250] (bacto-tryptone pancreatic digest of casein)	Applichem, Darmstadt
Phenol/Chloroform [Cat. No. A0889,0500]]	Applichem, Darmstadt
Polyethylenimine (PEI) [Cat. No. 23966]	Polysciences, Warrington
Ponceau S [Cat. No. 33429]	Serva, Heidelberg
NaF (Sodium Fluoride) [Cat. No. 201154-5G]	Sigma-Aldrich, St Louis
Na_3VO_4 (Sodium Orthovanadate) [Cat. No. 450243-10G]	Sigma-Aldrich, St Louis
SDS (sodium dodecyl sulfate) [Cat. No. 75746]	Sigma-Aldrich, St Louis
Streptomycin sulphate salt [Cat. No. S9137-256]	Sigma-Aldrich, St Louis
TEMED (N,N,N',N'-tetramethyl-ethane-1,2-diamine) [Cat. No. 1.10732.0100]	Merck, Darmstadt
Tris [Cat. No. A1086,5000]	Applichem, Darmstadt
Triton X-100 detergent [Cat. No. 8603]	Merck, Darmstadt
Tween-20 non-ionic detergent [Cat. No. 822184LE]	Merck, Darmstadt
Yeast extract granulated [Cat. No. 212750]	Becton-Dickinson, Heidelberg

7.1.1.2 Consumables

Name	Manufacturer
Cell culture dishes Falcon:	
6-well (1,0x10^6 cells per well); 24-well (2,0x10^5 cells per well);	TPP, Trasadingen
Cell culture flasks:	
25 ml (1,0x10^6 cells); 75 ml (1,0x10^7 cells); 175 ml (2,0x10^7 cells)	TPP, Trasadingen
Petri dishes for cell culture :	
60 mm (2,5x10^6 cells) 100 mm (7,0x10^6 cells), 150 mm (7,0x10^7 cells)	Startsedt, Nümbrecht
Conical test tubes 17x120 (15ml)	TPP, Trasadingen
Conical test tubes 30x115 (50ml), with and without feet	TPP, Trasadingen
Cryotubes 1,8 ml	Nunc, Kamstrupvej
Eppendorf tubes 1,5 and 2 ml	Sanstedt, Nümbrecht
Expendable cuvettes	Biodeal, Markkleeberg
Latex gloves	Unigloves, Troisdorf
Nitrile gloves	Unigloves, Troisdorf
PCR tubes	VWR International, West Chester
Sterile syringe filters PVDF 0,22µm	VWR International, West Chester
Sterile syringe filters PVDF 0,45µm	VWR International, West Chester
Strep-tactin beads [Cat No. 2-1201-002]	IBA, Göttigen
Transfection polypropylene tubes	TPP, Trasadingen
Whatmann blotting paper (WM Whatmann 3MM)	GE Healthcare, Freiburg
Visking dialysis tube type 20/32	Spectrummedical Industries Inc, Los Angeles

7.1.1.3 Equipment

Name	Manufacturer
Centrifuges	
Centrifuge 5424	Eppendorf, Hamburg
Rotor FA-45-24-11	
Centrifuge 5804R	Eppendorf, Hamburg
Rotors A-4-44 and F45-30-11	
Galaxy mini centrifuge	VWR International, West Chester
Sorvall RC5B Refrigerated Superspeed centrifuge	Thermo, Scientific, Dreieich
Rotors GSA and SS-34	

Generals

ABI Prism 7500 Fast Real-time PCR system	Invitrogen Life Technologies, Grand Island
Bacterial incubator 07-26860	Binder, Turtlingen
Bacterial incubator shaker Innova 44	New Brunswick Scientific, New Jersey
Bunsen burner Type 1020	Usbeck, Radevormwald
Branson sonifier 25C	Heinemann, Schwäbisch Gmünd
Cell incubators Excella ECO-1	New Brunswick Scientific, New jersey
Chemilumiscent imager Chemi-Smart 5100	PeqLab, Erlangen
Cryo storage system Cryo 1°C	NALGENE/Thermo Scientific, Rochester
Electroporator Genepulser Xcell	Bio-Rad, Munich
Electrophoresis power supply Power Source 250V	VWR International, West Chester
Fluorescence microscope Axiovert S 100	Carl Zeiss MicroImaging GmbH, Jena
Freezer -20°C	Liebherr, Bulle
Freezer -80°C	GFL, Burgwedel
Gel electrophoresis chamber Mini Elektroforese System	VWR International, West Chester
Gel electrophoresis chamber SUB-Cell GT	Bio-Rad, Munich
Ice machine AF100	Scotsman, Vernon Hills
Magnetic stirrer RH basic KT/C	IKA, Staufen
Microscope Axiovert S100	Carl Zeiss MicroImaging GmbH, Jena
Mini-Transblot (7.5 x 10 cm blotting area)	Bio-Rad, Munich
Model 583 Gel Dryer	BioRad Laboratories, Munich
Newbauer counting chamber	Assistant
Nitrogen tank ARPEGE70	Air liquide, Düsseldorf
Orbital shaker 0S-10	PeqLab, Erlangen
Petri dishes for bacteria	Sanstedt, Nümbrecht
pH-meter RHBKT/C WTW pH level 1	Inolab, Weilheim
SDS-PAGE chambers Mini-PROTEAN TetraCell	Bio-Rad, Munich
Semi-Dry Transfer Unit w/built-in Power Supply	Hoefer, San Francisco
Sterile laminar flow chambers	Bleymehl, Inden
Thermocycler Flexcycler	Analytik Jena, Jena
Thermocycler GeneAmp PCR System 2400	PerkinElmer, Waltham
Thermocycler T-Gradient	Biometra, Göttingen
Thermomixer 5326, confort and compact models	Eppendorf, Hamburg
UV Transiluminator Bio-Vision-3026	PeqLab, Erlangen
Transiluminator printer P93D	Mitsubishi, Rüsselsheim
Transiluminator VL-4C, 1x4W-254 nm	Vilber-Lourmat, Eberhardzell
Vacuum aspirator Vacumat 130	H.Saur, Reutlingen
Vortex VTX-3000L	Hartenstein, Würzburg
Water baths TW2 and TW12	Julabo, Seelbach
Water bath shaker C76	New Brunswick Scientific, New Jersey

Microscopes and associated equipment

Axio-Observer.Z1 fluorescence microscope	Carl Zeiss MicroImaging GmbH, Jena
Eclipse A1 laser scanning microscope	Nikon Instruments, Tokyo
Olympus BX60 wide field	Olympus, Tokyo
Mounting Medium Vectashield with DAPI [Cat. Nr: H-1200]	Vector Laboratories Inc, Burlingame
Microscope AE20	Motic, Wetzlar

Pipettes

Pipetboy	IBS Integrated Biosciences, Fernwald
Pipetman P1000	VWR International, West Chester
Pipetman P200	VWR International, West Chester
Pipetman P100	VWR International, West Chester
Pipetman P10	VWR International, West Chester
Pipettes for Pipetboy 5, 10, 25 ml	Sarstedt, Nümbrecht
Pippete tips for Pipetman P1000, 200, 100 and 10	VWR International, West Chester

Spectrometers

Nanodrop 1000	Peqlab, Erlangen

Software

Axiovision 4.8 software for Zeiss microscopes	Carl Zeiss MicroImaging GmbH, Jena
Chemi-Capt	Vilber-Lourmat, Eberhardzell
Graphpad Prism 5	Graphpad Software Inc, La Jolla
ImageJ 1.41o	NIH, Bethesda
Jmol	Open source, Jmol development team
ND-1000 V.3.0.7	PeqLab, Erlangen
ABI PRISM® 7000 Sequence Detection Systems 1.4	Invitrogen Life Technologies, Grand Island
SPSS	IBM, Armonk
Vector NTI 9	Invitrogen Life Technologies, Grand Island
Vision-Capt	Vilber-Lourmat, Eberhardzel

7.1.2 Enzymes, markers and kits

Name	**Manufacturer**
Enzymes modifying DNA, RNA and proteins	
Antartic Phosphatase [Cat. No.M0289L]	New England Biolabs, Ipswich
*Bam*HI [Cat. No. R0136]	New England Biolabs, Ipswich
*Bam*HI HF [Cat. No. R3136]	New England Biolabs, Ipswich

*Bgl*II [Cat. No. R0144]	New England Biolabs, Ipswich
Benzonase [Cat. No. D00111784]	Novagen, San Diego
Calf intestinal phosphatase (CIP) [Cat. No. M0290S]	New England Biolabs, Ipswich
Dpn I [Cat. No. ER1701]	New England Biolabs, Ipswich
*Eco*RI [Cat. No. R0101]	New England Biolabs, Ipswich
*Eco*RI HF [Cat. No. R3101]	New England Biolabs, Ipswich
*Eco*RV [Cat. No. R0195]	New England Biolabs, Ipswich
*Hind*III [Cat. No. R0104]	New England Biolabs, Ipswich
*Kpn*I [Cat. No. R0142]	New England Biolabs, Ipswich
Lysozyme 20 000 U/mg [Cat. No. 8259.1]	Applichem, Darmstad
Quick ligase [Cat. No. M2200S]	New England Biolabs, Ipswich
*Not*I [Cat. No. R0189]	New England Biolabs, Ipswich
Phusion Hot Start High-Fidelity DNA Polymerase [Cat. No. M0530S]	Fynnzimes, Thermo Scientific, Rochester
*Pme*I [Cat. No. R0560]	New England Biolabs, Ipswich
Proteinase K [Cat. No. 7528.2]	Carl-Roth, Karlsruhe
RNase A 100mg [Cat. No.A2760]	Applichem, Darmstad
*Sma*I [Cat. No. R0141]	New England Biolabs, Ipswich
T4 DNA Ligase 1000 units [Cat. No. M0202]	New England Biolabs, Ipswich
Taq DNA-Polymerase [Cat. No.01-1020]	PeqLab, Erlangen
TaqMan Fast Universal Master Mix	Invitrogen Life Technologies, Grand Island
*Xho*I [Cat. No. R0146]	New England Biolabs, Ipswich

DNA marker

Generuler ^{TM} 1kb DNA Ladder [Cat. No. SM0311]	Fermentas, Mannheim

Protein marker

PageRuler ^{TM} Prestained Protein Ladder [Cat. No. SM0671]	Fermentas, Mannheim

Kits

DNeasy 96 Blood and Tissue kit	Qiagen, Valencia, CA
ECL Plus detection kit [Cat. No. RPN2132]	Amersham/ GE Healthcare, Little Chalfont
EasyXpress Insect Kit II [Cat. No. 32561]	Qiagen, Hilden
Hi Yield Gel/PCR DNA Fragments Extraction Kit [Cat N0. 30 HYDF100-1]	SLG, Gauting
LipofectamineTM 2000 transfection kit	Invitrogen Inc., Carlsbad
Qiagen Plasmid Midi kit [Cat. No. 12145]	Qiagen, Hilden
QIAprep Spin Miniprep kit [Cat. No. 27104]	Qiagen, Hilden

7.1.3 Bacteria, cells and viruses

7.1.3.1 Bacteria

Name	Features	Reference
Top 10	F- mcrA Δ(mrr-hsdRMS-mcrBC) φ80lacZΔM15 ΔlacX74 nupG recA1 araD139 Δ(ara-leu)7697 galE15 galK16 rpsL(Str^R) endA1 λ$^-$	Invitrogen
XL1Blue	endA1, gyrA96, hsdR17 ($r_{k-}m_{K+}$), lac, recA1, relA1, supE44, thi, (F´, lacI^q, lacZ□M15, proAB$^+$, tet)	Stratagene
DH10B	F$^-$ endA1 recA1 galE15 galK16 nupG rpsL ΔlacX74 Φ80lacZΔM15 araD139 Δ(ara,leu)7697 mcrA Δ(mrr-hsdRMS-mcrBC) λ	Invitrogen
GS1783	DH10B λcI857 Δ(cro - bioA)<>araC - $P_{BAD,}$ I - SceI	Tischer et al, (150)

Table 1. Bacterial strains used for cloning and for two-step Red mediated recombination (GS1783).

7.1.3.2 Cells

Name	Features	Reference
293T/HEK	Human Embryonic Kidney (*HEK*) epithelial cell line transformed by human adenovirus 5 + SV40 T-antigen	ATCC.CRL-11268, (121)
CECs/CEFs	Chicken embryo fibroblasts/cells, primary cells, VALO SPF strain	Primary cells
CKCs	Chicken kidney cells; primary cells , SPF P2a strain	Primary cells
DF-1	Continuous chicken fibroblast cell line; spontaneously transformed, East Lansing Line (ELL-0)	ATCC #. CRL-12203 (61)

Table 2. Different cell lines used throughout this project.

7.1.4 Buffers and media

7.1.4.1 General Buffers

1x Phosphate saline buffer (1xPBS)
2 mM KH_2PO_4
10 mM Na_2HPO_4
137 mM NaCl
2,7 mM KLC, pH 7,3

1x Tris saline buffer (1xTBS)
50 mM Tris-Cl, pH 7.5
150 mM NaCl
Final pH 7,5

1x Tris-acetate-EDTA buffer (TAE)
(Diluted from 50X Stock)
40 mM Tris
1 mM $Na_2EDTAx2H_2O$
20 mM Acetic acid 99%, pH 8,0

10x Laemmli
1,25M Tris-HCl pH 6,8
10% SDS
0,2% bromophenol blue

Specific buffers for each of the performed techniques shall be mentioned in the methods section.

7.1.4.2 Media and supplements for cultivation of bacteria (*E.coli*)

Luria-Bertani medium (LB)
1% Bacto-tryptone
0,5% Bacto-Yeast extract
0,5% NaCl

Super Optimal broth with Catabolite repression (**SOC**)
20g/L Peptone/Tryptone
5g/L Yeast extract
0,5g/L NaCl
pH 7,5
after autoclaving:10 mM $MgCl_2$, 2,5 mM KCl, 56 mM Glucose

Product	Working concentration	Comment
Ampicillin (AMP)	100 µg/ml	in ddH_2O, storage -20°C
Kanamycin (KANA)	50 µg/ml	
Chloramphenicol (CAM)	30 µg/ml	in 96% EtOH, -20°C

Table 3. Antibiotics used for bacterial selection and respective dilutions.

7.1.4.3 Media and supplements for cultivation of mammalian cells

Fetal bovine serum (FBS)	Biochrom AG, Berlin
Minimum essential Medium Eagle (MEM)	Biochrom AG, Berlin
Dubellco's MEM (DMEM)	Biochrom AG, Berlin
Opti-MEM I (1x)	Invitrogen Life Technologies, Grand Island
L-alanyl-L-Glutamine	Biochrom AG, Berlin
Sodium Pyruvate	Biochrom AG, Berlin
Trypsin/EDTA 0,05%	GIBCO, Life Technologies, Grand Island

Antibiotic	**Working concentration**	**Comment**
Penicillin (P) Streptomycin (S)	100 U/ml	Diluted in MEM, stored at -20 °C

Table 4. Antibiotics used for maintenance of eukaryotic cells and respective dilutions.

7.1.5 Plasmids and BACs

7.1.5.1 Plasmids

Plasmid	**Features**	**Reference**
pcDNA3	Mammalian expression vector; T7prom, f1 ori, pBR322 ori, AmpR, pCMV, pSV40, NeoR	Invitrogen
pcDNA3-HA.USP	pcDNA3 with USP insertion between *Hind*III and *Xho*I restriction sites containing N-terminal HA tag	This work
pcDNA3-USP.HA	pcDNA3 with USP insertion between *Hind*III and *Xho*I restriction sites containing C-terminal HA tag	This work
pCDNA3-Meq	pcDNA3 with Meq insertion between *Hind*III and *Xho*I restriction sites	This work
pCeMM-CTAP(SG)	Eucharіotic expression vector; hCMV prom, ColE1 ori, AmpR, 5' LTR, IRES eGFP, CTAP	Bürckstümmer et al (18)
pCeMM-USP.CTAP	Insertion of USP sequence in pCeMM-CTAP vector using *Pme*I restriction site	This work

pGBKT7	Y2H bait expression vector; GAL4 DNA-binding domain, T7 prom, ADH1 prom, ADH1 term, TRP1 prom, f1 ori, 2μ ori, KanaR, NeoR	Clontech
pCAGGS-NLS/Cre	Bacteriophage P1 *CRE* gene for recombinase PR1 and PR2 promoter, CRE expression, AmpR, PuroR	Sternberg et al, (148)
pEP Kan-S	Mamalian expression vector; T7prom, f1 ori, SV40 ori, SV40 pr ,KanR, I-Sce-I restricion site, AmpR, ColE1 ori, NeoR	Tischer et al (150, 151)
pGA4	Bacterial expression vector; T7prom, f1ori,AmpR, Col E1 origin, *LacZ*prom	Geneart
pGA4-SynUSP.HA	pGA4 expressing codon-optimized SynUSP with C-terminal HA tag ; insertion between *Kpn*I and *Not*I restriction sites.	Geneart
pSynUSP.HA	Transfer vector based on pGA4-SynUSP.HA; *aphAI* and Sce-I inserted into SynUSP *Bg*lII restriction site	Dr. Keith Jarosinski (not published)
IRES-pSynUSP.HA	Insertion of IRES sequence at the N-terminus of SynUSP at *Eco*RV restriction site in pSynUSP.HA background	This work
pEP-eGFPin	*aphAI* gene insertion in eGFP; transfer construct for eGFP insertion during two-Red mutagenesis; AmpR	Tischer et al (95, 151), Brazeau et al (64)
pGex-6p-1	*E. coli* (*BL21*) expression vector; ptac, pBR322 ori, lac I q, AmpR, GST, PreScission_EK	GE Healthcare
pMDV USP	pGex-6p-1 with USP insertion between *BamHI* and *NotI* sites ; *aphAI* inserted into USP *EcoRI* restriction site	This work
pUC19	*E.coli* cloning vector; AmpR, ColE1 ori	New England Biolabs
pUC19-ICP4.eGFP	pUC19+insertion of ICP4.eGFP	Dr .Matthias Sieber/ Dr. Dušan Kunec (not published)
pICP4-SynUSP.aphAI	pUC19-HVT.ICP4.eGFP plus insertion of SynUSP-*aphAI* from pGA4-SynUSP-aphAI and inserted in *Not*I and *Eco*RI restriction sites (inserted by inverted PCR)	This work

Table 5. Plasmids used throughout this project.

7.1.5.2 BACs

A schematic representation of all clones can be found in the supplementary information, section 1, page 95.

BAC	Features	Reference
rRB-1B	Created from the MDV VV strain RB-1B	Petherbridge et al (124); spread competence restored by Jarosinski et al (67)
rBAC20	Created from avirulent strain 584Ap80C	Schumacher et al (142)
rΔUSP	Removal of the UL36 gene N-terminal 966 bp corresponding to MDV USP in the rRB-1B background	This work
rΔUSP-rev	Reinsertion of the UL36 gene MDV USP in the rΔUSP background by using pMDV USP as transfer plasmid	This work
rC98A	pRB-1B with cysteine to alanine mutation in position 98 of the UL36 gene	Jarosinski et al (66)
rC98A-SynUSP.HA	Insertion of synthetic codon-optimised HA-tagged gene (SynUSP.HA) upstream from UL36 gene, ectopically expressed but under same promoter. pSynUSP.HA used as transfer plasmid	Dr. Keith Jarosinski (not published)
rSynUSP.HAind	Removal of N-terminal 966bp MDV USP; independent expression of SynUSP.HA	Dr. Keith Jarosinski (not published)
rSynUSP.ind	Removal of HA tag from rSynUSP.HAind	This work
rSynUSP.HAlink	Removal of N-terminal 966bp MDV USP; linked expression of SynUSP.HA	Dr. Keith Jarosinski (not published)
rC98A- IRES SynUSP	Introduction of IRES.SynUSP in the C98A mutant at the C-terminus of UL36 using IRES-pSynUSP.HA as transfer plasmid	This work
rΔUSP- IRES SynUSP	Introduction of IRES.SynUSP in the ΔUSP mutant at the C-terminus of UL36 using IRES-pSynUSP.HA as transfer plasmid	This work
rC98A-SynUSP .Mini-F	Insertion of HVT.ICP4:SynUSP as replacement of xgpt region in the Mini-F sequence in the rC98A background. pICP4-SynUSP.*aphAI* used as transfer plasmid	This work

r ΔUSP-SynUSP .Mini-F	Insertion of HVT.ICP4:SynUSP as replacement of xgpt region in the Mini-F sequence in the rΔUSP background. pICP4-SynUSP.*aphAI* used as transfer plasmid	This work
rSynUSP.link	Removal of HA tag from rSynUSP.HAlink	This work
rSynUSP.link- rev	Reinsertion of viral USP sequence in the rSynUSPlink background	This work
rC98A-IRES.eGFP	Replacement of SynUSP by eGFP in rC98A-IRES.SynUSP using pEP-EGFPin as transfer plasmid	This work
rΔCysBox	Deletion of cysteine box in rRB-1B	This work
rΔCysBox-rev	Reinsertion of the cysteine box into rΔCys Box by using pMDV USP as transfer plasmid	This work

Table 6. MDV recombinants assembled throughout the project and respective parental bacterial artificial chromosomes.

7.1.6 Primers

Used primers were ordered from IDT, in the case of the long primers used for two-step Red-mediated recombination, whereas the primers used for sequencing, transfer plasmid and eucharyotic expression constructs assembly were ordered from Biomers and Metabion. All primers were designed by using Vector NTI 9.1 software from Invitrogen. DNA of plasmids and BACs indicated in the previous sections were used as templates. Sequencing of all clones (whole plasmid or PCR amplification of the mutated sequence, in the case of rMDVs) was performed both by LGC Genomics, Berlin and Starseq, Mainz.

Construct	**Direction**[a]	**Sequence (5´- 3´)**[b]
1.Constructs sequencing (not including T7, BGH, M13 forward and reverse):		
MDVUSP seq/ SynUSP seq	Forward	GTAGGAGCATCATTATACGAAAGAT
	Reverse	CGACGCATATTTTCAATCAT
SynUSP seq (internal)	Forward	GTAGGTGCCGTCCTCGCTTGTGGCG
	Reverse	CGCCACAAGCGAGGACGGCACCTAC
MDV USP seq (internal)	Forward	CTCAACGAGCTGCTTGATCC
	Reverse	GGCATATAGGACAGGCATGTATAG

IRES-pSynUSP.HA seq	Forward	TTTCCCAGTCACGACGTTGTAAAAC
	Reverse	CTTGTGGTCCTGCTGTACTTCCTGC
IRES.SynUSP/ eGFP BAC seq	Forward	TCGACGTCATAATAAAGTACAACAA
	Reverse	AGGGAACAACTGAGAACTAAAGTTG
IRES.SynUSP BAC seq (internal)	Forward	TCCTGCTGTACTTCCTGCAGTTGGT
	Reverse	ACCAACTGCAGGAAGTACAGCAGGA
Mini-F ICP4.SynUSP BAC insertion seq	Forward	GCCCAGCGTCTTGTCATT
	Reverse	GTTGCTACGCCTGAATAAG
Mini-F ICP4.SynUSP BAC insertion seq (internal)	Forward	TCGACGTCATAATAAAGTACAACAA
	Reverse	AGGGAACAACTGAGAACTAAAGTTG
2.Transfer plasmid generation		
pSynUSP.HA	Forward	CGAGCAGATCTGGAAGAAGAAGAGGGGCGACGTCTACTGC CTATCGTGGTAGGGATAACAGGGTAATCGATTT (*Bgl*II)
	Reverse	TGCACGAGATCTGCCAGTGTTACAACCAATTAACC (*Bgl*II)
IRES pSynUSP.HA	Forward	AAAAAGATATCCCGCCCCTCTCCCTCCCCC (*Eco*RV)
	Reverse	TTTTTGATATCGTTGTGGCCATATTATCAT (*Eco*RV)
pMDV USP	Forward	TTTTTGAATTCTATCTAGAAGAAAACACGCCCACTATAGGGA TAACAGGGTAATCGATTTA (*Eco*RI)
	Reverse	AAAAAGAATTCAAACTCCCCATATGAACTCGAAAATGCCAGT GTTACAACCAATTAACCAA (*Eco*RI)
pICP4-SynUSP.aphAI (plasmid)	Forward	ATATAGAATTCCTGCGGGAAATGGCAAAGG (*Eco*RI)
	Reverse	GAGACTGAATTCCTGCGGGAAATGGCA
pICP4-SynUSP.aphAI	Forward	ATATAGAATTCGCCACCATGACCGA (*Eco*RI)
	Reverse	ATATATGCGGCCGCTCATCAGTCGGCGGACACCACC (*Not*I)
3. Eukaryotic expression construct		
pcDNA3-HA. USP	Forward	AAAAAGCTTCCACCATG**TACCCATACGACGTCCCAGACTA CGCT**ACAGATTCTACTGACAGCAGACAAGC (*Hind*III)
	Reverse	TTTCTCGAGTCAATCAAAATCTGCCGACACTACTTTAC(*Xho*I)

pcDNA3-USP.HA	Forward	AAAAAGCTTCCACCATGACAGATTCTACTGACAGCAGAC (HindIII)
	Reverse	TTTCTCGAGTCA**AGCGTAGTCTGGGACGTCGTATGGGTA**A TCAAAATCTGCCGACACTACTTTAC (*Xho*I)
pcDNA3-Meq	Forward	TTTTAAGCTTATGTCTCAGGAGCCAGAGCCGG (*Hind*III)
	Reverse	TTTTCTCGAGTCAGGGTCTCCCGTCACCTGGAAAC (*Xho*I)
pCeMM-USP.CTAP	Forward	AAATTGTTTAAACATGACAGATTCTACTGACAGC (*Pme*I)
	Reverse	TTTAAGTTTAAACTCAAAATCTGCCGACACTAC (*Pme*I)
UL36I SC1	Forward	TTTTTCCCGGGAATGACAGATTCTACTGACAG (*Sma*I)
	Reverse	CCCGGGCTA ATCAAAATCTGCCGACACTACTTT (*Sma*I)
UL36I SC2	Forward	TTTTTCCCGGGAATGACAGATTCTACTGACAG (*Sma*I)
	Reverse	CCCGGGCTATCTCGAGTGTTTCCTGCTCAACGA (*Sma*I)
UL36I SC3	Forward	TTTTTCCCGGGAATGTCATCGTTGGCATTTCTTCGTATA (*Sma*I)
	Reverse	CCCGGGCTAATCTGACGATTCTGTAGAAGTGAC (*Sma*I)
UL36I SC4	Forward	TTTTTCCCGGGAATGCTTGACGATACCCATAGCACTATT (*Sma*I)
	Reverse	CCCGGGCTACCTTTCTATAAGGTCTATAGATTCAGATGC (*Sma*I)
UL36I SC5	Forward	TTTTTCCCGGGAATGTTATGGACACCACAATCAAGTTCG (*Sma*I)
	Reverse	CCCGGGCTACCTTTCTATAAGGTCTATAGATTCAGATGC (*Sma*I)
4.Two-step Red mediated recombination:		
rΔUSP	Forward	TGACAAGTTTGGTTAATCTCGGTTGTGGCCTAGAAGGCGGC ATTTTACACTCAATTTATATAGGGATAACAGGGTAATCG
	Reverse	TCGACGCATATTTTCAATCATATAAATTGAGTGTAAAATGCC GCCTTCTAGGCCACAACCGCCAGTGTTACAACCAATTA
rΔUSP-rev	Forward	TGACAAGTTTGGTTAATCTCGGTTGTGGCCTAGAAGGCGGA TCAAAATCTGCCGACACTA
	Reverse	TCGACGCATATTTTCAATCATATAAATTGAGTGTAAAATGAC AGATTCTACTGACAGCAG
rC98A-SynUSP.HA	Forward	GAGCTTATGTCGTTTCGACGCATATTTTCAATCATATAAATT GAGTGTAAGCCACCATGACCGACAGCAC
	Reverse	ATTTCCTGCAATTTGTAGTAGCTTGTCTGCTGTCAGTAGAAT CTGTCATTTCATCAGGCGTAGTCGGGCA
rΔUSP/C98A-IRES.SynUSP	Forward	TTTAAACAGTATACCGACACCTAATTCCATTCTTTTTTATTCA GTCGGCGGACACCACC

	Reverse	AATAGAGCTTTTCAAAATTAAAATGATCCTGACTGGATAACC GCCCCTCTCCCTCC
rC98A-IRES.eGFP	Forward	AAACAGTATACCGACACCTAATTCCATTCTTTTTTATTCACTT GTACAGCTCGTCCATGC
	Reverse	TGAAAAACACGATGATAATATGGCCACAACGATCGCCACCA TGGTGAGCAAGGGCGAGGAGCT
rSynUSP.HAind	Forward	TTTGGTTAATCTCGGTTGTGGCCTAGAAGGCGGATCAAA**CA TTTCATCA**GGCGTAGTCGGGCATAGGGATAACAGGGTAAT CGATTT
	Reverse	AGGTGGTGTCCGCCGACTACCCCTACGACGTGCCCGACTA CGCCTGATGAAATGTTTGATCCGCCTTCTAGGCGCCAGTGT TACAACCAATTAACC
rSynUSP.HAlink	Forward	TTTGGTTAATCTCGGTTGTGGCCTAGAAGGCGGATCAAAGG CGTAGTCGGGCACGTCGTAGGGATAACAGGGTAATCGATT
	Reverse	AGGTGGTGTCCGCCGACTACCCCTACGACGTGCCCGACTA CGCCTTTGATCCGCCTTCTAGGCGCCAGTGTTACAACCAAT TAACC
rC98A/ ΔUSP-SynUSP.Mini-F	Forward	ATTAAGGTGACACGCGCGGCCTCGAACACAGCTGCAGGCC TTCCCACAATCGCGAGGTCC
	Reverse	TAACGTCGACCCGGGTACCTCTAGATCCGCTAGCGCTTTAT CATCAGTCGGCGGACACCA
rSynUSP.ind	Forward	TCTCGGTTGTGGCCTAGAAGGCGGATCAAACATTTCATCAG TCGGCGGACACCACCTTGCTAGGGATAACAGGGTAATCG
	Reverse	GGCCAGGGAAGAGGACAACCGCAAGGTGGTGTCCGCCGA CTGATGAAATGTTTGATCCGCGCCAGTGTTACAACCAATTA
rSynUSP.link	Forward	GTTTGGTTAATCTCGGTTGTGGCCTAGAAGGCGGATCAAAG TCGCGGACACCACCTTGCTAGGGATAACAGGGTAATCGATT
	Reverse	GGCCAGGGAAGAGGACAACCGCAAGGTGGTGTCCGCCGA CTTGATCCGCCTTCTAGGCCGCCAGTGTTACAACCAATTAA CC
rSynUSP.link-rev	Forward	GTTTGGTTAATCTCGGTTGTGGCCTAGAAGGCGGATCAAAA TCTGCCGACACTACTTTAC
	Reverse	GACGCATATTTTCAATCATATAAATTGAGTGTAACCACCATG ACAGATTCTACTGACAG
rΔCysBox	Forward	ATGATATGACTGTATCTAATCCATACGCAAAAACTATACGGT TTCTAATACCAACCGCCATAGGGATAACAGGGTAATCG
	Reverse	TACGACTGATGTAACGGTAGTGGCGGTTGGTATTAGAAACC GTATAGTTTTTGCGTATGGGCCAGTGTTACAACCAATTA
rΔCysBox-rev	Forward	CACTTACACGGACTATACATGCCTG

	Reverse	ATGACAGATTCTACTGACAGCAGAC

Table 7. Primers used for transfer plasmid generation, eukaryotic expression, sequencing and two-step Red mediated recombination. [a] stands for directionality of the primer; [b] In the second table set (7.2), enzymatic cleavage sites used for cloning are indicated in brackets and underlined in the primer sequence; also, I-SceI restriction site in pSynUSP.HA primers and pEPkan-S binding sites in pMDV USP primers are underlined. In the third table set (7.3), restriction sites are also underlined and indicated in brackets, whereas the HA tags from pcDNA3-HA.USP and pCDNA3-USP.HA are indicated in bold. In the fourth table set (7.4), underlined nucleotides indicate pEPkanS1 binding sites, whereas bold stands for 2x STOP codon plus methionine insertion in rSynUSP.HAind.

7.1.7 Antibodies

7.1.7.1 Primary antibodies

Primary antibodies (abs) for IF were diluted in PBS+3% FCS. For WB, dilutions were made either in PBS+0,1% Tween-20 (PBST)+5% non-fat dry milk (NFDM)+0,02% NaN_3. Addition of sodium azide at a final concentration of 0,02% allows storage at 4°C and multiple usages.

Antibody	Company/Provider	Dilution WB	Dilution IF
Chicken serum anti-MDV	Jarosinski et al, 2005 (69)		1:2500
Rabbit anti-USP-1	Genscript	1:50	
Rabbit anti-HA (ab9110)	Abcam	1:1000	1:100
Rabbit anti-6xHis (ab 1187)	Abcam	1:2000	
Rabbit anti-Meq	Brown et al, 2009 (16)	1:3000	1:3000
Rabbit anti-eGFP (600-401-215)	Rockland	1:2000	

Table 8. Primary antibodies used for IF and WB, with respective dilutions.

7.1.7.2 Secondary antibodies

Secondary abs for IF were diluted PBS+3% FCS, whereas for WB the dilutions were done in PBST+5% NFDM, depending on the solution used for dilution of the primary ab. In both cases solutions were discarded after usage.

Antibody	Company	Dilution
IF		
Alexa Fluor 488 goat anti-chicken IgG (H+L) A11040	Invitrogen	1:500
Alexa Fluor 568 goat anti-chicken IgG (H+L) A11039	Invitrogen	1:500
Alexa Fluor 568 Goat Anti-Mouse IgG (H+L) A11004	Invitrogen	1:5000
Goat anti-rabbit IgG Florescein FITC Conjugate	Southern Biotech	1:5000
WB		
Goat anti-rabbit IgG Fc-HRP 4041-05	Southern Biotech	1:10000
Goat Anti-Mouse IgG (Fab specific)–Peroxidase antibody A9917-1ML	Sigma-Aldrich	1:5000

Table 9. Secondary antibodies used for IF and WB.

7.2 Methods

7.2.1 Basic molecular biology techniques

7.2.1.1 Plasmid and bacterial artificial chromosomes (BACs) preparation

7.2.1.1.1 Modified alkaline lysis at small scale

Plasmid purification was performed as previously described (132). Bacterial cultures (2-5 ml) were grown in LB media with appropriate antibiotics overnight (O/N) at 32°C (BACs) or 37°C (plasmids) in an incubator shaker at 220 rpm. Bacteria were pelleted at maximal speed in an Eppendorf 5424 centrifuge and resuspended in 300 µl buffer P1 (resuspension buffer, 50 mM tris, 10 mM EDTA pH 8,0) by vigorous vortexing. Then, 300 µl buffer P2 (lysis buffer, 0,2 M NaOH, 1% SDS) were added for alkaline cell lysis and incubated at room temperature (RT) for 5 minutes (min). After neutralization of the mixture by adding 300 µl of buffer P3 (neutralization buffer, 3 M potassium acetate, pH 5,5) to lysed bacteria and incubation for 5 min on ice, samples were centrifuged at 20,000xg for 5 min to remove cellular debris. The supernatant was transferred to a new tube to which 900 µl of Tris-buffered phenol/chloroform were added, followed by vortexing and centrifugation at 20,000xg for 10 min. The upper liquid phase was transferred to a new tube (using cut tips for BAC DNA) and 480 µl 100% isopropanol was added and mixed by inversion, followed by centrifugation at 20,000xg for 30 min to precipitate DNA. The DNA pellet obtained was washed twice with 70% ice-cold ethanol and dried at RT. Finally, the pellet was resuspended in 50 µl TE-RNAse A and incubated for 30 min at 37°C. DNA was either stored at 4 or -20°C until further use. For plasmid DNA transfection, which requires higher DNA purity, samples were prepared with QIAprep Spin Miniprep Kit according to manufacturer´s instructions.

7.2.1.1.2 Medium scale preparation (“Midiprep”)

For plasmid or BAC DNA preparation at larger scale and purity, the Plasmid Midi Kit (Qiagen) was used according to the manufacturer´s instructions. The “high copy protocol” was used for plasmids, whereas the “very low copy protocol” was used for BAC DNA.

7.2.1.2 Polymerase-chain reaction (PCR)

All PCR reactions for cloning, two-step Red mediated recombination and sequencing were performed using Phusion Hot Start High-Fidelity from Fynnzymes. For colony PCR and other diagnostic PCR assays, Peqlab's Taq polymerase was used. In both cases, the manufacturer's instructions were followed.

Double strand denaturation took place at 98°C for Phusion and 94ºC for Taq polymerase. Temperature profiles used for the annealing process varied on the enzyme and primers used; for Phusion PCR, the primer annealing temperature was first determined in Fynnzymes T_m calculator (http://www.finnzymes.fi/tm_determination.html) and the annealing temperature was determined by adding 3ºC to lower primer T_m; for Taq polymerase, annealing temperature corresponded to 5°C below melting point of the lowest T_m primer. The elongation time varied according to the polymerase used in terms of temperature and on the length of the DNA fragment to be amplified. For Phusion, elongation took place at 72ºC for 15 to 30 seconds (sec) per 1 Kb, whereas for Taq polymerase 1 Kb of target DNA is amplified every minute at 72ºC. These steps were repeated 25 to 35 times.

7.2.1.3 Cloning

All PCR products used for cloning were column purified using Hi Yield Gel/PCR DNA Fragments Extraction Kit from SLG according to the manufacturer's instructions and final concentrations of prepared DNA were measured with the Nanodrop instrument from Peqlab. Digestion of insert and plasmids was performed for 1 hour (h) with the appropriate enzyme(s) with the manufacturer's recommended buffer(s) and at the indicated temperature(s). Primers used for both transfer plasmid assembly and eukaryotic expression vectors are described in Table 7.2 and 7.3.

For pSynUSP.HA generation, the *aphAI* kanamycin resistance gene and an I-SceI restriction site were amplified from pEPKan-S plasmid (components of the kanamycin cassette) and inserted into the unique *Bgl*II site of pGA4-SynUSP.HA after dephosphorylation with 1 µl calf intestinal phosphatase (CIP) for 1 h at 37ºC. The same procedure was followed for generation of MDV USP transfer plasmid, pMDV USP; in this case, the kanamycin cassette was inserted into the unique *Eco*RI restriction site of a previously assembled pGex-6p-1-MDV USP plasmid.

For IRES-pSynUSP.HA transfer plasmid generation, an internal ribosome entry site (IRES) sequence was inserted upstream of SynUSP.HA in pSynUSP.HA by making use of the single *Kpn*I restriction site. In this case, and due to the fact that there is a *Kpn*I restriction site in the IRES sequence, blunting with T4 polymerase and dephosphorylation with Antarctic Phosphatase were performed, to allow the insertion of the IRES sequence, previously digested with blunt-cutting enzyme *Eco*RV.

For pICP4-SynUSP.*aphAI* generation, pUC19-ICP4-eGFP was amplified via inverse PCR in order to introduce restriction sites *Not*I and *Eco*RI, which were necessary for the cloning strategy without including the eGFP sequence. SynUSP+a*phAI* was amplified from pSynUSP.HA and ligated to inverse pUC19-ICP4, so that SynUSP+*aphAI* would be located immediately downstream from HVT ICP4 promoter. This HVT promoter was chosen in order to avoid homologous recombination with MDV ICP4 during the mutagenesis process.

For pcDNA3-HA.USP and pcDNA3-USP.HA generation, the N- and C-terminal HA tag were amplified by PCR together with the 322 N-terminal aa from rRB-1B BAC, using *Hind*III and *Xho*I restriction sites from pCDNA3 for insertion. For pcDNA3-Meq generation, the Meq sequence was amplified with specific primers from the rRB-1B BAC and cloned into pcDNA3 using same enzymes as above described.

For pCeMM.USP.CTAP generation, the 322 N-terminal aa from rRB-1B BAC were amplified and cloned into pCeMM-CTAP SG by using *Pme*I. Plasmid dephosphorylation was performed with 1 µl CIP for 1 h at 37ºC prior to ligation.

For pGBKT7 UL36I subclones generation, *Sma*I was used for digest of all inserts and plasmid at 25°C for 1 h; the plasmid was then dephopsphorylated for 1 h at 37°C with 1 µl CIP.

Digested inserts and vectors were separated on a 1% agarose gel at 100 volts for 30 min and gel-purified using the Hi Yield Gel/PCR DNA Fragments Extraction Kit from SLG according to the manufacturer's instructions. Insert and vector were added to the ligation mix in a 3:1 ratio using 50 ng vector as the constant. Ligations were either performed by using T4 ligase or quick ligase, according to the availability of the enzymes in stock. In the case of the T4 ligase, the ligation mix was prepared by using 1x ligase buffer,1 µl ligase and digested and purified insert and vector at a 3:1 ratio; the ligation mix was incubated O/N at 16°C. In the case of quick ligase, 2x quick ligase buffer was added to 1 µl ligase and the same proportion of insert and vector previously mentioned; incubation took place for 10 min at 25°C.

7.2.1.4 Plasmid transfection with PEI and lipofectamine

After testing by digestion and sequencing, high-quality plasmid DNA was transfected into DF-1 or 293T cells by using either the lipofectamine transfection reagent from Invitrogen or PEI reagent from Polysciences.

For lipofectamine transfection of $1,0x10^6$ cells, the manufacturer's instructions were followed. Briefly, 1 µg DNA was diluted in 100 µl Opti-MEM medium and incubated for 5 min prior to the addition 3 µl of lipofectamine reagent. After a 20 min incubation, the transfection mix was added dropwise to cells seeded into into one well of a 6-well plate the previous day.

For PEI transfection of $1,0x10^6$ cells, 1 µg DNA was diluted in 100 µl Opti-MEM and incubated for 5 min prior to the addition 10 µl of PEI reagent (1 mg/ml). After a 20 minute incubation, the transfection mix was added dropwise to cells seeded into one well of a 6-well plate the previous day.

7.2.2 Culture of *Escherichia coli* bacteria (*E. coli*)

7.2.2.1 Preparation of chemically competent cells with calcium chloride ($CaCl_2$)

For preparation of chemically competent cells, a single colony of *E. coli* (TOP10, XL1-blue, DH10B) previously plated on LB agar plates without antibiotics was grown shaking O/N in 5 ml LB medium at 37°C at 220 rpm in a shaking incubator. The following day, 1 ml of the O/N culture was inoculated into 100 ml LB in a 500 ml Erlenmeyer flask and grown at 37°C until a logarithmic growth of 0,45-0,6 $O.D._{600}$ was reached. After transfer of the culture to 50 ml pre-chilled polypropylene tubes and incubation for 5-10 min on ice, the bacteria were pelleted for 2 min at 1,000xg at 4°C and resuspended in 10 ml ice-cold 50 mM $CaCl_2$. After a second centrifugation step at 600xg for 10 min at 4°C, the supernatant was discarded and each pellet was resuspended in 10 ml ice-cold 50 mM $CaCl_2$ and incubated on ice for 30 min. After a last centrifugation at 400xg for 5 min at 4°C, the supernatant was discarded and each pellet was resuspended in 2 ml ice-cold 100 mM $CaCl_2$+15% sterile glycerol. One-hundred microliters of cells were aliquoted into pre-chilled Eppendorf tubes and bacteria were either promptly used or frozen at -80°C immediately for later use.

7.2.2.2 Transformation of chemically competent cells

Ligation mix was added to chemically competent bacteria. After 30 min incubation on ice, a 45 sec heat shock was performed in a water bath at 42°C, followed by a short (~2 min) incubation on ice. Bacteria were then grown in 1 ml SOC medium for 1 h at 37°C and plated on LB plates with the appropriate antibiotics, after centrifugation for 2 min at 2,500xg and incubation O/N at 37°C. The following day, individual colonies were replica-plated onto a master plate and inoculated into a LB broth culture for screening purposes; DNA alkaline lysis from O/N cultures was performed and DNA was digested with appropriate enzymes to check for correctness of the clones. Clones presenting the expected restriction digest pattern were sequenced with appropriate primers and 20% glycerol stocks were prepared for long-term storage at -80ºC.

7.2.2.3 Immunofluorescence procedures using coverslips

Transfected 293T cells grown in 24-wells were fixed with PFA 2% for 20 min at RT and then permeabilized with PBS 0,1% Triton X 100 for 5 min. After blocking for 30 min with 3% fetal calf serum (FCS) in PBS, samples were incubated for 1 h with primary antibody (ab) diluted in blocking buffer, washed three times for 5 min with PBS, incubated with appropriate secondary ab also diluted in the blocking solution for 1 h and washed again three times for 5 min with PBS. Coverslips were then carefully removed from 24-well and placed in slides with one drop of mounting media. After letting coverslips dry, samples were observed at the microscope.

7.2.3 Culture of eukaryotic cells

All cell types used in this project were grown at 37°C and under 5% CO_2 atmosphere. Chicken embryo cells (CECs) were freshly prepared in the beginning of every week from 10-day old specific-pathogen-free (SPF) VALO embryos using a standard protocol (136). Chicken kidney cells (CKCs) were used for some experiments where cells were freshly prepared from SPF P2 chicken kidneys, using standard protocols (136). Both primary chicken cells were kept at MEM 5% FCS with 1% penicillin/streptomycin (P/S). The continuous chicken cell line DF-1 were grown in DMEM with 10% FCS, 1% L-alalyl-L-Glutamine, 2 mM sodium pyruvate and 1% P/S, whereas 293T cells were grown in MEM with 10% FCS and 1% P/S.

Confluent monolayers were passaged after 1x PBS wash and detached with 0,05% trypsin-EDTA. Trypsin was inactivated by adding 5% FCS in growth media to detached cells, then cells were either split or seeded for further passaging or frozen in 1,8 ml cryotubes with 8% DMSO.

7.2.4 Construction of recombinant MDVs

7.2.4.1 BAC technology: a brief introduction

The first BACs were established in 1992 by cloning and propagation of a human gene in the single-copy *E. coli* F-plasmid (143), a procedure that allowed significant progress in genome sequencing projects (151). Since then, BACs have become an extremely valuable tool, allowing insertions of up to 300 Kb DNA, which can be stably propagated using the *E. coli* replication machinery (85). In 1997, a viral genome of MCMV was cloned for the first time into a BAC, stably propagated and importantly, infectious progeny was produced following reintroduction of cloned DNA in eurkaryotic cells (98). Whole genome cloning into BACs can be used for several purposes, such as recombinant vaccine development.

7.2.4.2 Red mutagenesis

In 1998, it was shown for the first time that it is possible to carry out mutations within BAC sequences by taking advantage of the *E. coli*-encoded Rec ET recombination proteins. This allowed the insertion of mutations within the BAC by including homologous sequences flanking the ends of the DNA to be mutated in a PCR product (85, 162). However, the *E. coli*-expressed intracellular Rec B/C/D exonuclease system, responsible for foreign DNA degradation, made the insertion of foreign DNA into BAC sequences difficult to achieve. Therefore, the discovery of the more efficient Red recombination system, based on the expression of a defective λ prophage within the same BAC carrier bacteria, constituted a important yet simple improvement, which allows linear DNA electroporation into bacteria and its maintenance within the bacteria prior to recombination occurrence (160). This system works through expression of phage “protector” *exo*, *bet* and *gam* genes (108, 150, 161), under a temperature-sensitive λ cI-repressor which is activated by temperature shift to 42°C for 15-30 min and inactived at 32°C (85). *Gam* inhibits RecB/C/D exonucleases responsible for linear DNA destruction (131), while the products of the *exo* and *beta* genes allow recombination of homologous sequences with the specific BAC genome (85). Integration of

the PCR product into the target sequences is mediated through homology between 30 to 50 bp-long PCR 5' ends and the borders of the region to be mutated (150). Selection of positive integrates is usually performed through selection markers, typically antibiotic resistance genes like *aphA*I, which confers resistance to kanamycin, although other positive selection markers, such as beta lactamases, which confer resistance to β-lactam antibiotics, can also be used (117).

7.2.4.3 Two-step Red mediated recombination or "en passant" mutagenesis

Based on the previously described Red recombination procedure, the two-step Red mediate recombination allows the insertion of PCR products by electroporation of the desired mutation, together with the positive selection marker a*phAI* kanamycin resistance gene, into the bacteria and integration into the BAC DNA, This is the first step in the two-step Red recombination technique, or "co-integration". In the second step or "resolution", complete removal of the kanamycin cassette is performed. Each PCR product also encodes a unique I-SceI restriction site that can be used to cleave the integrated sequences by *E. coli* expressing the endonuclease I-SceI. This enzyme has a 18 bp recognition site, which is rarely found in genomic sequences (28, 150). Both steps take place in GS1783 *E. coli* that carry the BAC DNA, the defective λ phage Rec system and I-SceI under L-arabinose induction (151).

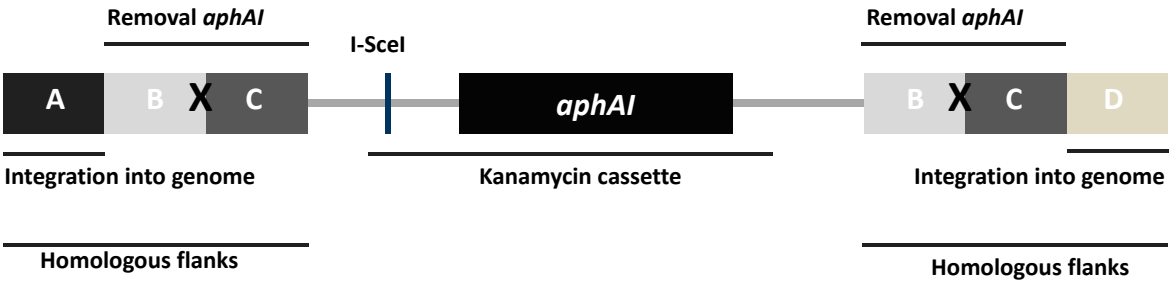

Figure 10. En passant mutagenesis PCR product amplified from pEPKan-S for deletions and insertion of point mutations and short sequences (e.g. tags) into the genome. Symbol X indicates possible location for introduction of point mutations and short sequences. The regions A and D, located at both extremities of the PCR product, allow integration of electroporated PCR product into the genome's desired locus, whereas the duplicated sequences B and C that allow *aphAI* removal recombine upon I-SceI cleavage during resolution, thus allowing complete removal of the kanamycin cassette.

The PCR products electroporated (Figure 10) in competent bacteria contain homologous flanks needed for integration into the BAC DNA, the above described kanamycin cassette with an I-SceI restriction site, and duplicated homologous sequences within the PCR product that allows the complete removal of the kanamycin cassette during the second Red recombination step.

The pEP Kan-S plasmid (150, 151) is the standard template for PCR product amplification for the generation of deletions and insertions of point mutations and short sequences (e.g.: tags). The full procedure is shown in Figure 11.

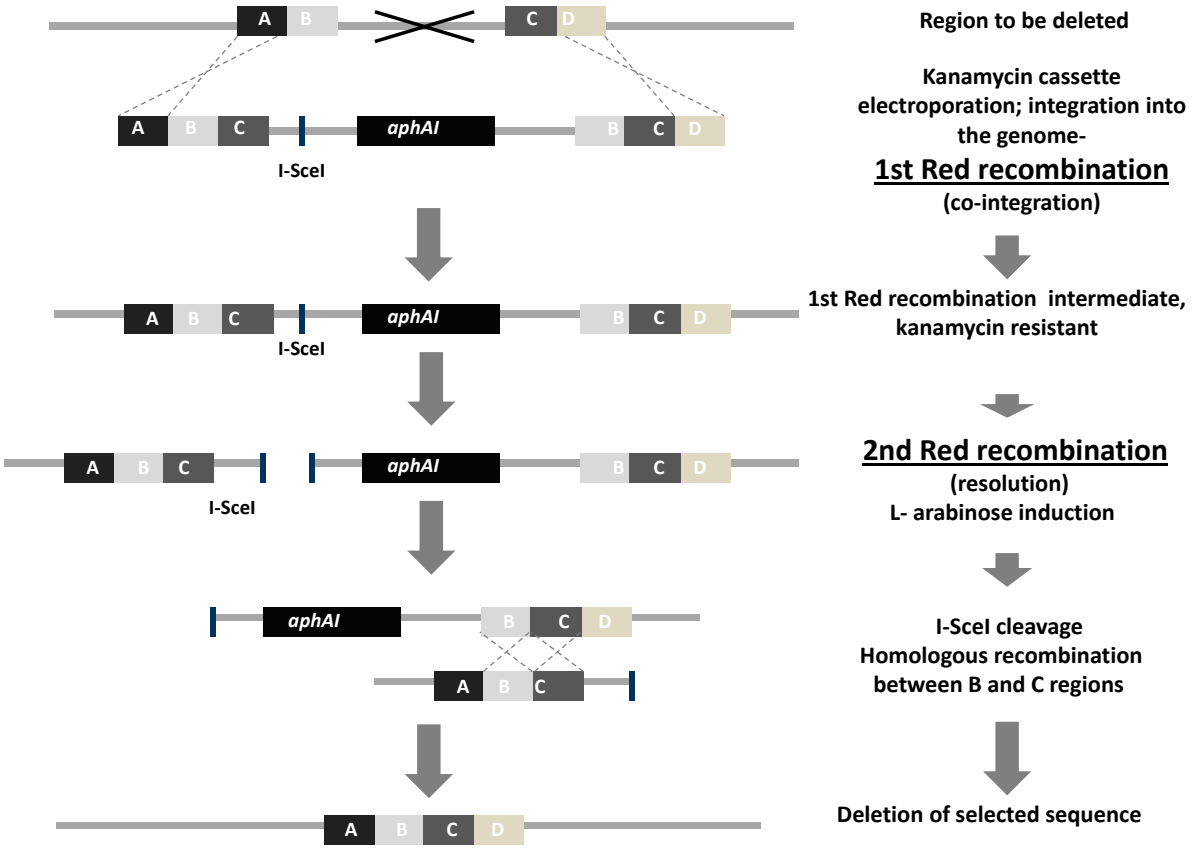

Figure 11. Schematic representation of the two-step Red mediated recombination protocol for deletion of selected sequences. Homologous flanks A and D allow the integration of the kanamycin cassette into the correct locus during the first Red recombination step or co-integration. After I-SceI induction with L-arabinose and incubation at 42ºC, the second recombination or resolution step occurs, resulting in recombination between the homologous sequences B and C; the kanamycin cassette is then removed. Figure adapted from Tischer et al. (151) and Osterrieder et al. (116).

For insertion of long sequences into the viral genome, an intermediate construct (transfer plasmid) must be assembled. This construct expresses the kanamycin cassette flanked by duplicated sequences of around 40 bp that are cloned into a unique restriction site within the sequence. Once standard cloning is performed and checked by sequencing, the PCR product used for recombination is amplified and electroporated into BAC-containing *E. coli*; the mutagenesis protocol is otherwise identical, as shown in Figure 12.

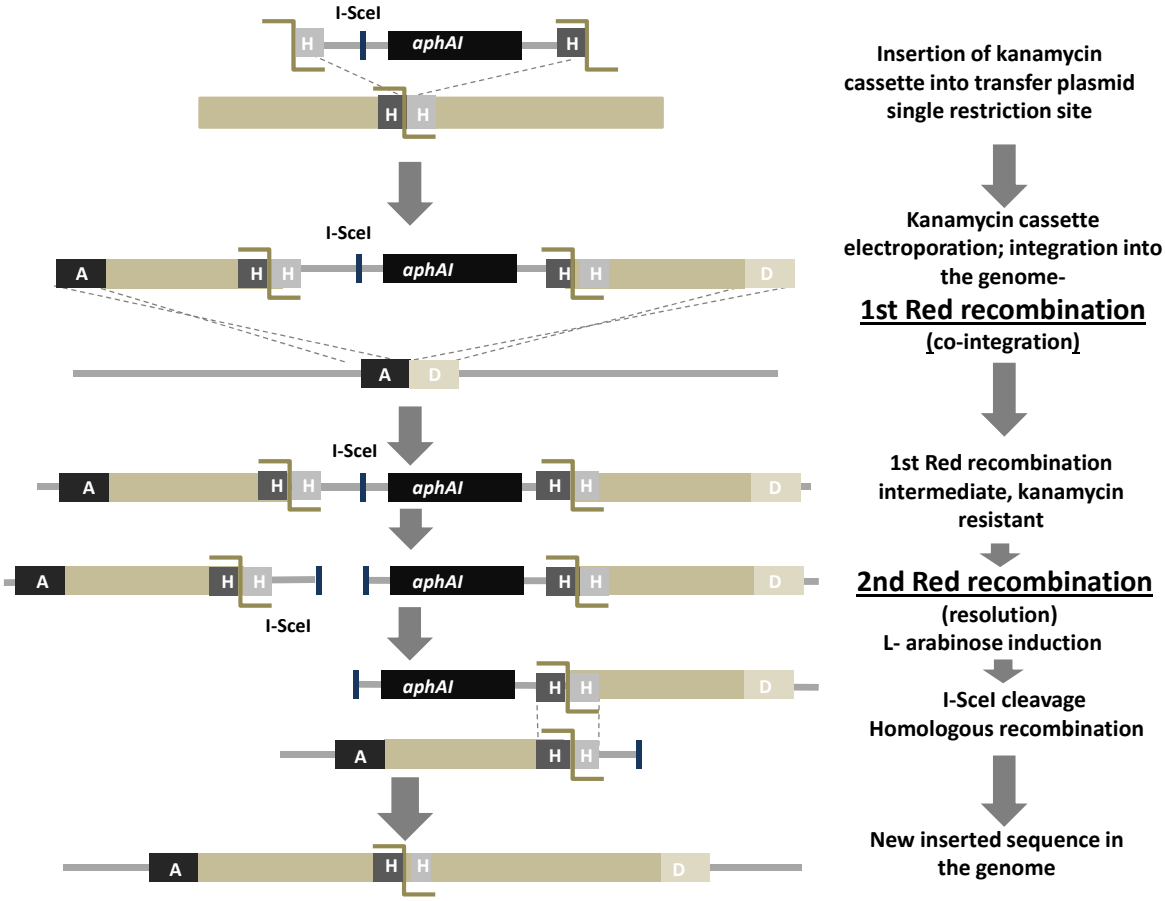

Figure 12. Schematic representation of the two-step Red mediated recombination procedure for insertion of long sequences into the viral genome. First, the kanamycin cassette with homologous sites (H) is cloned into the single restriction site of the sequence to be inserted, previously cloned into a plasmid. After PCR amplification with primers that add homologous flanks A and D, the first recombination step is performed in which the PCR product is integrated into the genome. The following process, resolution, is identical to what was previously described for sequence deletion. Figure adapted from Tischer et al (151).

7.2.4.4 En passant mutagenesis protocol

The following protocol was adapted from several references (67, 85, 150). First, a BAC-carrying GS1783 colony grown at 32ºC O/N in LB+CAM was resuspended in a small amount of LB+CAM (2-5 ml) and grown at 32°C O/N. The following day, 2-5 ml of fresh LB+CAM media was inoculated with 100 µl O/N culture and incubated at 32°C with shaking (220 rpm) for 2-4 h. Once $O.D._{600}$ of 0,4-0,8 is achieved, bacteria were incubated at 42°C for 15 min with 220 rpm shaking and kept on ice 20 min with rocking at the same speed. Bacteria were then spun down at 4°C for 5 min at 4,500×g, resuspended with wide-bore pipette tips in 1 ml ice-cold 10% glycerol and transferred into ice-cold 1,5 ml Eppendorf tubes. Bacteria were then spun down at 4°C for 5 min at 4,500×g and washed with 1 ml ice-cold 10% glycerol. After repeating this step three times, excess 10% glycerol was carefully removed and bacteria were gently resuspended with wide-bore pipette tips in 20-50 µl ice-cold 10% glycerol.

For the first mutagenesis step, bacteria were electroporated in ice-cold 0,1 cm cuvettes with 2-5 µl (~100 ng) *Dpn*I-digested gel purified PCR and carefully removed from the cuvette by adding 900 µl RT SOC or LB. After being incubated for 1 h at 32ºC, bacteria were spun down for 2 min at 4,500×g. After discarding most of the supernatant, bacteria were resuspended in residual media (~100 µl), plated on LB+KANA+CAM plates and incubated at 32ºC for 24-48 h. After screening some clones by restriction fragment length polymorphism (RFLP) or colony PCR, positive clones were grown O/N at 32ºC in 2 ml LB+CAM+KANA for resolution. The next day, 100 µl of the O/N culture were added to 2 ml of LB+CAM to maintain the BAC. After 2-4 h at 32°C and 220 rpm, 2 ml of LB+CAM+2% arabinose were added for induction of I-SceI. After shaking for another 60 min at 32°C, bacteria were incubated at 42°C at 220 rpm for 30 min to induce the expression of the Red recombination system. Bacteria were then grown at 32°C for another 1-4 h and diluted to 10^{-6} in LB; 100 µl of dilutions 10^{-5} and 10^{-6} were plated on LB+CAM+1% arabinose agar plates and incubated at 32°C for 24-48 h. Individual colonies (30-50) were picked and replica-plated of on LB+CAM and LB+CAM+KANA sensitive clones were further screened by RFLP or colony PCR. Specific primers were used to amplify the modified sequences by PCR with Phusion High Fidelity enzyme from Fynnzymes, purified with Hi Yield Gel/PCR DNA Fragments Extraction Kit from SLG and sequenced.

7.2.4.5 MDV BACs

The introduction of BAC technology in the MDV field (127), has had an important role in the study of MDV pathogenesis (67). BACs are particularly useful in MDV pathogenesis studies due to its strong cellular tropism and slow *in vitro* replication. Thanks to BAC technology introduction in the MDV field, mutagenesis in the genome can be performed in *E. coli* instead of in primary chicken cells, the only cell lines that support MDV growth (142).

The first MDV BAC was assembled in 2000 from the cell-culture passaged avirulent 584Ap80C strain and was named Bac20 (142); this was followed in 2003 by cloning of the mMDV CVI988 vaccine strain as a BAC (125), and in 2004 by the vvMDV strain RB-1B BAC (124). Most MDV BACs were assembled through replacement of the non-replication essential US2 gene (67, 117) by a mini-F sequence encoding for a CAM resistance gene. All generated MDV BACs showed no differences in their *in vitro* replication properties after reconstitution when compared with parental viruses (125, 142). In the case of the RB-1B BAC clone, this clone maintained its ability to efficiently cause tumours in experimentally infected chickens (124). However, due to mutations in the UL13 and UL44 genes, which encode for a serine/threonine protein kinase and gC, respectively (68), rB1-1B was impaired in its horizontal transmission capacity (11, 67, 69). All USP mutant viruses generated for this project were based on a restored spread-competent rRB-1B (67). In order to allow both *E. coli* BAC maintenance and minimum impairment of *in vivo* horizontal replication, the spread-competent rRB-1B has two *loxp* sites flanking the mini-F region, which allows for its removal following viral reconstitution by co-transfection with the CRE-expressing plasmid pCAGGS-NLS/Cre (67, 148).

7.2.4.5.1 Construction of USP MDV mutants presenting deletions

Six rMDV deletion mutants were generated during this project: rSynUSP.HAind, rSynUSP.HAlink, rSynUSP.ind, rSynUSP.link, rΔUSP and rΔCysBox. The kanamycin cassette was amplified from pEPkan-S (67, 150, 151) using appropriate primers described on Table 7.4. For generation of rSynUSP.HAind, rSynUSP.HAlink and rΔUSP, the N-terminal 966 bp (322 aa) of the UL36 gene, corresponding to the USP sequence that was previously analysed (66) were removed; for rSynUSP.ind and rSynUSP.link generation, the hemaglutinin (HA) tag located at the C-terminus of the SynUSP was removed; for rΔCysBox generation, the 66 bp (22 aa) encoded between the highly conserved glutamine (Q85) and

leucine (L106) residues and encompassing the active cysteine site (C98) (Figure 8) were removed.

7.2.4.5.2 Construction of rMDVs revertants

Revertant rMDVs created for this project rSynUSP.link-rev, rΔUSP-rev and ΔCysBox-rev were created by insertion of the 966 bp corresponding to MDV USP sequence of rRB-1B at the N-terminus of the mutant UL36 gene by using the primers described in Table 7.4. This sequence was amplified from the MDV transfer plasmid pMDV USP and used for two-step Red mediated recombination.

7.2.4.5.3 Insertion of ectopically expressed SynUSP at the 3´and 5´termini of the UL36 gene

For ectopic expression of MDV USP, the codon-optimized synthetic USP containing a C-terminal HA tag - SynUSP.HA - was used. This construct encoded the same aa sequence as wild-type USP, but alternative codons were used, as shown in Figure 13.

```
1    ATGACAGATT CTACTGACAG CAGACAAGCT ACTACAAATT GCAGGAAATA TTCAAGAACT ACATCGAACG CACCCATGCT
1    ATGACCGACA GCACCGATAG CAGGCAGGCC ACCACCAACT GCAGGAAGTA CAGCAGGACC ACAAGCAACG CCCCCATGCT
     M  T  D  S   T  D  S   R  Q  A   T  T  N  C   R  K  Y   S  R  T   T  S  N  A   P  M  L
81   AGCTGCGAAC GTGTTAAGAG ATAAATCGAC GTCTGGACTC TGTTCGCTTG ATCGAAAACA CGACCCATAT TTTGGGCAAA
81   GGCCGCCAAC GTGCTGAGGG ACAAGAGCAC CAGCGGCCTG TGCAGCCTGG ACAGGAAGCA CGACCCCTAC TTCGGCCAGA
      A  A  N   V  L  R  D   K  S  T   S  G  L   C  S  L  D   R  K  H   D  P  Y   F  G  Q  I
161  TTATGGATAA CCCTGAGGTA ATTCTAGATG AATGGGCAAA GATGGTGATA GATACGACTG ATGTAACGGT AGTGGCGGTT
161  TCATGGACAA CCCCGAGGTG ATCCTGGACG AGTGGGCCAA GATGGTGATC GACACCACCG ACGTGACCGT GGTGGCCGTG
       M  D  N   P  E  V   I  L  D  E   W  A  K   M  V  I   D  T  T  D   V  T  V   V  A  V
241  GGTATTAGAA ACCAGTTTGC TCCGGACCTA AGTCCTGCGT CTTCAGTTTC ATGTTTACGT TCATCGTTGG CATTTCTTCG
241  GGCATCAGGA ACCAGTTCGC CCCCGACCTG AGCCCCGCCA GCAGCGTGAG CTGCCTGAGA TCCAGCCTGG CCTTCCTGAG
     G  I  R  N   Q  F  A   P  D  L   S  P  A  S   S  V  S   C  L  R   S  S  L  A   F  L  R
321  TATAGTTTTT GCGTATGGAT TAGATACAGT CATATCATCA GATGCAATAG ATAGACTTTT ATTACAGGGA AAGGCCTGGA
321  GATCGTGTTC GCCTACGGCC TGGACACCGT GATCAGCAGC GACGCCATCG ACAGGCTGCT GCTGCAGGGC AAGGCCTGGA
      I  V  F   A  Y  G  L   D  T  V   I  S  S   D  A  I  D   R  L  L   L  Q  G   K  A  W  T
401  CAATAGCGAC TTCTGAAGAT GGGACATATA CAACGTGCGT TCCGCATGAT CTGCCGAATA GAATTATATC AAAAGATGCA
401  CCATCGCCAC AAGCGAGGAC GGCACCTACA CCACCTGCGT GCCCCACGAC CTGCCCAACA GGATCATCAG CAAGGACGCT
       I  A  T   S  E  D   G  T  Y  T   T  C  V   P  H  D   L  P  N  R   I  I  S   K  D  A
481  GGAGGAAATT TGTGTGTTGC ATTTTCGAGT TCATATGGGG AGTTTGAATT CTATCTAGAA GAAAACACGC CCACTATATT
481  GGCGGCAACC TGTGCGTGGC CTTCAGCAGC AGCTACGGCG AGTTCGAGTT CTACCTGGAA GAGAACACCC CCACCATCCT
     G  G  N  L   C  V  A   F  S  S   S  Y  G  E   F  E  F   Y  L  E   E  N  T  P   T  I  L
561  AGATACTCAA ATATCTGCGC GGACGTTCAT AGAACAAATA TGGAAAAAAA AGCGGGGTGA TGTTTATTGT TTAATTGTGG
561  GGATACCCAG ATCAGCGCCA GGACCTTCAT CGAGCAGATC TGGAAGAAGA AGAGGGGCGA CGTCTACTGC CTGATCGTGG
      D  T  Q   I  S  A  R   T  F  I   E  Q  I   W  K  K  K   R  G  D   V  Y  C   L  I  V  V
641  TTGGCGTTTT AGGAATTGGA GTGTACAGAT CCGGCGATGG AATTTATATT TTTGATCCGC ATGGACATGG GCATATAGGA
641  TGGGCGTGCT GGGCATCGGC GTGTACCGCA GCGGCGACGG CATCTACATC TTCGACCCCC ACGGCCACGG CCACATCGGC
```

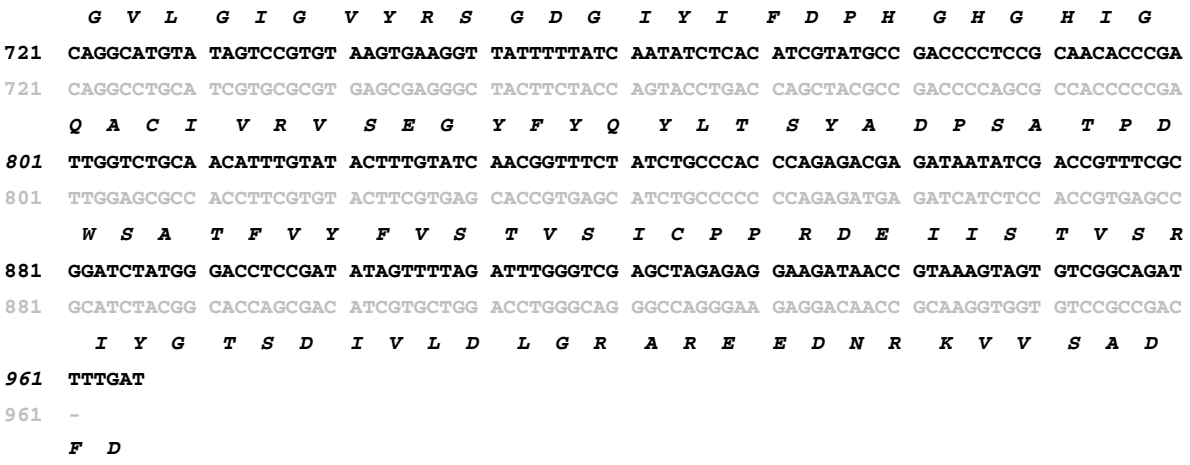

Figure 13. Comparison of the 320 aa codon-optimized SynUSP sequence developed by GeneArt with the wild-type MDV USP from the rRB-1B sequence. Different nucleotide sequences give origin to the same aa sequences. The active cysteine (first black box) and histidine residues important for catalysis (second black box) are highlighted. Picture courtesy of Dr. Dušan Kunec.

This sequence manipulation is essential to reduce the likelihood of homologous recombination between MDV USP and the ectopically expressed USP during the two-step Red recombination procedure.

For insertion of SynUSP.HA at the N-terminus of pUL36 for rC98A-SynUSP.HA assembly, the transfer plasmid pSynUSP.HA was used for amplification of the kanamycin cassette. For the insertion of the IRES.SynUSP sequence at the C-terminus of pUL36, IRES-pSynUSP.HA was used as transfer plasmid to generate rC98A-IRES.SynUSP and rΔUSP-IRES.SynUSP (Figure 12).

7.2.4.6 Calcium phosphate transfection

After generation of rMDVs and diagnostics such as RFLP analysis and sequencing, BAC DNAs were transfected into CECs by using the calcium phosphate method for virus reconstitution (132). First, 0,5-2,0 µg of highly pure BAC DNA prepared were diluted with sterile 10 mM Tris pH 7,5 to a 50 µl final volume in a polyethylene tube. Recombinant viruses destined to be used for *in vivo* experiments were transfected together with 0,1 µg CRE plasmid, for mini-F sequence removal. After adding 388 µl sterile millipore-purified water, the mix was incubated for 1-2 h at RT, shaking gently from time to time to dissolve the DNA. Sixty-two microliters 2 M $CaCl_2$ was then added in drops while gently mixing the tube and the

DNA mix was incubated O/N at 4ºC. Meanwhile, 1,0x10^6 CECs were seeded in one well of 6-well plate with 2 ml MEM supplemented with 5% FCS and 1% P/S.

The following day, 500 µl ice-cold 2x HEPES buffered saline (2x HBS; 140 mM NaCl, 1,5 mM $Na_2EDTAx2H_2O$ and 50 mM HEPES, pH 7,05) were added dropwise to the transfection mixture and incubated at RT for 15 min. Meanwhile, media was removed from CECs and 500 µl fresh media was added. After the incubation time, 500 µl of the transfection mixture was added to each well and gently mixed. After a 3-4 h incubation at 37°C, the transfection mixture was removed, the transfected wells washed once with PBS, then at RT with 1.5 ml 1x HBS+15% glycerol for 2 to 2 ½ min. After removal of the 1x HBS+15% glycerol, cells were gently washed with 2 ml 1x PBS for 1 min, then 2 ml MEM 5% supplemented with FCS and 1% P/S was added to each well. Serum concentration was decreased to 0,5% once the cells were confluent. For wild-type and revertant viruses, plaques appeared approximately 5 days post-transfection and the cells were then passaged to expand the virus.

7.2.4.7 Virus storage and titration

Replicating rMDVs were passaged two to three times prior to being frozen in 8% DMSO in 1 ml aliquots. Virus stocks were frozen slowly to -80°C and then frozen for longer storage periods in liquid nitrogen. Replication-impaired rMDVs were passaged one to two times more, in an attempt to increase viral titers.

For viral titration, one vial from each aliquoted viral stock was thawed and serially diluted to 10^{-4} in MEM media. Dilutions of 10^{-2} to 10^{-4} were mixed with fresh CECs/CKCs and plated in duplicate 6-wells with MEM 5% supplemented with FCS 1% and P/S. Once confluency was reached, serum concentration was decreased to 0,5%. After 6 days, all wells were fixed with 90% acetone and IF assays were performed using MDV-specific chicken serum, as described in the following section.

7.2.4.8 Plaque size assays

Due to the importance of the UL36 gene for viral replication, mutations in this region led to the generation of highly impaired viruses that could not be compared by using regular methods, such as multi-step growth kinetics and plaque size assays. Therefore, comparison of non-viable mutants was made by plaque size assays directly post-transfection.

For non-viable rMDV, $1{,}0x10^6$ fresh CECs were transfected by using the calcium phosphate method; for viable rMDV, 100 PFU were placed in 3 wells of a 6-well plate with $1{,}0x10^6$ fresh CECs/CKCs; in both cases cells were fixed 6 days later with 90% acetone for 10 min at -20ºC and then air dried. Standard IF assays were performed using polyclonal anti-MDV chicken serum, followed by anti-chicken IgY Alexa 488 secondary ab, both diluted in blocking solution (3% FCS in PBS). Following 1 h incubation with primary and secondary antibodies, three 5 min washing steps were performed in between. Plaque images from each virus were collected at 100x amplification and measured using the program Image J 1.410 (6) (http://rsbweb.nih.gov/ij/); 20 images were taken when possible from each virus for non-viable MDVs, while 60 pictures were taken for each viable virus per experiment. Relative plaque diameters were always compared with wild-type virus and revertant viruses when relevant. All experiments described were performed at least three times in an independent fashion.

7.2.4.9 Multi-step growth kinetics

Multi-step growth kinetic assays were performed simultaneously with all plaque size assays for viable MDV mutants; 100 PFU were plated with $1{,}0x10^6$ fresh CECs. One well was trypsinized daily for 6 days and serially diluted in fresh CECs, which were then fixed and stained after 6 days using IF assays described above.

7.2.4.10 Animal Studies

One animal experiment performed by Dr. Keith Jarosinski at Cornell University (Ithaca, NY, USA) provided important data regarding *in vivo* vC98A-SynUSP.HA phenotype and will therefore be described in the Results section.

SPF P2a chickens (MHC: $B^{19}B^{19}$) used for this experiment were obtained from Cornell University's departmental flocks and kept in isolation units, with water and food *ad libitum*. Ten 1-day-old chicks were infected intra-abdominally with 2,000 PFU of each rMDV and placed into different units with five age-matched, but uninfected contact birds. Whole blood was collected by wing-vein puncture at 4, 7, 10, 14, 21, 28 and 35 days pi. All animals were evaluated twice daily for clinical signs of disease and euthanized as soon as symptoms became apparent. At 13 weeks pi, the experiment was terminated and remaining birds were necropsied. Gross Marek´s disease lesions were observed during necropsy either after humane euthanasia or at the termination of the experiment.

7.2.4.11 Quantitative PCR (qPCR) analysis

pPCR assays were performed exactly as previously described (66, 67, 69). Briefly, DNA was extracted from chicken whole blood and MDV genomic copies measured using qPCR assays. Forty microliters of blood was mixed with 20 µl 0,1 M EDTA and frozen at −80°C until completion of the experiment. Ten microliters of the blood-EDTA mix was used for DNA preparation using the DNeasy 96 tissue kit from Qiagen according to the manufacturer's instructions. Final DNA preparations were eluted in 100 to 200 µl elution buffer heated to 70°C.

For the generation of standard curves in qPCR assays, a plasmid containing cellular inducible nitric oxide synthase (iNOS*)* and rRB-1B DNA were used. Serial 10-fold dilutions of each respective plasmid or BAC were used for generating standard curves, starting with approximately 500 pg of DNA. Total copy numbers were determined using the following formula: [(pg of input)(1 pmol/340 pg)(1/template size in bp)(1 mol/1,0x10^{12} pmol)]/(6,02 × 10^{23} copies/mol) (70), and standard curves were generated by plotting the threshold cycle values at each dilution with the total copies. The coefficient of regression was always >0.99 for standard curves.

MDV genome copies were determined using primers and probe specific for the MDV ICP4 gene and normalized against the iNOS gene. qPCR reactions were performed in an ABI Prism 7500 Fast Real-time PCR system and the results were analysed using Sequence Detection Systems version 1.4 software. Each qPCR mixture contained TaqMan Fast Universal Master Mix from Applied Biosystems, 9,5 µl DNA, 25 pmol of each gene-specific primer, and 10 pmol of the gene-specific probe in a 20 µl volume. Thermal cycling conditions were as follows: 95°C for 20 s, followed by 40 cycles at 95°C for 3 s and 60°C for 30 s. Using the standard curve generated for each gene, the numbers of *copies for* ICP4 *and* iNOS were determined by using the threshold cycle value for that sample.

7.2.5 Protein methods

7.2.5.1 Protein extraction with RIPA buffer and benzonase

Cells were scraped or trypsinised, pelleted by centrifugation, and washed twice with 1x PBS. RIPA I buffer (20 mM Tris-HCl, pH 7,5, 150 mM NaCl, 1% NP-40, 0.5% Na desoxycholate, 0,1% SDS) was then added to the pelleted cells in the appropriate proportion (50 µl per

1,0x10^6 cells) and cell pellet was resuspended with wide-bore pipette tip. The lysates were incubated on ice for 10 min with 0,5 µl of 25 U/µl stock of benzonase (12.5 U). Afterwards, an equal volume of RIPA II buffer (same as RIPA I but with 1 mM EDTA) was added and incubated on ice for another 10 min. The lysates obtained were then aliquoted to Eppendorf tubes, boiled for 5 min at 95°C with 4x loading buffer (400 µl 10x Laemmli, 400 µl 100% glycerol, 200 µl 14 M mercaptoethanol) and frozen at -80°C until used.

7.2.5.2 Western Blot

SDS-polyacrylamide gels were prepared according to Table 10. Previously denatured samples were loaded onto 10- or 15-well vertical gels and electrophoresed with 1x running buffer (19,2 M glycine, 5 M Tris pH 8,9, 10% SDS), initially at 70 V until the sample had traversed the stacking gel, then at 150-180 V for 30-45 min and finally at 200 Volts for the last 5 min. Proteins were transferred to nitrocellulose membranes in a semi-dry blotter system for 1,5 h at 2 mA/cm^2, using the three buffer transfer system composed of anode I (90% 0,3 M Tris pH 10,4, 10 % methanol) and II (90% 25 mM Tris pH 9,4, 10 % methanol (v/v)) and cathode (90% 25 mM Tris, pH 9,4 mM 6-N-caproic acid, 10 % methanol (v/v)). For pUL36 detection, cell lysates were separated by 5% SDS-PAGE at low speed and blotted in a wet transfer chamber for 3 h at constant 400mA (changing the ice pad in between).

Resolving gel	**10%**	**5%**
H_2O	2 ml	2,85 ml
1,5 M Tris-Cl pH 8,8	1,25 ml	1,25 ml
10% SDS	50 µl	50 µl
30% Acrylamid	1,5 ml	825 µl
10% APS	25 µl	25 µl
TEMED	2,5 µl	2,5 µl

Stacking gel	**4%**
H_2O	1,50 ml
1 M Tris-Cl pH 6,8	750 µl
10% SDS	25 µl
30% Acrylamid	325 µl
10% APS	12,5 µl
TEMED	2,5 µl

Table 10. Composition of the resolving and stacking gels used for SDS-PAGE.

After drying and blocking the blot for 30 min in 5% NFDM PBST, membranes were incubated O/N with specific abs diluted in blocking buffer at 4ºC with rocking. After three 5-min washing steps with PBST, membranes were incubated with horseradish peroxidase (HRP)-tagged secondary ab diluted in blocking buffer for 1 h, washed three times for 5 min with PBST and incubated with ECL Plus kit solution for 5 min prior to chemiluminescent detection.

7.2.5.3 Antibody anti-USP-1 blocking with USP-1 immunizing peptide

For testing the newly synthesized anti-USP-1 ab, blocking with the peptide used for immunization was performed, based in the indications provided by the Abcam troubleshooting guide (www.abcam.com/technical). First, in order to determine the smallest concentration that can be used for antigen detection, the ab was titrated (in the case of anti-USP-1, the obtained value was 1:5000). The ab was then diluted in 30 ml of freshly prepared 5% NFDM PBST at 1:5000 and divided into three portions prepared in the following fashion: tube 1, with anti-USP-1 ab only; tube 2, with 1 µg/ml (10 µg) immunizing USP-1 peptide, and tube 3, with non-specific 1 µg/ml VP1/2-1 peptide. After incubation O/N at 4 ºC on a rotating wheel, the three solutions were used for standard WB detection.

7.2.5.4 pcDNA3-HA.USP *In vitro* translation

EasyXpress Insect Kit II from Qiagen was used according to the manufacturer´s recommendations. pcDNA3-HA.USP was digested for 1 h with blunt-cutting enzyme *Sma*I (for protein yield increase) prior to transcription and purified with Hi Yield Gel/PCR DNA Fragments Extraction Kit from SLG.

7.2.5.5 TAP purification

Due to several technical problems, the pCeMM-USP.CTAP construct, originally meant to work in the context of a retroviral expression system (110), could not be used, neither for this purpose nor for regular two-step TAP purification from transiently expressed USP (18). However, a protocol adapted from another previously described TAP procedure (54) was successfully used to pull-down USP-CTAP using a single purification step with streptavidin beads, which bind to the streptavidin-binding peptide (SBP) present in pCeMM-CTAP tag. Briefly, 293T cells were grown to confluence in three T175 flasks and transfected with pCeMM-USP.CTAP using PEI, as previously described. The following day, cells were trypsinised, pelleted at 1,000xg for 10 min, resuspended in 10 ml lysis buffer (100 mM Tris, 5 mM EDTA, 250 mM NaCl, 50 mM NaF, 0,2 mM Na_3VO_4, pH 8,0; prior to usage, add 100 mM DTT, 100 mM PMSF, 10% Triton X-100 and ½ protease inhibitor tablet from Roche per 20ml) and homogenized on ice with an ice-cold Dounce homogenizer 10 times. After distributing volume in 2 ml Eppendorf tubes, cell lysates were spun down at 20,000xg for 30 min at 4°C. One-hundred microliters supernatant were kept for posterior analysis.

Meanwhile, 100 µl slurry of Strep-Tactin beads were washed once with lysis buffer and centrifuged at 1,000xg for 1 min. Supernatants from lysis were transferred to 15 ml tubes together with Strep-Tactin beads and kept in rotating shaker at 4°C for 30 min. Afterwards, beads were washed four times with ice-cold lysis buffer, with spinning at 1,000xg for 1 min. Meanwhile, elution buffer was prepared by adding 2,5 mM desthiobiotin (80 µl from previously prepared stock consisting in 200 mM desthiobiotin dissolved in 2,5 ml 100 mM Tris-HCl pH 8,0; heat-dissolved before addition) to 920 µl of lysis buffer. Elution was performed with 300 µl of elution buffer and beads were kept to check elution efficiency in 100 µl buffer. Fifty microliters of eluate were also kept for posterior WB analysis.

8 Results

8.1 Evaluating the role of the UL36-encoded USP in MDV replication

8.1.1 The presence of the N-terminus of UL36 is essential for MDV replication

It has been previously demonstrated that the MDV USP is present within the 322 N-terminal residues of the UL36-encoded large tegument protein (pUL36) of rRB-1B and that the conserved active cysteine is located at position 98 (C98) (Figure 8). In order to determine whether the USP located at the N-terminus of pUL36 is essential for viral replication, we deleted this region (rΔUSP) from rRB-1B. In addition, a revertant virus (rΔUSP-rev) was generated, in which the N-terminal 322 aa was restored. RFLP patterns from UL36 N-terminus removal and reconstitution are shown in Figure 14.

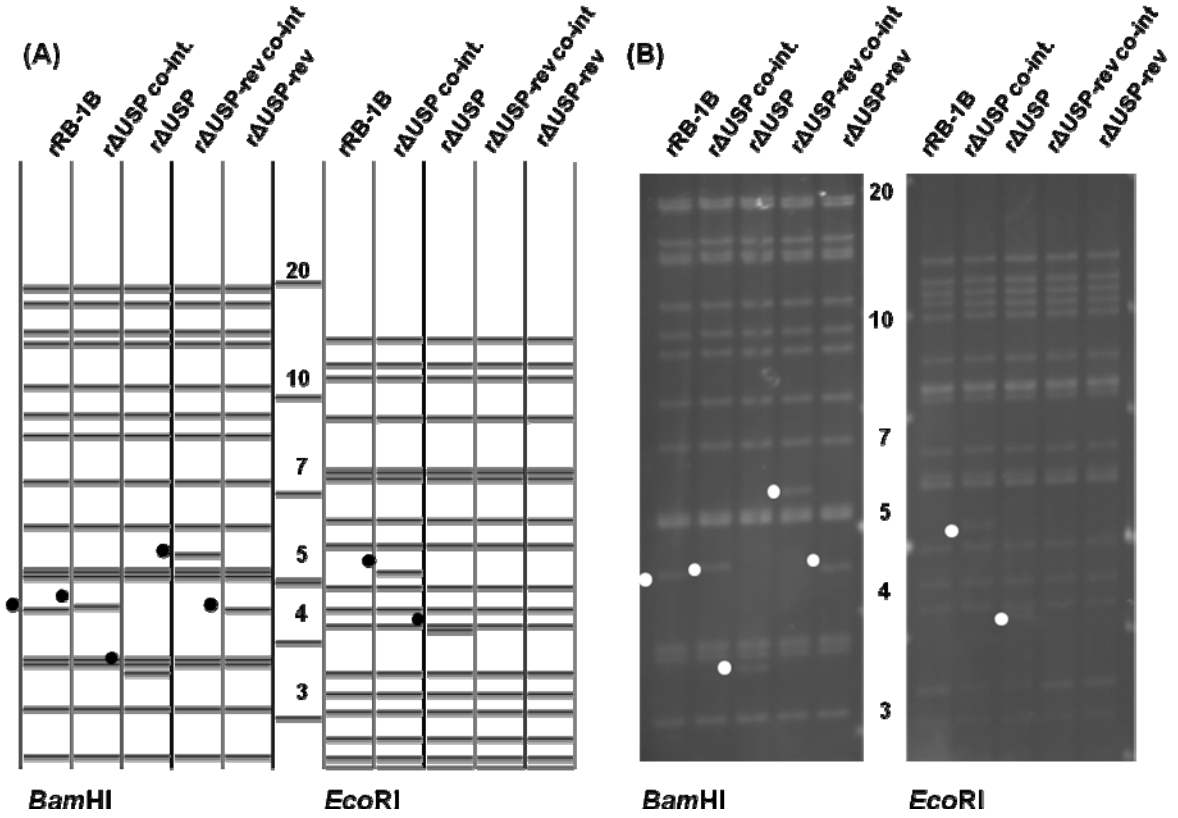

Figure 14. RFLP from rΔUSP and rΔUSP-rev clones, compared to wild-type virus and co-integrate rMDVs presenting kanamycin cassette. (A) Vector NTI 9.1 prediction using restriction enzymes *Bam*HI and *Eco*RI (B) RFLP patterns obtained using the same enzymes run through 0,8% agarose gels O/N at 65 V. Co-int stands for co-integrate clones.

Following reconstitution of viruses by transfection of BAC DNA into CECs, it was determined that vΔUSP was unable to replicate *in vitro*; only individually infected cells could be observed. In contrast, vΔUSP-rev replicated in a fashion that was comparable to parental vRB-1B when plaque size assay results were compared (Mann-Whitney U test; p>0,05) (Figure 15.B). Therefore, our data suggests that the N-terminal region of the pUL36 is essential for MDV replication.

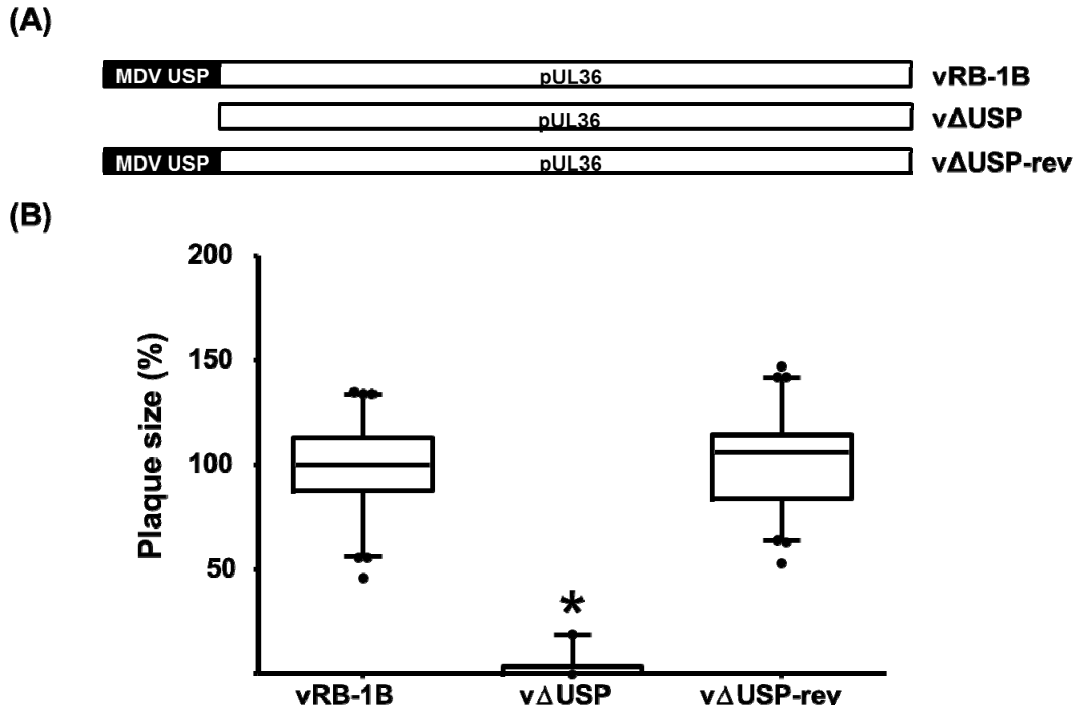

Figure 15. Importance of N-terminal UL36 region for viral replication. (A) Schematic representation of pUL36 from vRB-1B, vΔUSP and vΔUSP-rev. (B) Plaque area analysis of vRB-1B, ΔUSP and vΔUSP-rev after CECs transfection. Plaque sizes are shown as means from all plaque diameters obtained from each experiment, normalized with the respective wild-type diameters. Wiskers show 5 and 95% percentile values (the same applies to all the box plots presented in this thesis). Significant difference in replication (Kruskal-Wallis test, $p < 0.05$) is indicated with an asterisk (*).

8.1.2 Ectopically-expressed USP does not restore replication or tumourigenesis of vC98A

It was previously described that replacement of the highly conserved MDV USP active site cysteine by an alanine residue (rC98A) significantly impaired the resulting rMDV (vC98A) in its ability to induce lymphomas (66). However, it remained unclear whether MDV USP is required to be part of pUL36 to exert its functions in MDV replication and tumourigenesis. In order to address this question, a codon-optimized synthetic USP (SynUSP) was synthesized

and used for ectopic expression of MDV USP. SynUSP encodes the same aa sequence, but a different nucleotide sequence (Figure 13) to avoid illegitimate homologous recombination events between the two USPs during the two-step Red mediated recombination procedure. Also, SynUSP included a C-terminal HA tag (SynUSP.HA) for detection, as USP-specific abs are not to date available.

SynUSP.HA was first introduced at the 5' end of the UL36 gene in the rC98A background, in order to generate rC98A-SynUSP.HA; in this recombinant, SynUSP.HA is expressed under the control of the UL36 promoter and two stop codons located immediately downstream from the synthetic sequence separate SynUSP.HA from the rest of the UL36 ORF (Figure 16A).

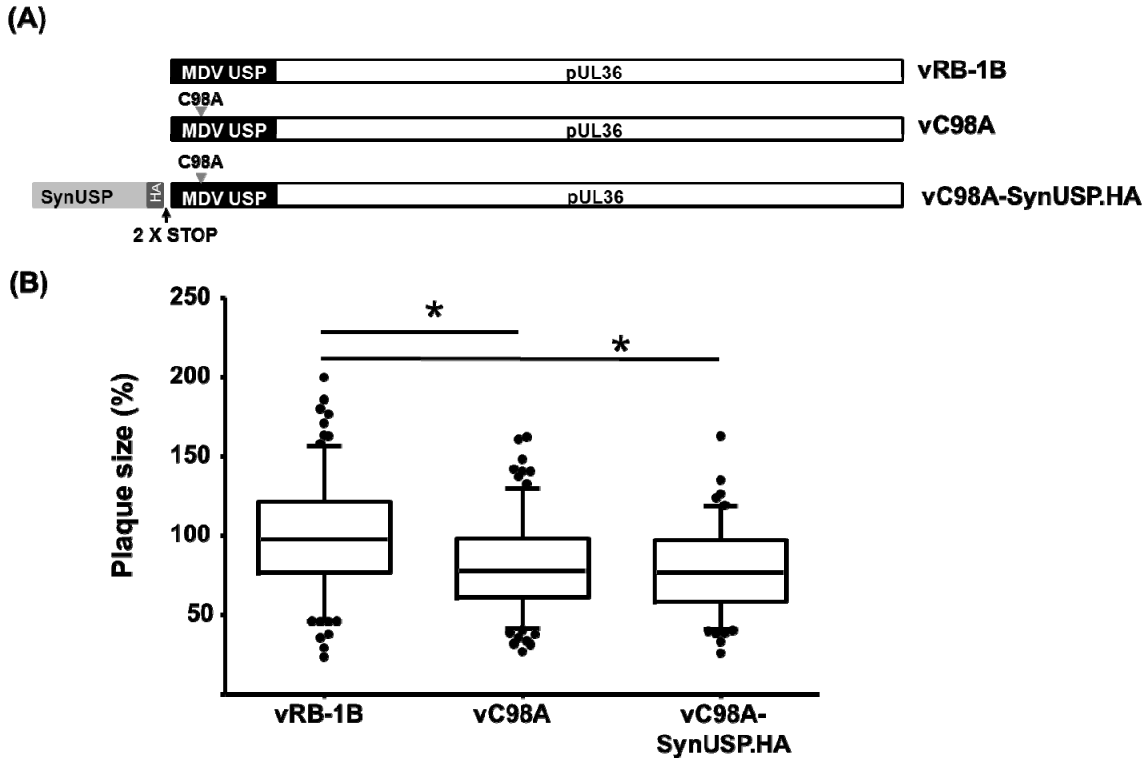

Figure 16. Ectopic expression of SynUSP.HA cannot rescue replication defective vC98A *in vitro*. (A) Schematic representation from vRB-1B, vC98A and vC98A-SynUSP.HA; (B) Plaque size analysis of vRB-1B, vC98A and vC98A-SynUSP.HA in fresh CKCs. vC98A-SynUSP.HA induced similar sized plaques compared to vC98A, and both were significantly less than wild-type virus. Significant differences between vRB-1B and mutant viruses vC98A and vC98A-SynUSP.HA (Mann-Whitney U test, $p < 0.05$) are indicated with an asterisk (*).

Reconstitution of rC98A-SynUSP.HA in CKCs resulted in virus (vC98A-SynUSP.HA) that replicated in a comparable fashion to vC98A (Mann-Whitney U test, p>0,05) using plaque size assays, and both vC98A and vC98A-SynUSP.HA produced plaque sizes significantly smaller compared to parental vRB-1B (Mann-Whitney U test, p<0,05). These results suggest

that ectopic expression of SynUSP at the 5' end of UL36 does not complement USP activity of vC98A.

Next, and in order to determine if ectopic expression of SynUSP can restore wild-type replication levels and tumourigenesis of vC98A, 1-day-old chicks were infected with vRB-1B, vC98A or two independent clones of vC98A-SynUSP.HA (1 and 2).

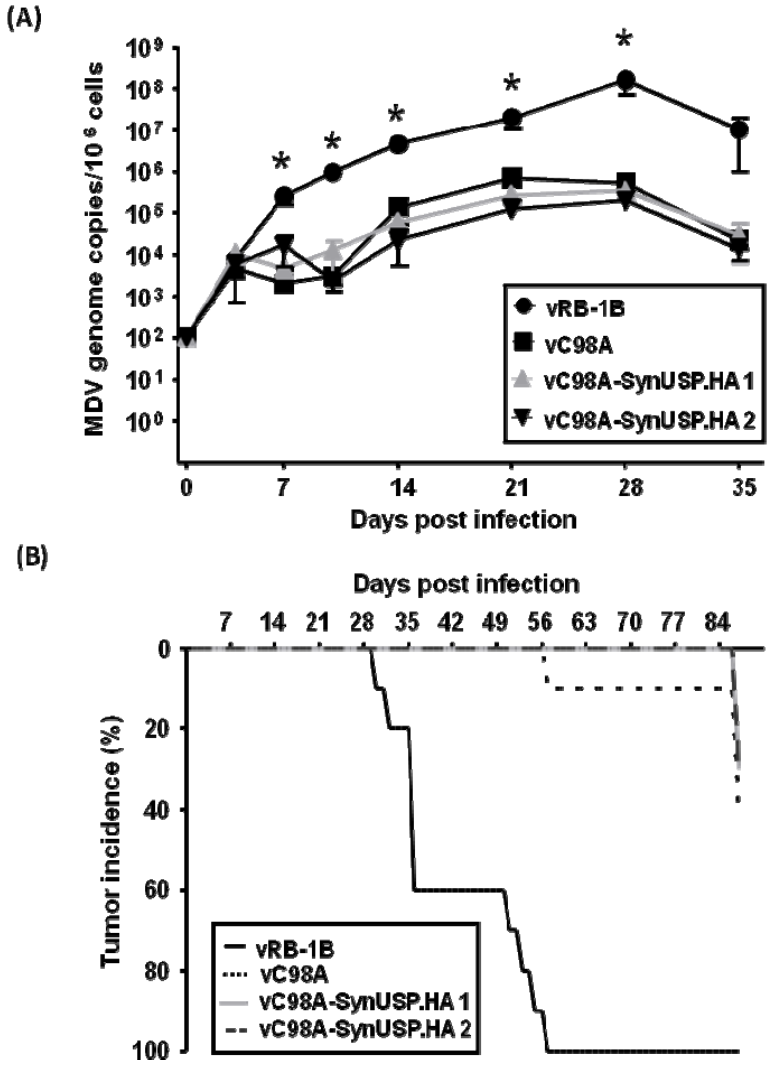

Figure 17. ***In vivo*** **replication and tumour incidence of vC98A-SynUSP.HA. (A) qPCR analysis of MDV genome copy numbers in whole blood of chickens infected with vRB-1B, vC98A or two independent clones of vC98A-SynUSP.HA. Mean MDV genome copy numbers per 1,0x10^6 cells of ten infected chickens per group are shown. Significant differences between vRB-1B and other groups (Mann-Whitney U tests, $p < 0.05$) are indicated with an asterisk (*); (B) Tumour incidence of chickens infected with vRB-1B, vC98A, or both vC98A-SynUSP.HA rMDVs until day 87 pi.**

This experiment clearly showed that replication of vC98A-SynUSP.HA in infected chickens was significantly limited when compared to vRB-1B (Figure 17A) and was, once again, comparable to vC98A (Kruskall-Wallis test, p<0,05). Furthermore, lymphomagenesis of both independent vC98A-SynUSP.HA clones was severely impaired when compared to vRB-1B and was comparable to vC98A (Figure 17B).

Our results demonstrate that ectopic expression of MDV USP as a separate protein outside the context of pUL36 was unable to restore efficient MDV replication and tumourigenesis of the enzymatically inactive vC98A.

To further confirm that ectopic expression of USP cannot restore efficient replication of USP deficient mutants, SynUSP was then expressed at the 3' end of the UL36 gene by utilizing an internal ribosome entry site (IRES), which was inserted immediately downstream of the UL36 ORF and immediately upstream of its poly-A tail as it can be observed in Figure 18 A.

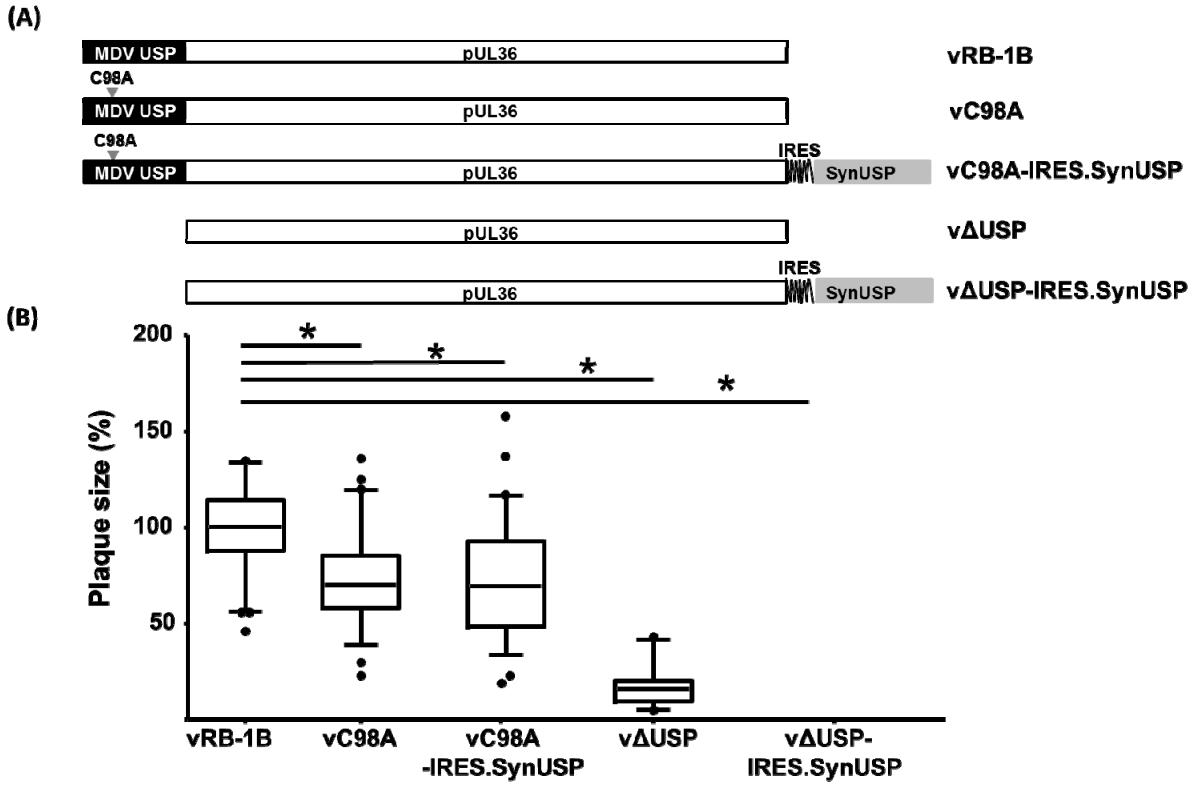

Figure 18. Ectopic expression of SynUSP by insertion of independently expressed IRES.SynUSP at the 3´-terminus of UL36. (A) Schematic representation from vRB-1B, vC98A-IRES.SynUSP, vC98A, vΔUSP-IRES.SynUSP and vΔUSP; (B) Plaque size assays following transfection showed that reversion of the phenotype could not be achieved by insertion of IRES.SynUSP at the C-terminus of UL36 protein. Differences between vC98A and vC98A-IRES.SynUSP areas were not significant (Mann-Whitney U test, p>0.05). Significant differences with vRB-1B are indicated with an asterisk (*).

The IRES.SynUSP sequence was inserted at the UL36 3´end in both the rC98A and rΔUSP background to compare the effect of SynUSP ectopic insertion in both settings: the enzymatically inactive clone and the structurally impaired clone, respectively. Obtained rMDVs were reconstituted in CECs and it was determined that expression of SynUSP at the 3' end of UL36 using an IRES did not rescue the phenotype of vC98A nor vΔUSP, as can be clearly be observed in Figure 18.B.

To show that IRES insertion immediately downstream from the UL36 ORF led to the expression of a functional SynUSP and in the absence of a confirmed USP region-specific ab, SynUSP was replaced by the enhanced green fluorescent protein (eGFP) in the rC98A-IRES.SynUSP background. As no fluorescent plaques were detectable and no eGFP could be detected with a eGFP-specific antibody in WB analyses, we concluded that USP function cannot be complemented by ectopic USP expression by means of an IRES motif, quite likely due to the sheer length of the UL36 ORF.

In order to answer the question of whether MDV USP activity is required to be linked to the UL36 protein to be able to exert wild-type function, the N-terminal 966 bp of UL36 corresponding to MDV USP were removed in vC98A-SynUSP.HA, leaving SynUSP.HA either in-frame (linked expression, vSynUSP.HAlink) or out-of-frame (independent expression, vSynUSP.HAind) of UL36 (Figure 19.A). The only difference between the two clones was the presence of two stop codons between the authentic UL36 gene and the SynUSP.HA sequence, reminiscent of vC98A-SynUSP.HA. As shown in Figure 19.B, both vMDVs expressing SynUSP.HA independently or linked to the UL36 ORF were replication-impaired, suggesting that the HA tag expressed at the C-terminus of SynUSP could be responsible for the observed impairment in viral replication. Therefore, the HA tag was removed from both vSynUSP.HAind and vSynUSP.HAlink. Interestingly, removal of the HA tag from vSynUSP.HAlink (vSynUSP.link) led to a virus that replicated similarly to vRB-1B (Figure **20**), unlike vSynUSP.ind, which was replication-impaired similarly to its parental virus vSynUSP.HAind (data not shown). These results suggested that SynUSP must be linked to pUL36 to be functional, and that having the HA tag at the C-terminus of SynUSP was lethal for its function.

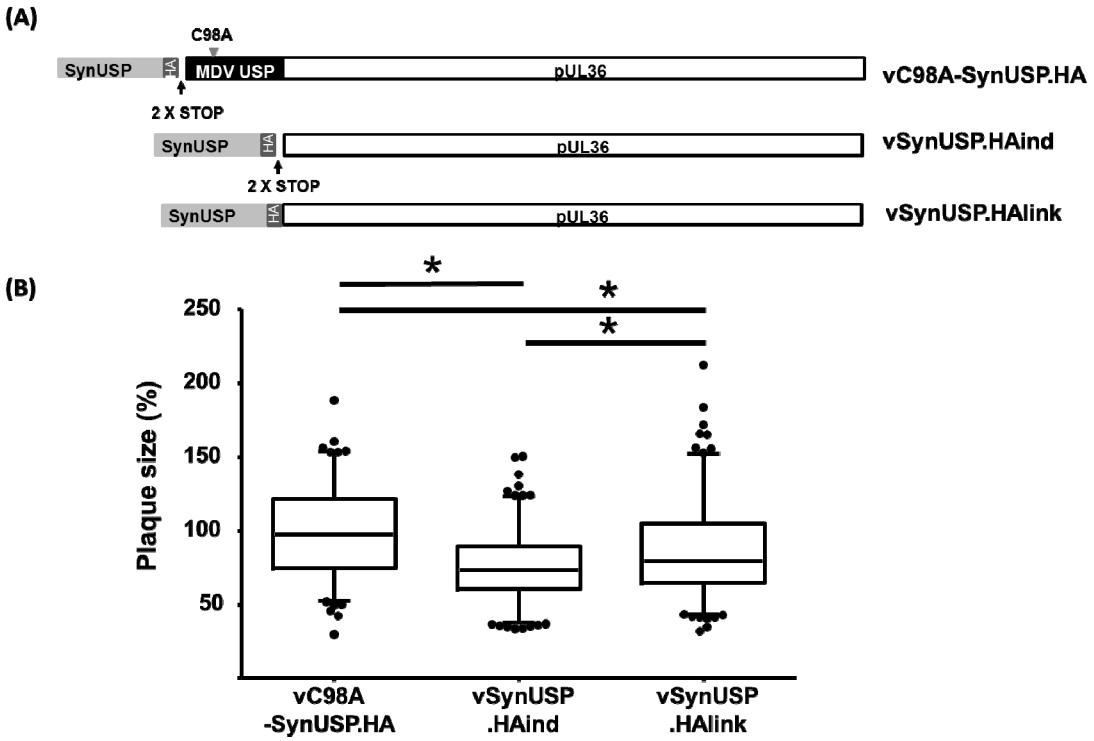

Figure 19. Evaluation of SynUSP linked and independent expression. (A) Schematic representation from vC98A-SynUSP.HA, vSynUSP.HAind and vSynUSP.HAlink; (B) Plaque size assays with vSynUSP.HAind and vSynUSP.HAlink with CKCs in comparison to parental virus vC98ASynUSP.HA. Both vSynUSP.HAind and vSynUSP.HAlink were severely impaired in their replication properties when compared to vC98A-SynUSP.HA (Kruskal-Wallis test, $p<0.05$), even if vSynUSP.HAlink replicates significantly better than vSynUSP.HAind; this impairment could be reverted after removal of HA tag in the SynUSP.HAlink mutant, but not in SynUSP.HAind (data not shown).

8.1.3 Insertion of SynUSP in the mini-F region does not lead to phenotype reversion

To evaluate whether USP complementation could be achieved by insertion of a functional enzyme in a completely distinct location in the genome under a different promoter, the SynUSP sequence was inserted in the mini-F region, downstream from an HVT ICP4 promoter, by using pICP4-SynUSP.*aphAI* as transfer plasmid. ICP4.SynUSP could therefore be removed by taking advantage of the *loxP* sites present at either end of the mini-F region, which would allow removal of SynUSP by co-transfection of rMDVs with pCAGGS-NLS/Cre, as previously described (67). The mutation was performed in rΔUSP (rΔUSP-ICP4.SynUSP) and in rC98A (rC98A-ICP4.SynUSP). Both mutants were then transfected with or without pCAGGS-NLS/Cre, in order to determine if ICP4.SynUSP maintenance would lead to phenotype reversion to wild-type, while its removal would lead to parental phenotype. However, even if no formal plaque size assay was performed, no difference between rMDV

transfection with and without pCAGGS-NLS/Cre could be detected in several independent experiments; in both cases, mutant viruses behaved like parental viruses, i.e. vΔUSP-ICP4.SynUSP was unable to grow, whereas vC98A-ICP4.SynUSP grew in an impaired fashion.

8.1.4 The exact base pair sequence of USP is important for replication *in vitro*

To determine if vSynUSP.link obtained after HA tag removal from vSynUSP.HAlink results in replication ability similarly to those of vRB-1B, a revertant virus (vSynUSP.link-rev) was generated and formal plaque size and multi-step growth kinetics assays were performed from titrated stocks (Figure.B and C).

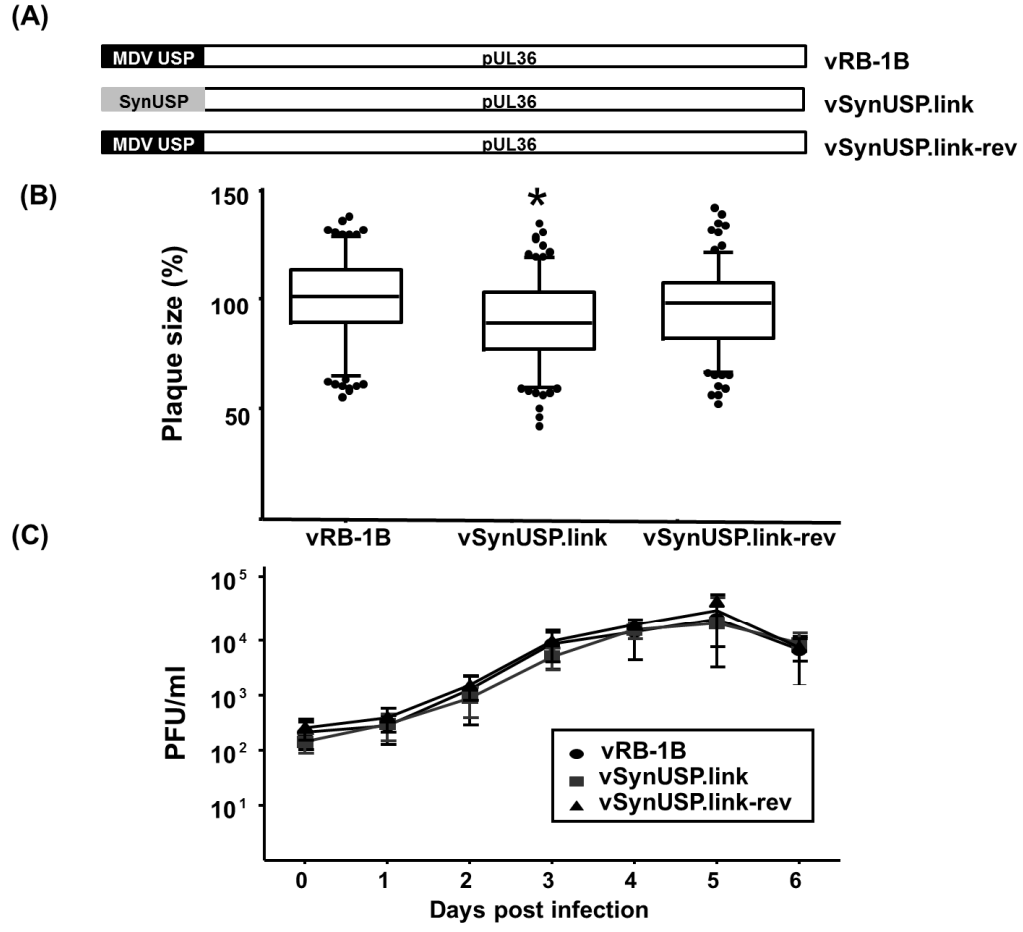

Figure 20. Replacement of MDV USP by SynUSP at the UL36 N-terminus. (A) Schematic representation from vRB-1B, vSynUSP.link and vSynUSP.link-rev; (B) Plaque size assay for comparison of vSynUSP.link with vRB-1B and vSynUSP.link-rev. vSynUSP.link shows slight replication impairment when compared to wild-type vRB-1B and vSynUSPlink-rev revertant (Kruskal-Wallis, $p<0.05$); (C) However, multi-step growth kinetic assays shows no difference between the three viruses at any time point (Kruskal-Wallis test, $p>0.05$). Significant difference in replication is indicated with an asterisk (*).

Following reconstitution of the recombinant viruses in CECs, vSynUSP.link replicated in a fashion comparable to those of parental and revertant virus with respect to multi-step growth kinetics (Figure 20.C) (Kruskal-Wallis test, $p>0.05$), but not in terms of plaque size (Kruskal-Wallis test, $p<0,05$), as it can be observed in Figure 20.B. These results suggest that the exact USP base pair sequence is important for MDV replication.

8.1.5 The enzymatic cysteine box is required for viral replication

Finally, in addition to the invariant active cysteine present within all htUSPs, there are also two residues which are highly conserved: a glutamine and leucine residue (Figure 8) (75). It has been shown that C98 is important for MDV USP function (66).

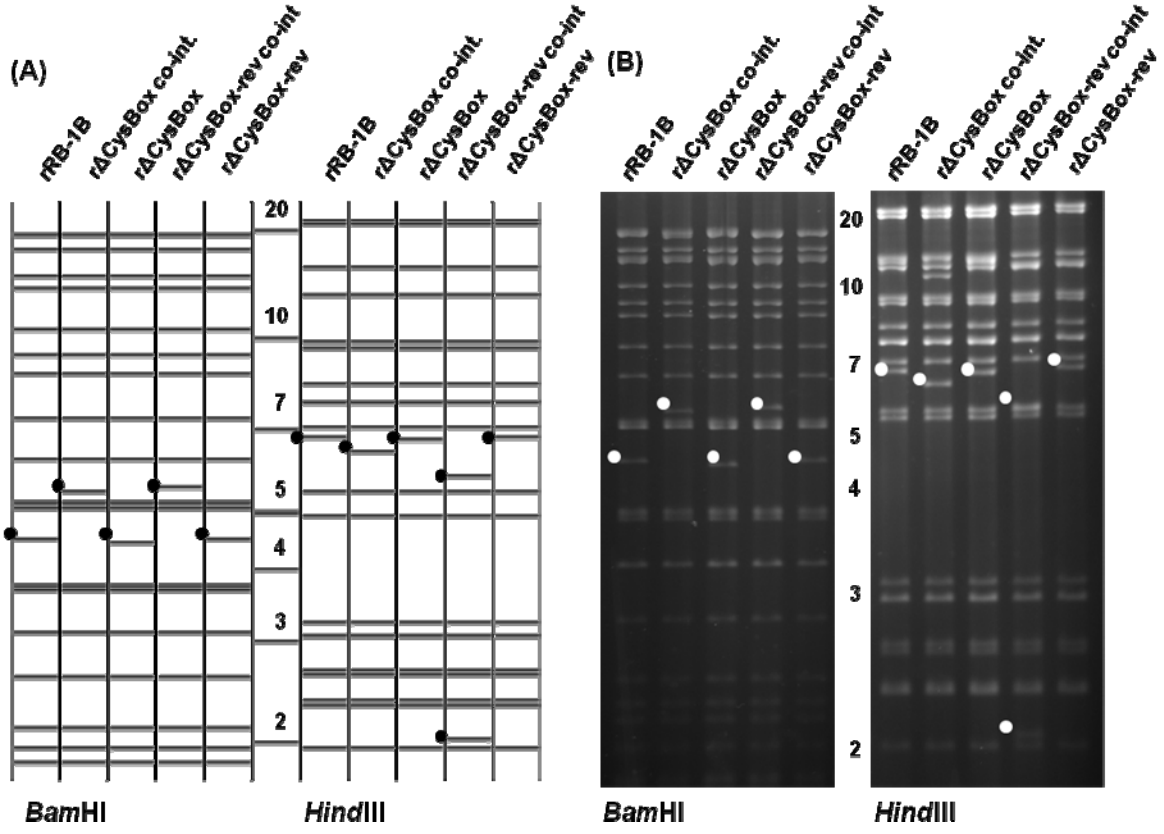

Figure 21. RFLP from rΔCysBox and rΔCysBox-rev clones, compared to wild-type rMDV and co-integrates rMDVs presenting kanamycin cassette. (A) Vector NTI 9.1 prediction with *Bam*HI and *Hind*III. (B) RFLP patterns in 0,8% agarose gels run O/N at 65 V. Co-int stands for co-integrate clones.

However, we were also interested in determining whether the whole Cys box region was required for MDV USP replication. In order to answer this question, the 22 aa comprising these residues were removed (ΔCysBox). A revertant virus was also generated (vΔCysBox-

rev). RFLP patterns from cysteine box removal and reconstitution are shown in Figure 21. Interestingly, removal from the Cys box rendered the virus completely unable to form plaques similar to removal of the complete MDV USP, while its revertant replicated similarly to vRB-1B (Figure 22.B). These results indicated that the region encompassing the Cys box, composed of 22 aa located at the N-terminus of UL36, is essential for MDV replication *in vitro*.

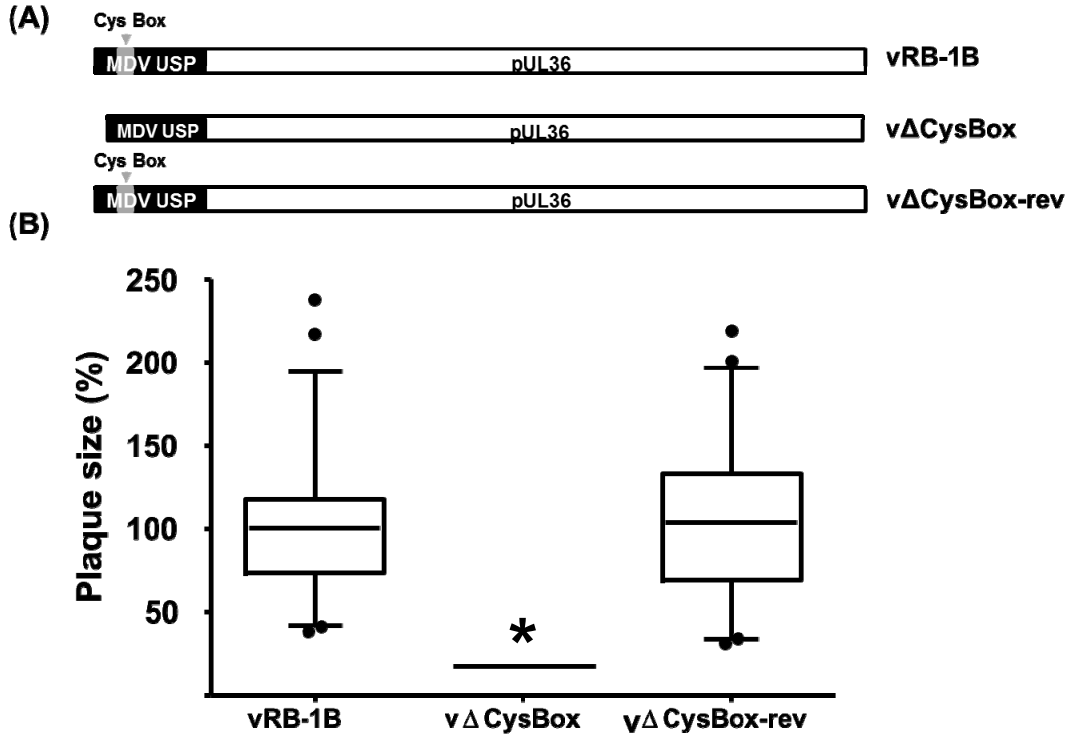

Figure 22. Importance of enzymatic cysteine box site for viral replication. (A) Schematic representation of vRB-1B, vΔCysBox and vΔCysBox-rev rMDVs. (B) Plaque area analysis of vRB-1B, ΔCysBox and vΔCysBox-rev after CECs transfection. Significant differences (Kruskal-Wallis test, $p < 0.05$) are indicated with an asterisk (*).

8.2 MDV USP interaction with oncoprotein Meq

8.2.1 Streptavidin pull-down of Meq by using USP.CTAP as a bait

In this set of experiments our aim was to discover possible interactors of MDV USP, similarly to what was observed for EBV (51, 155, 156), KSHV (134) and HSV-1(12), which could help to better understand the role these enzymes play in MDV replication and tumourigenesis. Our first hypothesis was that MDV USP was protecting viral and cellular proteins from degradation by the proteasome, namely the very potent oncogene Meq (71, 86, 88).

In order to determine whether Meq will co-precipitate with MDV USP, the N-terminal 966 bp of UL36 corresponding to MDV USP from rRB-1B were cloned in a C-terminal TAP expression plasmid that was called pCeMM-USP.CTAP. After transfection of the plasmid into 293T cells, pull-down assays were performed using an adaptation of a previously described protocol (54) either alone or together with vector expressing Meq (pcDNA3-Meq).

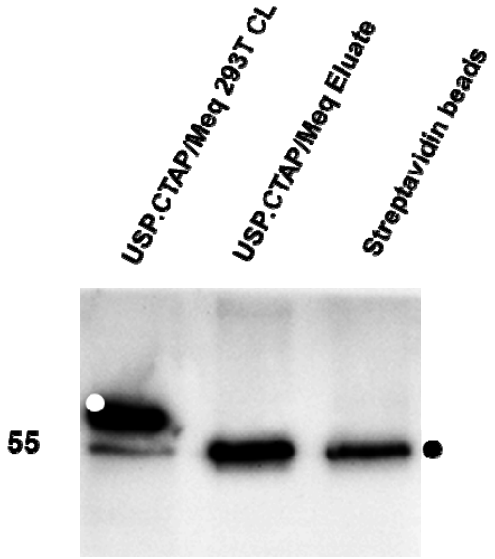

Figure 23. Streptavidin pull-down in 293T cell lysates co-trasfected with pCeMM-USP.CTAP and pcDNA3-Meq. Although both Meq (white dot, around 60 kDa) and USP.CTAP (black dot, 55 KDa) were detectable in the cell lysates, only USP.CTAP but not Meq can be seen in the eluate. PageRuler ^{TM} Prestained Protein Ladder from Fermentas was used as marker (kDa).

Although USP.CTAP could be pulled down by using this technique, Meq could not be detected in the eluate (Figure 23). Also, no other interesting candidates could be identified after analysis of MDV USP-only pull-down assay by mass spectroscopy (data not shown).

8.2.2 Co-localization assays for Meq and USP.HA

IF was performed in order to determine if MDV USP and Meq interact upon transient transfection. For this experiment, 293T cells were co-transfected with both pcDNA3-Meq and pcDNA3-USP.HA, fixed and stained with anti-HA and anti-Meq abs. Confocal microscopy was performed but no co-localization of Meq and MDV USP was detected (Figure 24).

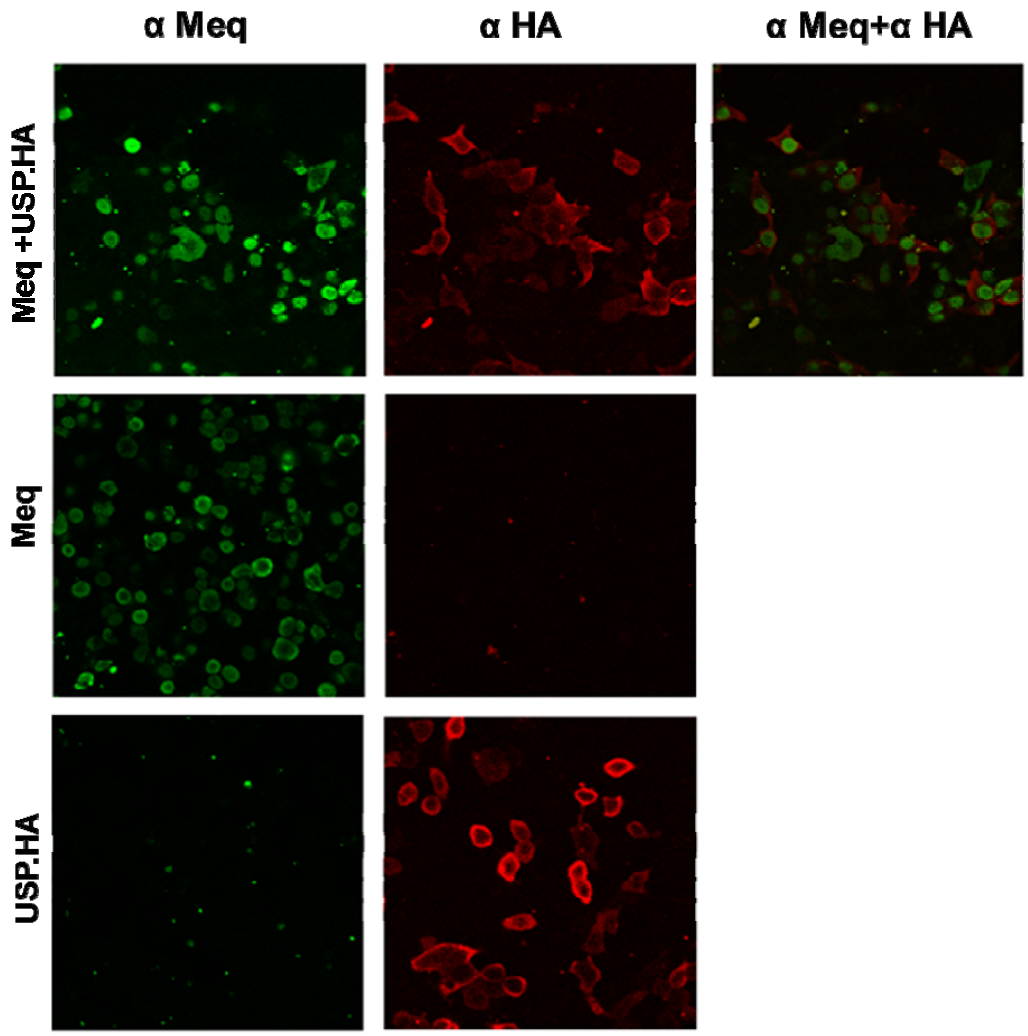

Figure 24. Confocal microscopy images from 293T cells co-transfected with pCDNA3-Meq and pCDNA3-USP.HA. Meq and USP.HA are found in distinct cellular compartments. Pictures taken by Dr. Benedikt Kaufer at 630x amplification.

While Meq was predominantly present in the nucleus, as previously described in the literature (89), MDV USP was found distributed in the cytoplasm in a diffuse fashion.

8.2.3 Yeast two-hybrid assays (Y2H)

To identify potential MDV USP targets, Y2H studies were initiated, in collaboration with Professor Jürgen C. Haas, Dr. Ola Hassanin and Clark Russell from the University of Edinburgh. Due to its length, pUL36 had been previously divided into three fragments (I, II and III), subcloned in both prey and bait plasmids (pGADT7 and pGBKT7 from Clontech Matchmaker Gold Yeast Two-Hybrid System, respectively) and used for interaction studies

with chicken and MDV genome libraries. The N-terminal fragment UL36I prey construct was found to interact with several baits from the MDV library, which is not yet confirmed by a corresponding pUL36I bait construct.

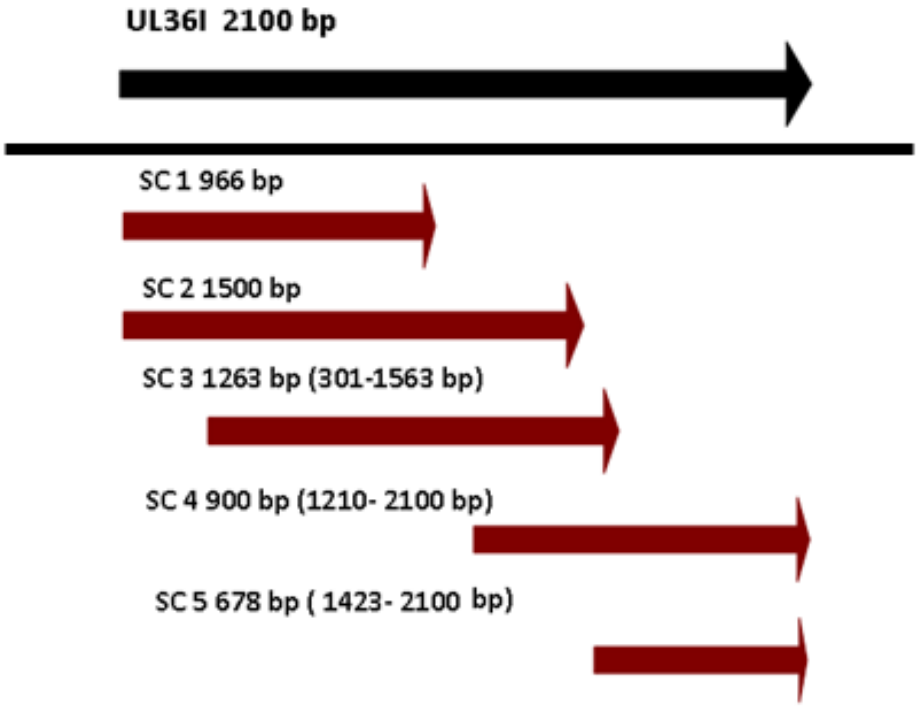

Figure 25. N-terminal subclones from the UL36I fragment.

In order to better determine which portions of the N-terminus of pUL36 are involved in the detected interactions, five fragments from the UL36I fragment were cloned into pGBKT7 bait plasmid (Figure 25). These clones will be used in further Y2H assays for determination of viral and cellular interactors by using both MDV and chicken cell Y2H libraries. Preliminary assays with a Y2H mammalian genome collection library performed by Professor Jürgen C. Haas and Clark Russell indicated some potentially interesting MDV USP interactors, including a E3 ligase (UBE3B), two small GTPase activating proteins (ARGGAP, ARHGAP19) and a regulator of apoptosis (FAIM2), among other hits that are listed in the supplementary information, section 2, page . Further experiments are required for validation of these results and also to know whether similar interactions are found in the chicken cell Y2H library background.

8.3 Detection of putative independently-expressed MDV USP in infected CECs

Detection of MDV pUL36 by using specific abs both in IF and WB has not been possible so far. As previously described (Figure 19), the presence of an HA tag at the C-terminus of SynUSP in vSynUSP.HAlink had a detrimental impact on MDV replication. Also, insertion of FLAG and 6xHis tags at the N-terminus of UL36 did not give positive results in IF, even if the HA tag inserted at the C-terminus of the ectopically expressed N-terminal SynUSP was detectable both by IF and WB. Therefore, after a failed attempt to produce mouse antibodies against two GST-purified peptides specific for two regions of pUL36, anti-peptide antibodies specific for pUL36 were developed. In order to maximize the chances of obtaining a functional ab that would allow us to study both cellular location and MDV pUL36 post-translational cleavage four peptides were used: two specific for the 322 aa region corresponding to MDV USP, and two corresponding to the remaining portion of MDV pUL36; the sequences of the used peptides are shown in Table 11.

Peptide	Sequence	Modifications
USP-1	MTDSTDSRQATTNC	N-terminal acetylation
USP-2	CGTSDIVLDLGRARE	C-terminal amidation
VP1/2-1	KRRRPLWTPQSSSEC	N-terminal acetylation
VP1/2-2	CLLTRRDFRNASRGA	C-terminal amidation

Table 11. Peptides used for ab generation by Genscript. Modifications were introduced in these sequences as indicated in order to increase peptide antigenicity.

Due to very little specificity detected in preliminary test-bleeds, all four sera were purified by Genscript using affinity chromatography. Cell lysates from vRB-1B- or vBac20-infected CECs as wells from pcDNA3-HA.USP transfected DF-1 were separated in a 10% polyacrylamide gel. Separated proteins were transferred to a membrane and the membrane incubated with anti-USP-1 and USP-2 abs that had been diluted 1:50 in 5% NFDM PBST. While the anti-USP-2 ab gave a very unspecific reaction (data not shown), the anti-USP-1 ab was reactive with bands of the predicted size of MDV USP (Figure 26.A).

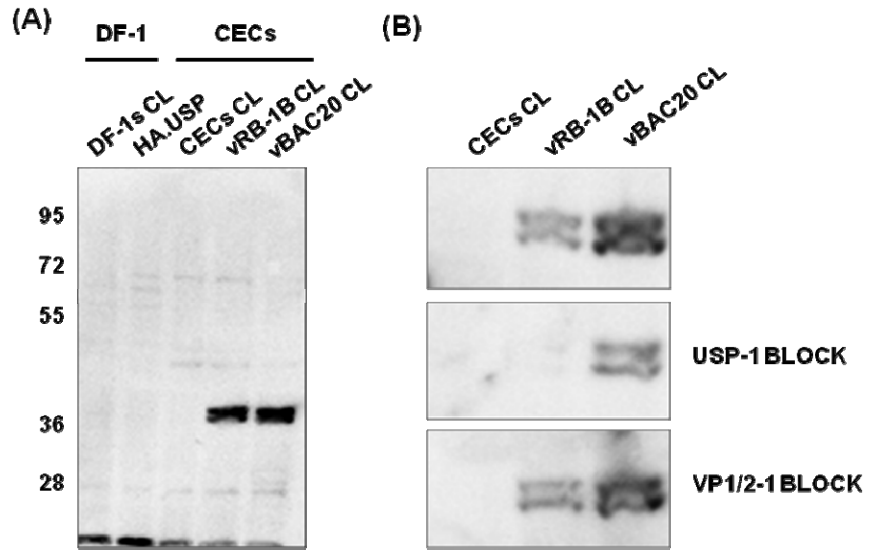

Figure 26. Specific signal obtained after incubation of several MDV USP-expressing cell lysates upon anti-USP-1 antibody incubation. (A) Incubation with anti-USP-1 ab of both transfected and infected cell lysates. PageRuler ™ Prestained Protein Ladder from Fermentas was used as marker (kDa); (B) USP-1 peptide can specifically block anti-USP-1 ab signal after ab solution O/N incubation in 5% NFDM PBST, unlike unspecific VP1/2-1 peptide.

Two specific bands with a molecular mass of approximately 40 kDa in size were consistently observed in both vRB-1B and vBac20-infected CECs, as well as in cell lysates from CECs infected with vSynUSP.link and vSyn.link-rev (Figure 27).

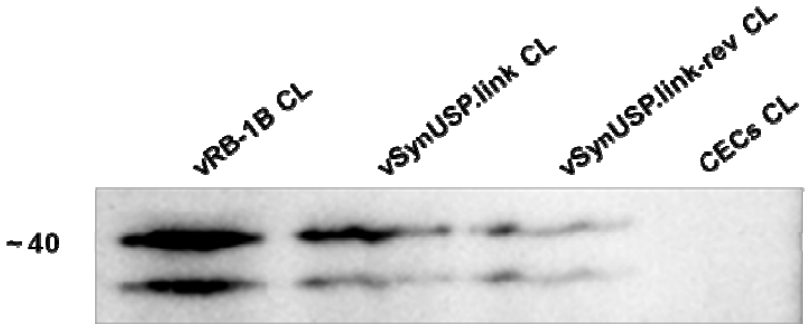

Figure 27. Same anti-USP-1 antibody signal observed for vSynUSP.link and vSynUSP.link-rev. PageRuler ™ Prestained Protein Ladder from Fermentas was used as marker (kDa).

However, these bands could not be identified in cell lysates from growth-defective vMDV, both presenting alterations in the USP region, such as vC98A or vC98A.IRES.SynUSP (data not shown). This is very likely due to a lower concentration of the protein, as these viruses

have considerably lower titers when compared to those of wild-type or revertant viruses. Differences in band intensity in Figure 27 are also likely due to different viral titers.

Intriguingly enough, the anti-USP-1 ab could not detect the 36 kDa pcDNA3-HA.USP construct transfected in DF-1s (Figure 26) and 293T cells (data not shown). After issues in efficiency of transfection were evaluated and determined to likely not be a significant factor using anti-HA IF assays and eGFP transfection controls, *in vitro* transcription/translation of pCDNA3-HA.USP was performed. Results obtained are shown in Figure 28. pcDNA3-HA.USP can be detected with rabbit anti-HA ab diluted 1:1000 in 5% NFDM, but not by the anti-USP-1 ab at 1:50 dilution in the same blocking buffer.

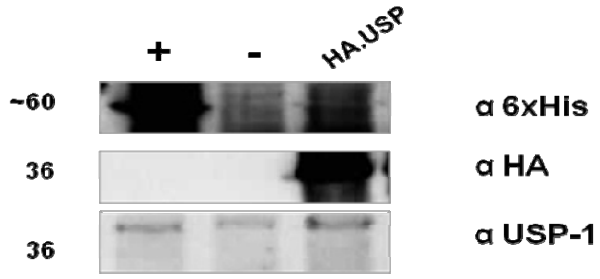

Figure 28. *In-vitro* translation assay for pcDNA3-HA.USP obtained with EasyXpress Insect Kit II from Qiagen. Samples were loaded in three different gels and run simultaneously prior to being incubated O/N with anti-6xHis, anti-HA and anti-USP-1 abs. The positive control is a ~60 kDa protein detected with anti-6xHis ab. PageRuler ™ Prestained Protein Ladder from Fermentas was used as marker (kDa)

However, if the reactivity of the two bands were indeed specific, the data would be consistent with what has been for HSV-1 (75, 154), HCMV (154) and EBV (50, 51) that all express a form of USP cleaved from pUL36.

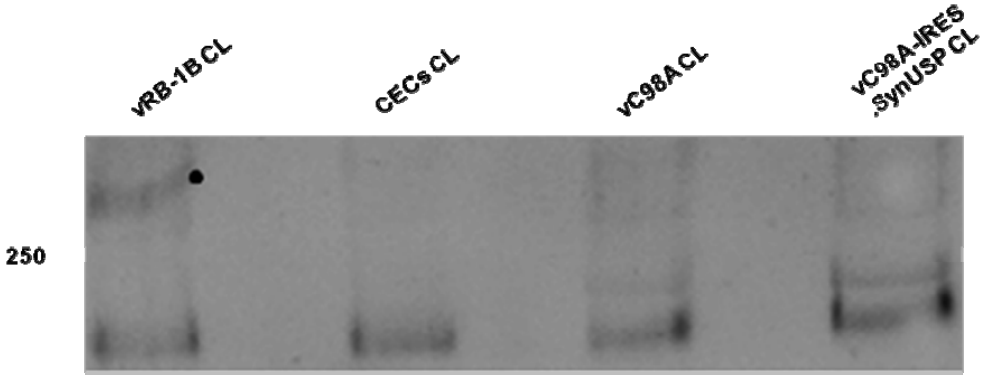

Figure 29. Detection of MDV pUL36 with anti-USP-1 antibody. A protein >250 kDa was detected in vRB-1B-infected CECs cell lysates (black dot). PageRuler ™ Prestained Protein Ladder from Fermentas was used as marker (kDa).

Thus far, detection of the non-cleaved form of the ~330 kDa pUL36 with anti-VP1/2-1 and VP1/2-2 abs could not be observed in infected cell lysates. A band with more than 250 kDa in size could be detected once in vRB-1B-infected cell lysates with anti-USP-1 ab (Figure 29). However, this result could not be replicated to date. MDV-expressed large proteins are particularly difficult to detect in WB, not only due to the virus' strict cell association, which makes virion purification from supernatants next to impossible, but also to the relatively low MDV titers when compared to other viruses such as HSV-1, PRV, HCMV and SCMV, in which large tegument protein detection has been achieved, not only from purified virions, but also from cell lysates (4, 87, 106, 154). Therefore, the described results would need further confirmation.

Regarding IF, several experimental approaches were taken using various conditions of fixation and staining of CECs infected with vRB-1B and Bac20, as well in DF-1 cells transfected with USP constructs; however, all abs gave unspecific signals for both USP and pUL36.

9 Discussion

Since their discovery, htUSPs have garnered much interest, not only due to their function in virus replication and pathogenesis, but also as possible targets for antiviral therapy (140). One of the first proposed hypotheses following htUSP discovery in HSV-1 was that it played an important role in the protection of viral and cellular proteins from proteasomal degradation (75, 84). Therefore, considerable efforts have been devoted to discover interaction partners of htUSPs (12, 51, 134, 155). Most substrates known so far have been identified in gammaherpesviruses. These studies strongly indicate that htUSPs are involved not only in multiple steps of virus replication, but can also eventually hinder DNA repair mechanisms (50, 51, 155, 156) and contribute to avoidance of cellular immune responses during virus infection (134). Also, some recent reports have shown that htUSPs play an important role in stabilizing the large tegument protein pUL36, in which it is embedded, by self-deubiquitination (12).

Regarding MDV USP, the only published report clearly showed that abrogation of USP activity by mutation of the cysteine active site had severe impact on viral pathogenesis (66). This observation led to the hypothesis that MDV USP could contribute to tumourigenesis by deubiquitinating Meq, the potent MDV-encoded oncoprotein (71, 88, 92), or eventually cellular proteins involved in cell cycle regulation. In order to determine whether MDV USP and Meq interact, TAP and IF experiments were performed. However, no interaction between MDV USP and Meq could be shown using TAP (Figure 23) and no other interesting candidates could be identified after analysis of MDV USP-only pull-down assays by mass spectroscopy. Also, no co-localization of Meq and MDV USP was observed by confocal microscopy in 293T cells co-transfected with pcDNA3-HA.USP and pcDNA3-Meq (Figure 24); while Meq is predominantly present in the nucleus as previously described (89), MDV USP was found distributed in the cytoplasm in a diffuse fashion. However, it cannot be excluded that the highly conserved N-terminal NLS1, active both in HSV-1 (4) and PRV (106), is part of a putative MDV USP cleaved form, which would allow USP transport into the nucleus in case this NLS was functional in MDV as well. However, as Meq is a MDV-specific protein and the USP active site is highly conserved throughout all herpesviruses subfamilies, it is also possible that USP functions are highly conserved among herpesviruses, thus reducing the likelihood of USP interactions with virus-specific proteins, in spite of the high homology of Meq's bZIP with the ones encoded by the Jun/Fos family of cellular transcription factors (89). In order to determine which viral and cellular proteins interact with MDV USP in

the MDV and chicken cell Y2H library background, further Y2H experiments shall be performed by Professor Jürgen C. Haas and Clark Russell at the University of Edinburgh; preliminary hits identified in a mammalian genome collection library are promissing but need further validation.

Unlike the MDV USP interaction studies, experiments performed for this project with recombinant MDV presenting alterations in the USP region showed some interesting phenotypes. First, it has been clearly shown that the removal of the N-terminal 322 aa from the UL36 large tegument protein encompassing the USP (ΔUSP) is lethal for virus replication (Figure 15.B), as well as the removal of only 22 aa from the highly conserved USP cysteine box of the 3358 aa long MDV UL36 large tegument protein (Figure 22 B). It has been previously shown that sequential deletions at the C-terminus of PRV pUL36 also led to severe impairment of viral replication, with the notable exception of a 709 aa deletion between residues 2087 and 2795 of the 3084 aa PRV pUL36. This virus replicates with a 10-fold decrease of titers when compared to wild-type virus (14). Also the deletion of seven residues of the highly conserved UL36 NLS led to a virus that is unable to spread unless it infects UL36 complementing cell lines (3). However, we knew from the previous report on MDV USP (66) that the enzymatically inactive vC98A was still able to replicate, albeit in an impaired fashion, as previously described in the literature for PRV (15), MHV-68 (56) and HCMV (154), but not for HSV-1 (12). The fact that 22 aa residues that constitute the cysteine box within the MDV USP are essential for virus replication, whereas an enzymatically inactive DUB still allows virus replication, suggests a structural rather than enzymatic role of USP in MDV replication. Although it is currently not possible to formally support or refute this hypothesis, we surmise that the USP domain is a functional part of the UL36 protein and may play a role in virus assembly (tegumentation) or virus entry and egress, as has been described for HSV-1 (3, 40, 130) and PRV (15). Also the fact that MDV USP sequence is essential for MDV replication seems to support such an interpretation of the results.

To perform USP complementation experiments, a 320 aa codon-optimized SynUSP was synthesized. Insertion at the N-terminus of the UL36 gene as replacement of the original MDV USP sequence (vSynUSP.link) led to replication of the resulting viruses that was comparable to parental vRB-1B and revertant viruses (Figure 20.C) in the multi-step growth kinetics, but not in the plaque sizes (Figure 20.B), thus suggesting that the nucleotide sequence of USP may present specific domais that are optimal for MDV replication. Also, none of the complementation assays in which SynUSP was expressed either under the UL36 promoter at the C- (Figure 16.B) or at the N-terminus of pUL36 (Figure 18 B), or under the HVT ICP4 promoter within the mini-F cassette both in the enzymatically inactive vC98A and

in the structurally impaired vΔUSP backgrounds were successful in rescuing the wild-type phenotype. Therefore, with these recombinant MDVs it was not possible to further investigate the functional role of MDV USP. Replacement of SynUSP by eGFP in the C-terminus of rC98A-IRES.SynUSP did not lead to fluorescent plaques. This is most likely due to the inability of the ribosome to bind the IRES sequence after the long 10 kb UL36 mRNA is translated. In the case of the HVT ICP4.SynUSP insertion in the mini-F sequence, there may be two reasons for the observed non-reversion of phenotypes: either the immediate early (IE) HVT ICP4 promoter is not appropriate for SynUSP expression, as UL36 is expressed with late kinetics, or SynUSP can only be expressed under the control of the authentic UL36 promotor. However, we are limited by the absence of a confirmed USP-specific ab. It is, therefore, not possible to determine whether SynUSP expression actually occurs. In order to test this hypothesis, a late gene promoter such as HVT-expressed gB promoter (147) could eventually be used instead of ICP4 for SynUSP expression in the same location.

As the ectopic expression of SynUSP at the C-terminus from the UL36 ORF did not result in restoration of tumourigenesis (Figure 17.B), the exact role of MDV USP in tumourigenesis remains unclear at this time. However, based on the data provided by the performed experiments with MDV USP recombinants, we hypothesize that the decreased MDV-induced tumourigenesis observed in the absence of an active USP is due predominantly to MDV replication impairment, rather than to a direct MDV USP interference in tumourigenesis.

In order to identify MDV USP and pUL36 expression, several tags were inserted into the MDV genome, both at the N-terminus of the UL36 ORF and in the ectopically expressed HA tagged SynUSP. Even if vC98A-SynUSP.HA grew slightly more robustly in comparison to vC98A, the HA tag present in the context of the whole UL36 gene was deleterious for viral replication, as shown in Figure 19 and Figure 20 by mutants vSynUSP.HAlink and vSynUSP.link. However, it is interesting to note that vSynUSP.HAind was able to grow, even if in a severely impaired fashion when compared to wild-type virus, in spite of being expressed independently from pUL36. HA tag removal from rSynUSP.HA.ind did not change this phenotype (data not shown), but curiously enough, a virus presenting the same two stop codons between MDV USP and pUL36 was unable to grow (data not shown). The only difference between this virus and vSynUSP.ind is that MDV USP is 322 aa long, whereas SynUSP is 320 aa long (Figure 13). The question that still remains is why the insertion of two stop codons two aa downstream in the pUL36 sequence seems to completely eliminate viral replication. Therefore, it would be interesting to insert an IRES immediately downstream from SynUP.HA in the vC98A-SynUSP.HA background in order to determine whether this virus' impairment is due not to insufficient complementation but to low pUL36 expression levels.

Also the removal of the HA from SynUSP.HA in vC98A-SynUSP.HA could show whether the observed impairment is due once again to the presence of the tag.

Regarding the production of USP and pUL36-specific antibodies, after an unsuccessful attempt to produce polyclonal mouse abs specific for two fragments of the UL36 protein, four anti-peptide rabbit abs were commercially developed. While no conclusive result has been obtained for three of the antibodies to date, two specific 40 kDa bands could be identified in MDV-infected cell lysates with one of the generated abs (anti-USP-1) (Figure 26). So far, it is still unclear whether all htUSPs are cleaved from the large tegument protein and expressed as a separate protein, or whether they perform their major functions only in the context of the pUL36. HSV-1 USP is expressed both independently (75) and as post-translationally cleaved form of pUL36, with either having DUB activity (154). A similar situation is described for HCMV, in which both the non-cleaved form and a ~38 kDa catalytic fragment were found to interact with an HAUbVME DUB detection probe, previously used for identification of other USPs (75, 139) and for structural studies (140). However, in the case of SCMV, only the uncleaved form of the large tegument protein was found to bind Ub (154). In addition, a 325 aa N-terminal fragment of EBV BPLF1 transfected in HeLa cells could actively cleave both Ub and NEDD8 bound to GFP (50, 51). Taken together, these observations indicate that at least some htUSPs can be expressed independently from the large tegument protein in members of all herpesviruses subfamilies. Therefore, the 40 kDa bands observed with anti-USP-1 in MDV may correspond to a cleaved form of pUL36, which could be active on its own. However, in spite of its specificity in infected cell lysates, anti-USP-1 ab could not detect USP in cell lysates of DF-1 cells transfected with pcDNA3-HA.USP (Figure 26) and pcDNA3-USP.HA (data not shown). *In vitro* translation assays using pcDNA3-HA.USP were also not successfully detected with the antibody (Figure 28). These results can indicate that the two 40kDa bands observed in the infected vMDV cell lysates are not specific for USP, that the N-terminal UL36 region is unstable in the absence of other viral proteins, or that, for some unknown reason, anti-USP-1 ab is unable to specifically detect USP expressed by pcDNA3-HA.USP. Therefore, we are still unable to to conclusively determine whether the two bands detected by anti-USP-1 are specific for USP.Therefore, further characterization of this ab is necessary, not only by using other eukaryotic expression clones, but also by finding a reliable MDV infection control. Also, the fact that two bands are observed may indicate the occurrence of post-translational modifications, such as phosphorylation. Regarding WB detection of the uncleaved protein, the >250 kDa band detected with anti-USP-1 (Figure 29) could correspond to pUL36, but this observation needs to be confirmed by further experiments using different cell lysis techniques, gel concentrations and constitutions, as well as other antibody incubation conditions as the ones used in this project.

In conclusion, although no data could be provided regarding MDV USP interaction partners, this report further defines the importance of MDV USP for virus replication with four important findings. First, the N-terminal UL36 region encompassing USP is essential for MDV replication beyond its enzymatic activity, as the enzymatically inactive vC98A is still able to replicate, whereas the Cys box mutant virus, vΔCysBox, is not. Second, ectopic expression of MDV USP did not restore virus replication and tumourigenesis in replication-defective viruses, suggesting that MDV USP is an integral part of the UL36 large tegument protein in order to be functional. Third, the primary nucleotide sequence of USP seems to present domains that are important for virus replication. Fourth, the insertion of the HA tag at the C-terminus of the USP strongly impairs viral replication. Finally, two bands with an approximate moleclular mass of 40 kDa were identified by WB using a USP-specific antibody, which could eventually correspond to a cleaved MDV pUL36 product encompassing USP.

10 Summary

Marek´s disease (MD) is a poultry disease with a worldwide distribution. The disease is caused by MD virus (MDV), an alphaherpesvirus in the *Mardivirus* genus. MDV causes neurological symptoms and CD4+ T cell visceral lymphomas, which eventually lead to the death of the affected animals. First described in 1907 by Jozef Marek as a slowly progressing chronic polyneuritis, MD became a major worry for poultry producers due to the severity of symptoms and the lack of effective control measures until vaccines were developed in the 1960s. The various vaccines have resulted in a reduction of disease incidence, but not in sterilizing immunity, which has led to constantly increasing virulence of circulating field strains, ultimately leading to the selection of highly virulent viruses. These strains continue to threaten chickens and it is, therefore, important to study MDV genes involved in viral pathogenesis. In addition to the MDV-encoded oncoprotein Meq and the viral telomerase, the UL36 gene plays an essential role in MDV pathogenesis. This gene was recently found to encode a deubiquitinase (DUB). The ubiquitin-specific protease (USP) is embedded in the N-terminal part of the large tegument protein (pUL36). The USP is highly conserved among herpesviruses and replacement of its putative active site cysteine by an alanine had a profound effect on *in vitro* replication and *in vivo* tumourigenesis. However, in these previous studies it was not possible to determine which proteins interact with MDV USP, and also if the observed effects were due to structural significance of the N-terminus of the UL36-encoded large tegument protein or solely to its enzymatic activity.

In this dissertation, USP-Meq interaction studies were performed and several mutant viruses based on the very virulent RB-1B MDV strain were constructed by two-step Red mediated recombination. The mutants were designed to allow differentiation between USP enzymatic and structural function. Even if the interaction between MDV USP and Meq could not be confirmed, it was shown that both the N-terminal UL36 region and its highly-conserved USP cysteine box are essential for viral replication. Also, ectopical expression of a functional, synthetic USP (SynUSP) in several locations of the MDV genome could not compensate for the absence of a (functional) USP, suggesting that the large tegument protein can only exert its functions if USP is expressed in frame within the UL36 protein. We concluded from our studies that MDV USP has a structural role beyond its enzymatic activity, which implies that the decreased tumourigenesis observed in the absence of an active USP is partly due to MDV replication impairment and not to a direct activity of USP in tumourigenesis.

Additionally, specific antibodies for MDV USP and for pUL36 were produced. Two 40 kDa bands were detected with one of the antibodies in MDV-infected cell lysates, which could correspond to cleaved MDV USP, similar to what was previously identified in other herpesviruses.

11 Zusammenfassung

Die vom UL36-Gen Kodierte Ubiquitin-Spezifische Protease des Virus der Marek‘schen Krankheit (MDV) und seine Rolle in Replikation und Tumourigenese

Die Marek’sche Krankheit (MD) ist eine weltweit verbreitete Erkrankung von Geflügel. Das Virus der Marek’schen Krankheit (MDV), der Auslöser der Erkrankung, wird innerhalb der Alphaherpesviren zum Genus *Mardivirus* gezählt. Neben neurologischen Symptomen führt die Infektion mit MDV auch zur Entstehung von CD4+ T-Zelllymphomen welche schließlich zum Tod des betroffenen Tieres führen. Nach der Erstbeschreibung der Krankheit als langsam fortschreitende, chronische Polyneuritis im Jahre 1907 durch den Tierarzt Jozef Marek, entwickelte sich MD aufgrund der schwerwiegenden Symptomatik sowie dem Fehlen von effektiven Kontrollmechanismen zu einem großen Problem für die Geflügelindustrie. Die Entwicklung und Einführung von Impfstoffen in den 1960iger Jahren konnte die Inzidenz der Marek’schen Krankheit zwar reduzieren, jedoch wird durch die Vakzination keine sterile Immunität erreicht. Dieser Umstand hat in den letzten Jahrzehnten zur Selektion von hochvirulenten Viren geführt, die sich in einer steigenden Virulenz der zirkulierenden Feldstämme niederschlägt. Da entsprechende Stämme auch weiterhin Geflügelbestände weltweit bedrohen, ist es von entscheidender Bedeutung die für die virale Pathogenese verantwortlichen Gene zu untersuchen. Neben dem von MDV kodierten Onkoprotein Meq sowie der viralen Telomerase ist auch das Gen UL36 an der Pathogenese des Virus beteiligt. In diesem Zusammenhang wurde das Genprodukt pUL36 kürzlich als Deubiquitinase (DUB) beschrieben. Die für die Funktion entscheidene Ubiquitin-spezifische Protease (USP) befindet sich dabei in dem N-terminalen Teil des pUL36. Zudem ist die USP innerhalb der Herpesviren hochkonserviert und der Austausch des katalytischen Cysteins im aktiven Zentrum des Proteins hat einen ausgeprägten Effekt auf die Replikation *in vitro* sowie die Tumourgenese *in vivo*. In vorhergehenden Studien war es nicht möglich die Interaktionspartner der MDV USP zu identifizieren. Ungeklärt blieb zudem ob der beschriebene Einfluss auf die Pathogenese von struktureller oder enzymatischer Natur ist.

In der vorliegenden Dissertation wurden USP-Meq–Interaktionsstudien durchgeführt. Außerdem wurden, mit Hilfe einer zweistufigen Red-Mutagenese, virale USP-Mutanten erzeugt, die auf dem sehr virulenten MDV Stamm RB-1B basierten. Die Mutanten wurden dabei so konstruiert, dass sie eine Unterscheidung zwischen enzymatischer und struktureller Funktion der USP erlauben. Obwohl eine direkte Interaktion zwischen Meq und USP nicht nachweisbar war, konnte gezeigt werden, dass die N-terminale Region sowie die

hochkonservierte USP Cystein-Box des pUL36 für die virale Replikation essentiell sind. Des Weiteren konnte die ektopische Expression einer synthetischen aber funktionalen USP (SynUSP) innerhalb verschiedener Positionen des MDV-Genoms nicht die Abwesenheit der originalen Sequenz kompensieren. Dieses Ergebnis implizierte, dass das Tegumentprotein pUL36 seine Funktion nur ausführen kann wenn die USP im selben Leserahmen exprimiert wird. Aus unseren Untersuchungen folgerten wir, dass MDV USP neben seiner enzymatischen Funktion auch eine strukturelle Rolle innerhalb des Proteins besitzt. Die verminderte Tumourgenese, die in der Abwesenheit einer aktiven USP beobachtet wurde, ist daher wahrscheinlich durch die generelle Beeinträchtigung der viralen Replikation zu erklären und nicht etwa durch eine direkte Aktivität der USP im Prozess der Krebsentstehung.

Abschließend wurden spezifische Antikörper gegen das MDV USP sowie pUL36 produziert. Zwei Banden von etwa 40 kDa konnten mit einem der Antikörper in Lysaten infizierter Zellen detektiert werden. Ähnlich wie bei anderen Herpesviren beobachtet, korrespondierten diese Banden in ihrer Größe mit einer gespalten USP.

12 References

1. 2004. Sequence and comparative analysis of the chicken genome provide unique perspectives on vertebrate evolution. Nature **432:**695-716.
2. **Abaitua, F., T. Daikoku, C. M. Crump, M. Bolstad, and P. O'Hare.** 2011. A single mutation responsible for temperature-sensitive entry and assembly defects in the VP1-2 protein of herpes simplex virus. J Virol **85:**2024-36.
3. **Abaitua, F., M. Hollinshead, M. Bolstad, C. M. Crump, and P. O'Hare.** 2012. A Nuclear localization signal in herpesvirus protein VP1-2 is essential for infection via capsid routing to the nuclear pore. J Virol **86:**8998-9014.
4. **Abaitua, F., and P. O'Hare.** 2008. Identification of a highly conserved, functional nuclear localization signal within the N-terminal region of herpes simplex virus type 1 VP1-2 tegument protein. J Virol **82:**5234-44.
5. **Abaitua, F., R. N. Souto, H. Browne, T. Daikoku, and P. O'Hare.** 2009. Characterization of the herpes simplex virus (HSV)-1 tegument protein VP1-2 during infection with the HSV temperature-sensitive mutant tsB7. J Gen Virol **90:**2353-63.
6. **Abramoff, M. D. M., Paulo J.; Ram, Sunanda J.** 2004. Image processing with ImageJ. Biophotonics international **Volume: 11:**pp. 36-42.
7. **Amerik, A. Y., and M. Hochstrasser.** 2004. Mechanism and function of deubiquitinating enzymes. Biochim Biophys Acta **1695:**189-207.
8. **Baigent, S. J., and F. Davison.** 2004. 6 - Marek's disease virus: Biology and life cycle, p. 62-ii. *In* D. Fred and N. Venugopal (ed.), Marek's Disease. Academic Press, Oxford.
9. **Batterson, W., D. Furlong, and B. Roizman.** 1983. Molecular genetics of herpes simplex virus. VIII. further characterization of a temperature-sensitive mutant defective in release of viral DNA and in other stages of the viral reproductive cycle. J Virol **45:**397-407.
10. **Beckmann, J. S., F. Maurer, M. Delorenzi, and L. Falquet.** 2005. On ubiquitin ligases and cancer. Hum Mutat **25:**507-12.
11. **Blondeau, C., N. Chbab, C. Beaumont, K. Courvoisier, N. Osterrieder, J. F. Vautherot, and C. Denesvre.** 2007. A full UL13 open reading frame in Marek's disease virus (MDV) is dispensable for tumour formation and feather follicle tropism and cannot restore horizontal virus transmission of rRB-1B in vivo. Vet Res **38:**419-33.
12. **Bolstad, M., F. Abaitua, C. M. Crump, and P. O'Hare.** 2011. Autocatalytic activity of the ubiquitin-specific protease domain of herpes simplex virus 1 VP1-2. J Virol **85:**8738-51.
13. **Borchers, K., D. Lieckfeldt, A. Ludwig, H. Fukushi, G. Allen, R. Fyumagwa, and R. Hoare.** 2008. Detection of Equid herpesvirus 9 DNA in the trigeminal ganglia of a Burchell's zebra from the Serengeti ecosystem. J Vet Med Sci **70:**1377-81.
14. **Bottcher, S., B. G. Klupp, H. Granzow, W. Fuchs, K. Michael, and T. C. Mettenleiter.** 2006. Identification of a 709-amino-acid internal nonessential region within the essential conserved tegument protein (p)UL36 of pseudorabies virus. J Virol **80:**9910-5.
15. **Bottcher, S., C. Maresch, H. Granzow, B. G. Klupp, J. P. Teifke, and T. C. Mettenleiter.** 2008. Mutagenesis of the active-site cysteine in the ubiquitin-specific protease contained in large tegument protein pUL36 of pseudorabies virus impairs viral replication in vitro and neuroinvasion in vivo. J Virol **82:**6009-16.
16. **Brown, A. C., L. P. Smith, L. Kgosana, S. J. Baigent, V. Nair, and M. J. Allday.** 2009. Homodimerization of the Meq viral oncoprotein is necessary for induction of T-cell lymphoma by Marek's disease virus. J Virol **83:**11142-51.

17. **Bucks, M. A., K. J. O'Regan, M. A. Murphy, J. W. Wills, and R. J. Courtney.** 2007. Herpes simplex virus type 1 tegument proteins VP1/2 and UL37 are associated with intranuclear capsids. Virology **361:**316-24.
18. **Burckstummer, T., K. L. Bennett, A. Preradovic, G. Schutze, O. Hantschel, G. Superti-Furga, and A. Bauch.** 2006. An efficient tandem affinity purification procedure for interaction proteomics in mammalian cells. Nat Methods **3:**1013-9.
19. **Calnek, B. W.** 1986. Marek's disease--a model for herpesvirus oncology. Crit Rev Microbiol **12:**293-320.
20. **Calnek, B. W.** 2001. Pathogenesis of Marek's disease virus infection. Curr Top Microbiol Immunol **255:**25-55.
21. **Cardone, G., W. W. Newcomb, N. Cheng, P. T. Wingfield, B. L. Trus, J. C. Brown, and A. C. Steven.** 2012. The UL36 Tegument Protein of Herpes Simplex Virus 1 Has a Composite Binding Site at the Capsid Vertices. J Virol.
22. **Catic, A., and H. L. Ploegh.** 2005. Ubiquitin--conserved protein or selfish gene? Trends Biochem Sci **30:**600-4.
23. **Cebrian, J., C. Kaschka-Dierich, N. Berthelot, and P. Sheldrick.** 1982. Inverted repeat nucleotide sequences in the genomes of Marek disease virus and the herpesvirus of the turkey. Proc Natl Acad Sci U S A **79:**555-8.
24. **Chang, J. T., M. F. Schmid, F. J. Rixon, and W. Chiu.** 2007. Electron cryotomography reveals the portal in the herpesvirus capsid. J Virol **81:**2065-8.
25. **Chau, V., J. Tobias, A. Bachmair, D. Marriott, D. Ecker, D. Gonda, and A. Varshavsky.** 1989. A multiubiquitin chain is confined to specific lysine in a targeted short-lived protein. Science **243:**1576-1583.
26. **Churchill, A. E., L. N. Payne, and R. C. Chubb.** 1969. Immunization against Marek's disease using a live attenuated virus. Nature **221:**744-7.
27. **Clinton, M., D. Zhao, D. McBride, S. Nandi, H. A. McQueen, M. J. McGrew, P. M. Hocking, P. D. Lewis, and H. M. Sang.** 2010. Somatic sex identity is cell autonomous in the chicken. Nature **464:**237-U115.
28. **Colleaux, L., L. d'Auriol, M. Betermier, G. Cottarel, A. Jacquier, F. Galibert, and B. Dujon.** 1986. Universal code equivalent of a yeast mitochondrial intron reading frame is expressed into E. coli as a specific double strand endonuclease. Cell **44:**521-33.
29. **Coller, K. E., J. I. Lee, A. Ueda, and G. A. Smith.** 2007. The capsid and tegument of the alphaherpesviruses are linked by an interaction between the UL25 and VP1/2 proteins. J Virol **81:**11790-7.
30. **Copeland, A. M., W. W. Newcomb, and J. C. Brown.** 2009. Herpes simplex virus replication: roles of viral proteins and nucleoporins in capsid-nucleus attachment. J Virol **83:**1660-8.
31. **Costa, M. D., and H. L. Paulson.** 2011. Toward understanding Machado-Joseph disease. Prog Neurobiol.
32. **Cramer, S. D., G. A. Campbell, B. L. Njaa, S. E. Morgan, S. K. Smith, 2nd, W. R. t. McLin, B. W. Brodersen, A. G. Wise, G. Scherba, I. M. Langohr, and R. K. Maes.** 2011. Pseudorabies virus infection in Oklahoma hunting dogs. J Vet Diagn Invest **23:**915-23.
33. **Davison, A. J.** 2002. Evolution of the herpesviruses. Vet Microbiol **86:**69-88.
34. **Davison, A. J., R. Eberle, B. Ehlers, G. S. Hayward, D. J. McGeoch, A. C. Minson, P. E. Pellett, B. Roizman, M. J. Studdert, and E. Thiry.** 2009. The order Herpesvirales. Arch Virol **154:**171-7.
35. **Davison, A. J., B. L. Trus, N. Cheng, A. C. Steven, M. S. Watson, C. Cunningham, R. M. Le Deuff, and T. Renault.** 2005. A novel class of herpesvirus with bivalve hosts. J Gen Virol **86:**41-53.
36. **Delecluse, H. J., and W. Hammerschmidt.** 1993. Status of Marek's disease virus in established lymphoma cell lines: herpesvirus integration is common. J Virol **67:**82-92.

37. **Delecluse, H. J., S. Schuller, and W. Hammerschmidt.** 1993. Latent Marek's disease virus can be activated from its chromosomally integrated state in herpesvirus-transformed lymphoma cells. EMBO J **12:**3277-86.
38. **Deng, B., C. M. O'Connor, D. H. Kedes, and Z. H. Zhou.** 2007. Direct visualization of the putative portal in the Kaposi's sarcoma-associated herpesvirus capsid by cryoelectron tomography. J Virol **81:**3640-4.
39. **Desai, P., G. L. Sexton, J. M. McCaffery, and S. Person.** 2001. A null mutation in the gene encoding the herpes simplex virus type 1 UL37 polypeptide abrogates virus maturation. J Virol **75:**10259-71.
40. **Desai, P. J.** 2000. A null mutation in the UL36 gene of herpes simplex virus type 1 results in accumulation of unenveloped DNA-filled capsids in the cytoplasm of infected cells. J Virol **74:**11608-18.
41. **Donovan, T. A., M. D. Schrenzel, T. Tucker, A. P. Pessier, B. Bicknese, M. D. Busch, A. G. Wise, R. Maes, M. Kiupel, C. McKnight, and R. W. Nordhausen.** 2009. Meningoencephalitis in a polar bear caused by equine herpesvirus 9 (EHV-9). Vet Pathol **46:**1138-43.
42. **Ellegren, H.** 2001. Hens, cocks and avian sex determination. A quest for genes on Z or W? EMBO Rep **2:**192-6.
43. **Fadly, A. M.** 2008. Neoplastic diseases, p. 405-407. *In* A. M. F. Y. M. Saif, John R. Glisson , Larry R. McDougald , L. K. Nolan , David E. Swayne (ed.), Diseases of poultry, 11th ed. Wiley-Blackwell.
44. **Fortier, G., E. van Erck, S. Pronost, P. Lekeux, and E. Thiry.** 2010. Equine gammaherpesviruses: pathogenesis, epidemiology and diagnosis. Vet J **186:**148-56.
45. **Fragnet, L., M. A. Blasco, W. Klapper, and D. Rasschaert.** 2003. The RNA subunit of telomerase is encoded by Marek's disease virus. J Virol **77:**5985-96.
46. **Fuchs, W., H. Granzow, B. G. Klupp, M. Kopp, and T. C. Mettenleiter.** 2002. The UL48 tegument protein of pseudorabies virus is critical for intracytoplasmic assembly of infectious virions. J Virol **76:**6729-42.
47. **Fuchs, W., B. G. Klupp, H. Granzow, and T. C. Mettenleiter.** 2004. Essential function of the pseudorabies virus UL36 gene product is independent of its interaction with the UL37 protein. J Virol **78:**11879-89.
48. **Fukushi, H., T. Tomita, A. Taniguchi, Y. Ochiai, R. Kirisawa, T. Matsumura, T. Yanai, T. Masegi, T. Yamaguchi, and K. Hirai.** 1997. Gazelle herpesvirus 1: a new neurotropic herpesvirus immunologically related to equine herpesvirus 1. Virology **227:**34-44.
49. **Gao, G., and H. Luo.** 2006. The ubiquitin-proteasome pathway in viral infections. Can J Physiol Pharmacol **84:**5-14.
50. **Gastaldello, S., S. Callegari, G. Coppotelli, S. Hildebrand, M. Song, and M. G. Masucci.** 2012. Herpes virus deneddylases interrupt the cullin-RING ligase neddylation cycle by inhibiting the binding of CAND1. J Mol Cell Biol **4:**242-51.
51. **Gastaldello, S., S. Hildebrand, O. Faridani, S. Callegari, M. Palmkvist, C. Di Guglielmo, and M. G. Masucci.** 2010. A deneddylase encoded by Epstein-Barr virus promotes viral DNA replication by regulating the activity of cullin-RING ligases. Nat Cell Biol **12:**351-61.
52. **Gibson, W.** 1981. Structural and nonstructural proteins of strain Colburn cytomegalovirus. Virology **111:**516-37.
53. **Gibson, W., and B. Roizman.** 1972. Proteins specified by herpes simplex virus. 8. Characterization and composition of multiple capsid forms of subtypes 1 and 2. J Virol **10:**1044-52.
54. **Glatter, T., A. Wepf, R. Aebersold, and M. Gstaiger.** 2009. An integrated workflow for charting the human interaction proteome: insights into the PP2A system. Mol Syst Biol **5:**237.
55. **Glickman, M. H., and A. Ciechanover.** 2002. The ubiquitin-proteasome proteolytic pathway: destruction for the sake of construction. Physiol Rev **82:**373-428.

56. **Gredmark-Russ, S., M. K. Isaacson, L. Kattenhorn, E. J. Cheung, N. Watson, and H. L. Ploegh.** 2009. A gammaherpesvirus ubiquitin-specific protease is involved in the establishment of murine gammaherpesvirus 68 infection. J Virol **83:**10644-52.
57. **Gredmark, S., C. Schlieker, V. Quesada, E. Spooner, and H. L. Ploegh.** 2007. A functional ubiquitin-specific protease embedded in the large tegument protein (ORF64) of murine gammaherpesvirus 68 is active during the course of infection. J Virol **81:**10300-9.
58. **Greenwood, A. D., K. Tsangaras, S. Y. Ho, C. A. Szentiks, V. M. Nikolin, G. Ma, A. Damiani, M. L. East, A. Lawrenz, H. Hofer, and N. Osterrieder.** 2012. A Potentially Fatal Mix of Herpes in Zoos. Curr Biol.
59. **Hershko, A., and A. Ciechanover.** 1998. The ubiquitin system. Annu Rev Biochem **67:**425-79.
60. **Hicke, L., and R. Dunn.** 2003. Regulation of membrane protein transport by ubiquitin and ubiquitin-binding proteins. Annu Rev Cell Dev Biol **19:**141-72.
61. **Himly, M., D. N. Foster, I. Bottoli, J. S. Iacovoni, and P. K. Vogt.** 1998. The DF-1 chicken fibroblast cell line: transformation induced by diverse oncogenes and cell death resulting from infection by avian leukosis viruses. Virology **248:**295-304.
62. **Homa, F. L., and J. C. Brown.** 1997. Capsid assembly and DNA packaging in herpes simplex virus. Reviews in Medical Virology **7:**107-122.
63. **Ichimura, Y., T. Kirisako, T. Takao, Y. Satomi, Y. Shimonishi, N. Ishihara, N. Mizushima, I. Tanida, E. Kominami, M. Ohsumi, T. Noda, and Y. Ohsumi.** 2000. A ubiquitin-like system mediates protein lipidation. Nature **408:**488-92.
64. **Isaacson, M. K., and H. L. Ploegh.** 2009. Ubiquitination, ubiquitin-like modifiers, and deubiquitination in viral infection. Cell Host Microbe **5:**559-70.
65. **Jainkittivong, A., and R. P. Langlais.** 1998. Herpes B virus infection. Oral Surg Oral Med Oral Pathol Oral Radiol Endod **85:**399-403.
66. **Jarosinski, K., L. Kattenhorn, B. Kaufer, H. Ploegh, and N. Osterrieder.** 2007. A herpesvirus ubiquitin-specific protease is critical for efficient T cell lymphoma formation. Proc Natl Acad Sci U S A **104:**20025-30.
67. **Jarosinski, K. W., N. G. Margulis, J. P. Kamil, S. J. Spatz, V. K. Nair, and N. Osterrieder.** 2007. Horizontal transmission of Marek's disease virus requires US2, the UL13 protein kinase, and gC. J Virol **81:**10575-87.
68. **Jarosinski, K. W., and N. Osterrieder.** 2010. Further analysis of Marek's disease virus horizontal transmission confirms that U(L)44 (gC) and U(L)13 protein kinase activity are essential, while U(S)2 is nonessential. J Virol **84:**7911-6.
69. **Jarosinski, K. W., N. Osterrieder, V. K. Nair, and K. A. Schat.** 2005. Attenuation of Marek's disease virus by deletion of open reading frame RLORF4 but not RLORF5a. J Virol **79:**11647-59.
70. **Jarosinski, K. W., R. Yunis, P. H. O'Connell, C. J. Markowski-Grimsrud, and K. A. Schat.** 2002. Influence of genetic resistance of the chicken and virulence of Marek's disease virus (MDV) on nitric oxide responses after MDV infection. Avian Dis **46:**636-49.
71. **Jones, D., L. Lee, J. L. Liu, H. J. Kung, and J. K. Tillotson.** 1992. Marek disease virus encodes a basic-leucine zipper gene resembling the fos/jun oncogenes that is highly expressed in lymphoblastoid tumours. Proc Natl Acad Sci U S A **89:**4042-6.
72. **Jovasevic, V., L. Liang, and B. Roizman.** 2008. Proteolytic cleavage of VP1-2 is required for release of herpes simplex virus 1 DNA into the nucleus. J Virol **82:**3311-9.
73. **Kaiser, P., and L. Huang.** 2005. Global approaches to understanding ubiquitination. Genome Biol **6:**233.
74. **Karlin, S., E. S. Mocarski, and G. A. Schachtel.** 1994. Molecular evolution of herpesviruses: genomic and protein sequence comparisons. J Virol **68:**1886-902.
75. **Kattenhorn, L. M., G. A. Korbel, B. M. Kessler, E. Spooner, and H. L. Ploegh.** 2005. A deubiquitinating enzyme encoded by HSV-1 belongs to a family of cysteine proteases that is conserved across the family Herpesviridae. Mol Cell **19:**547-57.

76. **Kaufer, B. B., S. Arndt, S. Trapp, N. Osterrieder, and K. W. Jarosinski.** 2011. Herpesvirus Telomerase RNA (vTR) with a Mutated Template Sequence Abrogates Herpesvirus-Induced Lymphomagenesis. PLoS Pathog **7:**e1002333.
77. **Kaufer, B. B., K. W. Jarosinski, and N. Osterrieder.** 2011. Herpesvirus telomeric repeats facilitate genomic integration into host telomeres and mobilization of viral DNA during reactivation. J Exp Med **208:**605-15.
78. **Kelly, B. J., B. Mijatov, C. Fraefel, A. L. Cunningham, and R. J. Diefenbach.** 2012. Identification of a single amino acid residue which is critical for the interaction between HSV-1 inner tegument proteins pUL36 and pUL37. Virology **422:**308-16.
79. **Kerscher, O., R. Felberbaum, and M. Hochstrasser.** 2006. Modification of proteins by ubiquitin and ubiquitin-like proteins. Annu Rev Cell Dev Biol **22:**159-80.
80. **Kim, J. H., K. C. Park, S. S. Chung, O. Bang, and C. H. Chung.** 2003. Deubiquitinating enzymes as cellular regulators. Journal of Biochemistry **134:**9-18.
81. **Klupp, B. G., W. Fuchs, H. Granzow, R. Nixdorf, and T. C. Mettenleiter.** 2002. Pseudorabies virus UL36 tegument protein physically interacts with the UL37 protein. J Virol **76:**3065-71.
82. **Ko, D. H., A. L. Cunningham, and R. J. Diefenbach.** 2010. The major determinant for addition of tegument protein pUL48 (VP16) to capsids in herpes simplex virus type 1 is the presence of the major tegument protein pUL36 (VP1/2). J Virol **84:**1397-405.
83. **Koch, M., S. Camp, T. Collen, D. Avila, J. Salomonsen, H. J. Wallny, A. van Hateren, L. Hunt, J. P. Jacob, F. Johnston, D. A. Marston, I. Shaw, P. R. Dunbar, V. Cerundolo, E. Y. Jones, and J. Kaufman.** 2007. Structures of an MHC class I molecule from B21 chickens illustrate promiscuous peptide binding. Immunity **27:**885-99.
84. **Komander, D., M. J. Clague, and S. Urbe.** 2009. Breaking the chains: structure and function of the deubiquitinases. Nat Rev Mol Cell Biol **10:**550-63.
85. **Lee, E. C., D. Yu, J. Martinez de Velasco, L. Tessarollo, D. A. Swing, D. L. Court, N. A. Jenkins, and N. G. Copeland.** 2001. A highly efficient Escherichia coli-based chromosome engineering system adapted for recombinogenic targeting and subcloning of BAC DNA. Genomics **73:**56-65.
86. **Lee, L. F., B. Lupiani, R. F. Silva, H. J. Kung, and S. M. Reddy.** 2008. Recombinant Marek's disease virus (MDV) lacking the Meq oncogene confers protection against challenge with a very virulent plus strain of MDV. Vaccine **26:**1887-92.
87. **Leelawong, M., J. I. Lee, and G. A. Smith.** 2012. Nuclear egress of pseudorabies virus capsids is enhanced by a subspecies of the large tegument protein that is lost upon cytoplasmic maturation. J Virol.
88. **Levy, A. M., O. Gilad, L. Xia, Y. Izumiya, J. Choi, A. Tsalenko, Z. Yakhini, R. Witter, L. Lee, C. J. Cardona, and H. J. Kung.** 2005. Marek's disease virus Meq transforms chicken cells via the v-Jun transcriptional cascade: a converging transforming pathway for avian oncoviruses. Proc Natl Acad Sci U S A **102:**14831-6.
89. **Liu, J. L., and H. J. Kung.** 2000. Marek's disease herpesvirus transforming protein MEQ: a c-Jun analogue with an alternative life style. Virus Genes **21:**51-64.
90. **Liu, J. L., S. F. Lin, L. Xia, P. Brunovskis, D. Li, I. Davidson, L. F. Lee, and H. J. Kung.** 1999. MEQ and V-IL8: cellular genes in disguise? Acta Virol **43:**94-101.
91. **Loret, S., G. Guay, and R. Lippe.** 2008. Comprehensive characterization of extracellular herpes simplex virus type 1 virions. J Virol **82:**8605-18.
92. **Lupiani, B., L. F. Lee, X. Cui, I. Gimeno, A. Anderson, R. W. Morgan, R. F. Silva, R. L. Witter, H. J. Kung, and S. M. Reddy.** 2004. Marek's disease virus-encoded Meq gene is involved in transformation of lymphocytes but is dispensable for replication. Proc Natl Acad Sci U S A **101:**11815-20.
93. **Luxton, G. W., J. I. Lee, S. Haverlock-Moyns, J. M. Schober, and G. A. Smith.** 2006. The pseudorabies virus VP1/2 tegument protein is required for intracellular capsid transport. J Virol **80:**201-9.

94. **McGeoch, D. J., M. A. Dalrymple, A. J. Davison, A. Dolan, M. C. Frame, D. McNab, L. J. Perry, J. E. Scott, and P. Taylor.** 1988. The complete DNA sequence of the long unique region in the genome of herpes simplex virus type 1. J Gen Virol **69 (Pt 7):**1531-74.
95. **McMahon, B., and R. M. Hanson.** 2008. A toolkit for publishing enhanced figures. J Appl Crystallogr **41:**811-814.
96. **McNabb, D. S., and R. J. Courtney.** 1992. Analysis of the UL36 open reading frame encoding the large tegument protein (ICP1/2) of herpes simplex virus type 1. J Virol **66:**7581-4.
97. **McNabb, D. S., and R. J. Courtney.** 1992. Characterization of the large tegument protein (ICP1/2) of herpes simplex virus type 1. Virology **190:**221-32.
98. **Messerle, M., I. Crnkovic, W. Hammerschmidt, H. Ziegler, and U. H. Koszinowski.** 1997. Cloning and mutagenesis of a herpesvirus genome as an infectious bacterial artificial chromosome. Proceedings of the National Academy of Sciences of the United States of America **94:**14759-14763.
99. **Mettenleiter, T. C.** 2002. Herpesvirus assembly and egress. J Virol **76:**1537-47.
100. **Mettenleiter, T. C., B. G. Klupp, and H. Granzow.** 2006. Herpesvirus assembly: a tale of two membranes. Curr Opin Microbiol **9:**423-9.
101. **Mettenleiter, T. C., B. G. Klupp, and H. Granzow.** 2009. Herpesvirus assembly: an update. Virus Res **143:**222-34.
102. **Mijatov, B., A. L. Cunningham, and R. J. Diefenbach.** 2007. Residues F593 and E596 of HSV-1 tegument protein pUL36 (VP1/2) mediate binding of tegument protein pUL37. Virology **368:**26-31.
103. **Millard, S. M., and S. A. Wood.** 2006. Riding the DUBway: regulation of protein trafficking by deubiquitylating enzymes. J Cell Biol **173:**463-8.
104. **Mitchell, M. S., and V. B. Rao.** 2006. Functional analysis of the bacteriophage T4 DNA-packaging ATPase motor. Journal of Biological Chemistry **281:**518-527.
105. **Mizushima, N., T. Noda, T. Yoshimori, Y. Tanaka, T. Ishii, M. D. George, D. J. Klionsky, M. Ohsumi, and Y. Ohsumi.** 1998. A protein conjugation system essential for autophagy. Nature **395:**395-8.
106. **Mohl, B. S., S. Bottcher, H. Granzow, J. Kuhn, B. G. Klupp, and T. C. Mettenleiter.** 2009. Intracellular localization of the pseudorabies virus large tegument protein pUL36. J Virol **83:**9641-51.
107. **Morrow, C., and F. Fehler.** 2004. 5 - Marek's disease: A worldwide problem, p. 49-61. *In* D. Fred and N. Venugopal (ed.), Marek's Disease. Academic Press, Oxford.
108. **Murphy, K. C.** 1998. Use of bacteriophage lambda recombination functions to promote gene replacement in Escherichia coli. Journal of Bacteriology **180:**2063-2071.
109. **Nair, V.** 2005. Evolution of Marek's disease -- a paradigm for incessant race between the pathogen and the host. Vet J **170:**175-83.
110. **Naviaux, R. K., E. Costanzi, M. Haas, and I. M. Verma.** 1996. The pCL vector system: rapid production of helper-free, high-titer, recombinant retroviruses. J Virol **70:**5701-5.
111. **Newcomb, W. W., and J. C. Brown.** 2010. Structure and capsid association of the herpesvirus large tegument protein UL36. J Virol **84:**9408-14.
112. **Newcomb, W. W., and J. C. Brown.** 2009. Time-dependent transformation of the herpesvirus tegument. J Virol **83:**8082-9.
113. **Nijman, S. M., M. P. Luna-Vargas, A. Velds, T. R. Brummelkamp, A. M. Dirac, T. K. Sixma, and R. Bernards.** 2005. A genomic and functional inventory of deubiquitinating enzymes. Cell **123:**773-86.
114. **Okazaki, W., H. G. Purchase, and B. R. Burmester.** 1970. Protection against Marek's disease by vaccination with a herpesvirus of turkeys. Avian Dis **14:**413-29.
115. **Osterrieder, K., and J.-F. Vautherot.** 2004. 3 - The genome content of Marek's disease-like viruses, p. 17-31. *In* D. Fred and N. Venugopal (ed.), Marek's Disease. Academic Press, Oxford.

116. **Osterrieder, N., J. P. Kamil, D. Schumacher, B. K. Tischer, and S. Trapp.** 2006. Marek's disease virus: from miasma to model. Nat Rev Microbiol **4:**283-94.
117. **Parcells, M. S., A. S. Anderson, J. L. Cantello, and R. W. Morgan.** 1994. Characterization of Marek's disease virus insertion and deletion mutants that lack US1 (ICP22 homolog), US10, and/or US2 and neighboring short-component open reading frames. J Virol **68:**8239-53.
118. **Parcells, M. S., S. F. Lin, R. L. Dienglewicz, V. Majerciak, D. R. Robinson, H. C. Chen, Z. Wu, G. R. Dubyak, P. Brunovskis, H. D. Hunt, L. F. Lee, and H. J. Kung.** 2001. Marek's disease virus (MDV) encodes an interleukin-8 homolog (vIL-8): characterization of the vIL-8 protein and a vIL-8 deletion mutant MDV. J Virol **75:**5159-73.
119. **Pasdeloup, D., D. Blondel, A. L. Isidro, and F. J. Rixon.** 2009. Herpesvirus capsid association with the nuclear pore complex and viral DNA release involve the nucleoporin CAN/Nup214 and the capsid protein pUL25. J Virol **83:**6610-23.
120. **Paul-Pierre, P.** 2004. 1 - Introduction, p. 1-7. *In* D. Fred and N. Venugopal (ed.), Marek's Disease. Academic Press, Oxford.
121. **Pear, W. S., G. P. Nolan, M. L. Scott, and D. Baltimore.** 1993. Production of high-titer helper-free retroviruses by transient transfection. Proc Natl Acad Sci U S A **90:**8392-6.
122. **Pellet, P. E., Roizman, B.** 2007. The Family Herpesviridae: A brief introduction, 5th edition ed, vol. Volume 2. Lippincott Williams & Wilkins, a Wolters Kluwer Business, 530 Walnut street, Philadelphia, PA 19106 USA.
123. **Peter M, B.** 2004. 2 - Marek's disease: Long and difficult beginnings, p. 8-16. *In* D. Fred and N. Venugopal (ed.), Marek's Disease. Academic Press, Oxford.
124. **Petherbridge, L., A. C. Brown, S. J. Baigent, K. Howes, M. A. Sacco, N. Osterrieder, and V. K. Nair.** 2004. Oncogenicity of virulent Marek's disease virus cloned as bacterial artificial chromosomes. J Virol **78:**13376-80.
125. **Petherbridge, L., K. Howes, S. J. Baigent, M. A. Sacco, S. Evans, N. Osterrieder, and V. Nair.** 2003. Replication-competent bacterial artificial chromosomes of Marek's disease virus: novel tools for generation of molecularly defined herpesvirus vaccines. J Virol **77:**8712-8.
126. **Pickart, C. M., and M. J. Eddins.** 2004. Ubiquitin: structures, functions, mechanisms. Biochim Biophys Acta **1695:**55-72.
127. **Reddy, S. M., B. Lupiani, I. M. Gimeno, R. F. Silva, L. F. Lee, and R. L. Witter.** 2002. Rescue of a pathogenic Marek's disease virus with overlapping cosmid DNAs: use of a pp38 mutant to validate the technology for the study of gene function. Proc Natl Acad Sci U S A **99:**7054-9.
128. **Rispens, B. H., H. van Vloten, N. Mastenbroek, H. J. Maas, and K. A. Schat.** 1972. Control of Marek's disease in the Netherlands. I. Isolation of an avirulent Marek's disease virus (strain CVI 988) and its use in laboratory vaccination trials. Avian Dis **16:**108-25.
129. **Rispens, B. H., H. van Vloten, N. Mastenbroek, J. L. Maas, and K. A. Schat.** 1972. Control of Marek's disease in the Netherlands. II. Field trials on vaccination with an avirulent strain (CVI 988) of Marek's disease virus. Avian Dis **16:**126-38.
130. **Roberts, A. P., F. Abaitua, P. O'Hare, D. McNab, F. J. Rixon, and D. Pasdeloup.** 2009. Differing roles of inner tegument proteins pUL36 and pUL37 during entry of herpes simplex virus type 1. J Virol **83:**105-16.
131. **Sakaki, Y., A. E. Karu, S. Linn, and H. Echols.** 1973. Purification and properties of the gamma-protein specified by bacteriophage lambda: an inhibitor of the host RecBC recombination enzyme. Proc Natl Acad Sci U S A **70:**2215-9.
132. **Sambrook, J.** 2001. Molecular cloning : a laboratory manual / Joseph Sambrook, David W. Russell. Cold Spring Harbor Laboratory, Cold Spring Harbor, N.Y. :.
133. **Santin, E. R., C. E. Shamblin, J. T. Prigge, V. Arumugaswami, R. L. Dienglewicz, and M. S. Parcells.** 2006. Examination of the effect of a naturally occurring mutation in glycoprotein L on Marek's disease virus pathogenesis. Avian Dis **50:**96-103.

134. **Schat, K. A., B. W. Calnek, and J. Fabricant.** 1981. Influence of the bursa of Fabricius on the pathogenesis of Marek's disease. Infect Immun **31:**199-207.
135. **Schat, K. A., B. W. Calnek, J. Fabricant, and H. Abplanalp.** 1981. Influence of oncogenicity of Marek' disease virus on evaluation of genetic resistance. Poult Sci **60:**2559-66.
136. **Schat KA, P. H.** 1998. p. pp. 223–234. *In* G. J. Swayne DE, Jackwood MW, Pearson JE, Reed WM (ed.), A Laboratory Manual for the Isolation and Identification of Avian Pathogens. Am Assoc Avian Pathol, Kennett Square, PA.
137. **Schat, R. L. W. a. K. L.** 2008. Sub-section Neoplastic diseases, Marek´s disease p. 407-475. *In* A. M. F. Y. M. Saif , John R. Glisson , Larry R. McDougald , L. K. Nolan , David E. Swayne (ed.), Diseases of Poultry, 11th ed, vol. 1. Wiley-Blackwell.
138. **Schipke, J., A. Pohlmann, R. Diestel, A. Binz, K. Rudolph, C. H. Nagel, R. Bauerfeind, and B. Sodeik.** 2012. The C-terminus of the large Tegument Protein pUL36 Contains Multiple Capsid Binding Sites that Function differently During Assembly and Cell Entry of Herpes Simplex Virus. J Virol.
139. **Schlieker, C., G. A. Korbel, L. M. Kattenhorn, and H. L. Ploegh.** 2005. A deubiquitinating activity is conserved in the large tegument protein of the herpesviridae. J Virol **79:**15582-5.
140. **Schlieker, C., W. A. Weihofen, E. Frijns, L. M. Kattenhorn, R. Gaudet, and H. L. Ploegh.** 2007. Structure of a herpesvirus-encoded cysteine protease reveals a unique class of deubiquitinating enzymes. Mol Cell **25:**677-87.
141. **Schmaus, S., H. Wolf, and F. Schwarzmann.** 2004. The reading frame BPLF1 of Epstein-Barr virus: a homologue of herpes simplex virus protein VP16. Virus Genes **29:**267-77.
142. **Schumacher, D., B. K. Tischer, W. Fuchs, and N. Osterrieder.** 2000. Reconstitution of Marek's disease virus serotype 1 (MDV-1) from DNA cloned as a bacterial artificial chromosome and characterization of a glycoprotein B-negative MDV-1 mutant. J Virol **74:**11088-98.
143. **Shizuya, H., B. Birren, U. J. Kim, V. Mancino, T. Slepak, Y. Tachiiri, and M. Simon.** 1992. Cloning and stable maintenance of 300-kilobase-pair fragments of human DNA in Escherichia coli using an F-factor-based vector. Proc Natl Acad Sci U S A **89:**8794-7.
144. **Smith, J. D., and E. De Harven.** 1973. Herpes simplex virus and human cytomegalovirus replication in WI-38 cells. I. Sequence of viral replication. J Virol **12:**919-30.
145. **Smith, T. W., D. M. Albert, N. Robinson, B. W. Calnek, and O. Schwabe.** 1974. Ocular manifestations of Marek's disease. Invest Ophthalmol **13:**586-92.
146. **Sonaiya, E. B., S. E. J. Swan, and Food and Agriculture Organization of the United Nations.** 2004. Small-scale poultry production : technical guide. Food and Agriculture Organization of the United Nations, Rome.
147. **Sonoda, K., M. Sakaguchi, H. Okamura, K. Yokogawa, E. Tokunaga, S. Tokiyoshi, Y. Kawaguchi, and K. Hirai.** 2000. Development of an effective polyvalent vaccine against both Marek's and Newcastle diseases based on recombinant Marek's disease virus type 1 in commercial chickens with maternal antibodies. J Virol **74:**3217-26.
148. **Sternberg, N., B. Sauer, R. Hoess, and K. Abremski.** 1986. Bacteriophage P1 cre gene and its regulatory region. Evidence for multiple promoters and for regulation by DNA methylation. J Mol Biol **187:**197-212.
149. **Svobodova, S., S. Bell, and C. M. Crump.** 2011. Analysis of the interaction between the essential HSV-1 tegument proteins VP16 and VP1/2. J Virol.
150. **Tischer, B. K., G. A. Smith, and N. Osterrieder.** 2010. En passant mutagenesis: a two step markerless red recombination system. Methods Mol Biol **634:**421-30.
151. **Tischer, B. K., J. von Einem, B. Kaufer, and N. Osterrieder.** 2006. Two-step red-mediated recombination for versatile high-efficiency markerless DNA manipulation in Escherichia coli. Biotechniques **40:**191-7.

152. **Trus, B. L., W. Gibson, N. Cheng, and A. C. Steven.** 1999. Capsid structure of simian cytomegalovirus from cryoelectron microscopy: evidence for tegument attachment sites. J Virol **73:**2181-92.
153. **Vittone, V., E. Diefenbach, D. Triffett, M. W. Douglas, A. L. Cunningham, and R. J. Diefenbach.** 2005. Determination of interactions between tegument proteins of herpes simplex virus type 1. J Virol **79:**9566-71.
154. **Wang, J., A. N. Loveland, L. M. Kattenhorn, H. L. Ploegh, and W. Gibson.** 2006. High-molecular-weight protein (pUL48) of human cytomegalovirus is a competent deubiquitinating protease: mutant viruses altered in its active-site cysteine or histidine are viable. J Virol **80:**6003-12.
155. **Whitehurst, C. B., S. Ning, G. L. Bentz, F. Dufour, E. Gershburg, J. Shackelford, Y. Langelier, and J. S. Pagano.** 2009. The Epstein-Barr virus (EBV) deubiquitinating enzyme BPLF1 reduces EBV ribonucleotide reductase activity. J Virol **83:**4345-53.
156. **Whitehurst, C. B., C. Vaziri, J. Shackelford, and J. S. Pagano.** 2012. Epstein-Barr Virus BPLF1 Deubiquitinates PCNA and Attenuates Polymerase eta Recruitment to DNA Damage Sites. J Virol **86:**8097-106.
157. **Whitley, R.** 1996. Herpesviruses. *In* B. S (ed.), Medical Microbiology, 4th ed. The University of Texas Medical Branch at Galveston, Galveston (TX).
158. **Witter, R. L.** 1997. Increased virulence of Marek's disease virus field isolates. Avian Dis **41:**149-63.
159. **Witter, R. L., K. Nazerian, H. G. Purchase, and G. H. Burgoyne.** 1970. Isolation from turkeys of a cell-associated herpesvirus antigenically related to Marek's disease virus. Am J Vet Res **31:**525-38.
160. **Yu, D., H. M. Ellis, E. C. Lee, N. A. Jenkins, N. G. Copeland, and D. L. Court.** 2000. An efficient recombination system for chromosome engineering in Escherichia coli. Proc Natl Acad Sci U S A **97:**5978-83.
161. **Zagursky, R. J., and J. B. Hays.** 1983. Expression of the phage lambda recombination genes exo and bet under lacPO control on a multi-copy plasmid. Gene **23:**277-92.
162. **Zhang, Y., F. Buchholz, J. P. Muyrers, and A. F. Stewart.** 1998. A new logic for DNA engineering using recombination in Escherichia coli. Nat Genet **20:**123-8.
163. **Zhou, Z. H., D. H. Chen, J. Jakana, F. J. Rixon, and W. Chiu.** 1999. Visualization of tegument-capsid interactions and DNA in intact herpes simplex virus type 1 virions. J Virol **73:**3210-8.

13 Supplementary Information

Section 1: Schematic representation of all the vMDVs assembled throughout the project. The order in which schemes are displayed is the same from chapter 7.1.5.2, where all rMDVs descriptions are indicated.

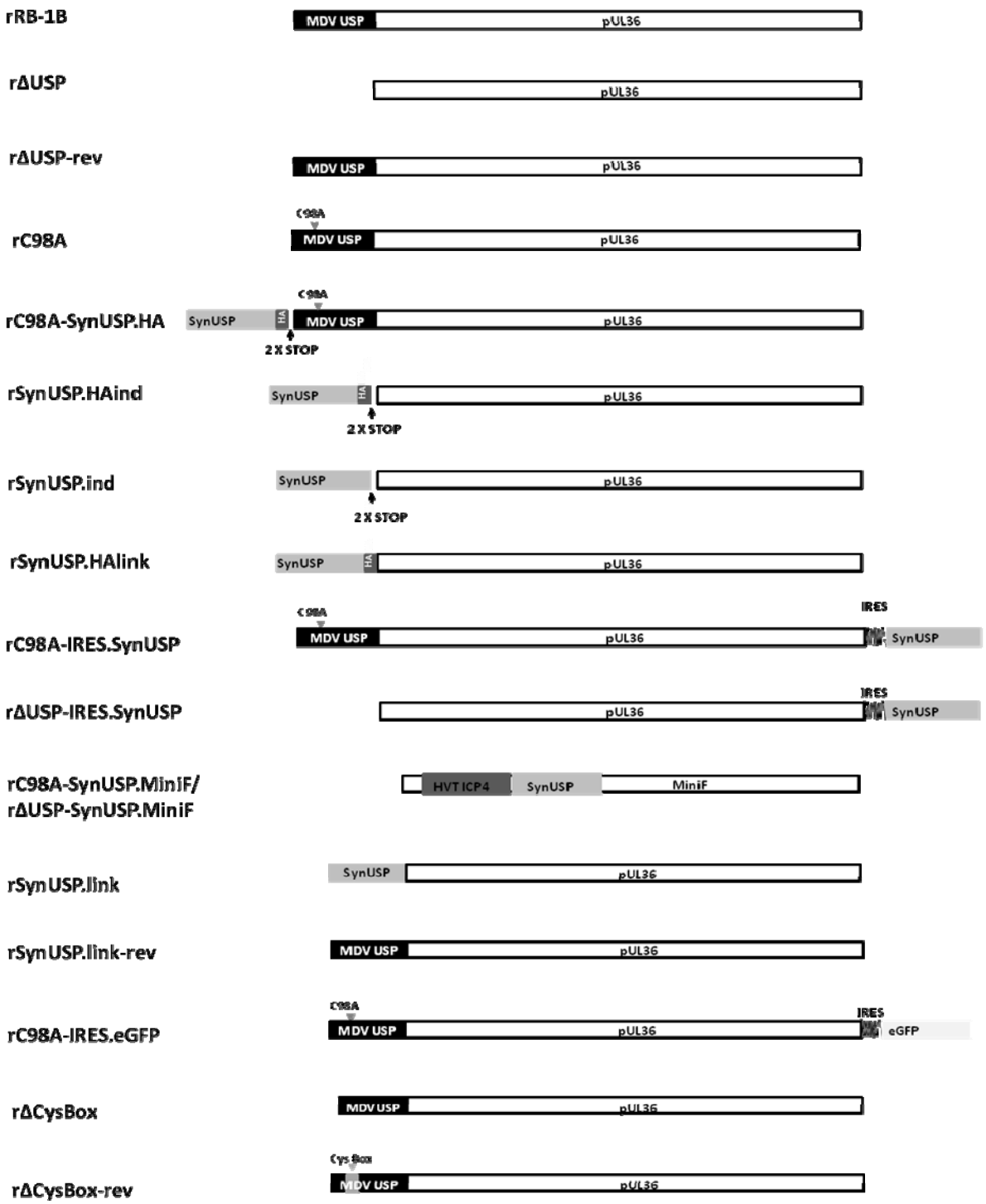

Section 2: List of positive hits found for UL36I SC-1 clone in a mammalian genome collection library by Professor Jürgen C. Haas and Clark Russell from the University of Edinburgh. Highlighted hits correspond to the ones that were found to be more significant.

Hit	Accession number	Max score	Total score	Query coverage	E-value
2-hydroxyacyl-CoA lyase 1 (HACL1)	NM_012260.2	571	668	62%	4,00E-160
ADP-ribosylation factor-like 17A (ARL17A), transcript variant 1	NM_001113738.1	346	346	42%	1,00E-92
anaphase promoting complex subunit 13 (ANAPC13), transcript variant 3	NM_001242375.1	414	414	50%	3,00E-113
androgen-induced 1 (AIG1)	NM_016108.2	1325	1325	86%	0
ArfGAP with SH3 domain, ankyrin repeat and PH domain 1	NM_018482.2	204	204	33%	9,00E-50
aspartylglucosaminidase (AGA), transcript variant 1, mRNA	NM_000027.3	1469	1469	98%	0
barrier to autointegration factor 1 (BANF1), transcript variant 2	NM_001143985.1	497	497	55%	6,00E-138
cerberus 1, cysteine knot superfamily, homolog (Xenopus laevis) (CER1)	NM_005454.2	1443	1443	96%	0
chromosome 1 open reading frame 210 (C1orf210), transcript variant 1	NM_182517.2	632	632	61%	2,00E-178
chromosome 1 open reading frame 212 (C1orf212)	NM_001164824.1	516	516	56%	1,00E-143
chromosome 14 genomic contig, alternate assembly	NW_001838121.1	475	927	38%	4,00E-131
chromosome 21 open reading frame 128 (C21orf128), non-coding RNA	NR_027243.1	889	889	70%	0
chromosome 22 genomic contig, GRCh37.p5	NT_011520.12	401	401	47%	3,00E-109
chromosome 6 open reading frame 123 (C6orf123)	NR_026773.1	320	320	44%	7,00E-85
CYP1B1 antisense RNA 1 (CYP1B1-AS1), non-coding RNA	NR_027252.1	791	791	67%	0
EH domain binding protein 1 (EHBP1), transcript variant 2	NM_001142614.1	575	575	58%	3,00E-161
ER lipid raft associated 1 (ERLIN1)	NM_006459.3	1186	1186	96%	0
family with sequence similarity 105, member B (FAM105B)	NM_138348.4	1482	1482	96%	0
family with sequence similarity 134, member B (FAM134B)	NM_019000.3	1437	1437	96%	0
Fas apoptotic inhibitory molecule 2 (FAIM2)	**NM_012306.3**	**278**	**278**	**86%**	**2,00E-72**
fatty acid binding protein 4, adipocyte (FABP4)	NM_001442.2	730	730	65%	0
glucuronidase, beta pseudogene	NR_024054.1	520	520	56%	8,00E-145
glutathione S-transferase kappa 1 (GSTK1), nuclear gene encoding mitochondrial protein, transcript variant 1	NM_015917.2	1253	1253	84%	0
growth arrest-specific 2 like 3 (GAS2L3)	NM_174942.1	309	309	44%	1,00E-81

histone cluster 1, H2am (HIST1H2AM)	NM_003514	726	726	64%	0
Homo sapiens phosphotriesterase related, transcript variant 2	NM_030664.3	1382	1382	96%	0
hydroxysteroid (17-beta) dehydrogenase 7 pseudogene 2 (HSD17B7P2)	NR_003086.1	1247	1247	93%	0
lysosomal protein transmembrane 4 alpha (LAPTM4A)	NM_014713.4	1284	1284	93%	0
major histocompatibility complex, class II, DO beta	NM_002120.3	169	169	17%	4,00E-39
major histocompatibility complex, class II, DP beta 1 (HLA-DPB1)	NM_002121.5	1345	1345	94%	0
microsomal glutathione S-transferase 1 (MGST1), transcript variant 1d	NM_145764.1	863	863	69%	0
ORM1-like 2 (S. cerevisiae) (ORMDL2)	NM_014182.4	846	846	67%	0
plexin domain containing 2 (PLXDC2)	NM_032812.7	713	1318	97%	0
regulator of chromosome condensation 1 (RCC1), transcript variant 3, mRNA	NM_001269.4	1454	1454	96%	0
Rho GTPase activating protein 19 (ARHGAP19)	**NM_001204300.1**	**189**	**189**	**30%**	**2,00E-45**
ribosomal protein L39-like (RPL39L)	NM_052969.1	289	289	41%	3,00E-75
RWD domain containing 4 (RWDD4)	NM_152682.2	1040	1040	76%	0
S100 calcium binding protein A12 (S100A12)	NM_005621.1	484	484	56%	4,00E-134
ST8 alpha-N-acetyl-neuraminide alpha-2,8-sialyltransferase 1	NM_003034.3	436	436	50%	1,00E-119
synapse associated protein 1 (SYAP1)	NM_032796.3	1303	1303	97%	0
synaptojanin 2 binding protein (SYNJ2BP)	NM_018373.2	809	809	69%	0
syndecan 4 (SDC4)	NM_002999.3	1103	1103	90%	0
synovial sarcoma, X breakpoint 2B (SSX2B)	NM_001164417.1	1037	1037	77%	0
ubiquitin protein ligase E3B (UBE3B), transcript variant 3, mRNA	**NM_183415.1**	**1166**	**1166**	**77%**	**0**
vacuolar protein sorting 25 homolog (S. cerevisiae) (VPS25)	NM_032353.2	979	979	72%	0
zinc finger protein 544 (ZNF544)	NM_014480.2	451	451	45%	3,00E-124
zinc finger protein 585A (ZNF585A), transcript variant 2	NM_199126.1	396	534	57%	2,00E-107

14 List of publications

14.1 Scientific publications

Veiga, I. B., K. W. Jarosinski, B. B. Kaufer, and N. Osterrieder, 2012. Marek's disease virus (MDV) ubiquitin-specific protease (USP) performs critical functions beyond its enzymatic activity during virus replication. Virology, 2013 Mar 15;437(2):110-7. doi: 10.1016/j.virol.2013.01.003. Epub 2013 Feb 9.

Chbab, N., A. Egerer, **I. Veiga**, K. W. Jarosinski, and N. Osterrieder. 2010. Viral control of vTR expression is critical for efficient formation and dissemination of lymphoma induced by Marek's disease virus (MDV). Vet Res 41:56. doi: 10.1051/vetres/2010026. Epub 2010 Apr 29.

Duarte, A., **I. Veiga**, and L. Tavares. 2009. Genetic diversity and phylogenetic analysis of Feline Coronavirus sequences from Portugal. Vet Microbiol 138:163. doi: 10.1016/j.vetmic.2009.03.009. Epub 2009 Mar 13.

14.2 Talks and poster presentations (conference proceedings)

Veiga I., Jarosinski K., Kaufer B., Azab W., Reum A., Osterrieder N.. Talk “Characterisation of Marek’s disease virus mutants presenting alterations in the UL36-encoded ubiquitin-specific protease region”, 9th Symposium on MDV and Avian herpesviruses in Berlin, Germany, 24th-28th June 2012

Veiga I., Jarosinski K., Kaufer, B. Osterrieder, N.. Poster “The role of the UL36-encoded viral ubiquitin-specific protease in Marek’s disease virus replication”, 36th Annual International Herpesvirus Workshop (IHW) in Gdansk, Poland, 24th-28th July 2011

Veiga I., Jarosinski K., Kaufer B., Osterrieder N.. Poster “Analysis of Marek’s Disease Virus Mutants with Alterations of the Viral Ubiquitin-Specific Protease”, 21st German Society of Virology (GfV) Congress, Freiburg, Germany, 22nd-25th March 2011

Veiga I., Jarosinski K., Osterrieder N.. Poster “Analysis of Marek’s Disease Virus Mutants with Alterations of the Viral Ubiquitin-Specific Protease”, 5th International Workshop on the Molecular Pathogenesis of Marek's Disease Virus & 1st Symposium on Avian Herpesviruses, Athens Georgia USA, 17th-20th October 2010

Veiga I., Jarosinski K., Osterrieder N.. Poster “Analysis of Marek’s Disease Virus Mutants with Alterations of the Viral Ubiquitin-Specific Protease”, 4th European society of Virology (ESV) Congress, Chernobbio, Italy; 7th-11th April 2010

15 Acknowledgments

No one is an island, and PhD students are no exception. It would not have been possible to endure this extreme experience without a good back-up team to get me through it.
First of all, I would like to thank my supervisor, Professor Klaus Osterrieder, for giving me the opportunity to do my doctoral thesis in his lab, for funding assistance, for his ideas and, last but not least, for never saying no to my holidays.I would also thank my co-supervisors Dr. Elke Genersch, which had to come all the way from Brandenburg for the thesis committee meetings, and Dr. Thorsten Wollf.
Then, I would like to thank Dr. Keith Jarosinski, ex-Cornelian now running his own lab in Iowa, that handed me over the MDV UL36 USP project (very happily, he told me later on, for reasons that I can now perfectly comprehend), but who luckily for me never really stopped caring about it completely. Thanks a lot for all the encouragement and support!
Also, I would like to thank Dr. Benedikt Kaufer for giving me new ideas for the project, for advice during difficult times and for providing me with some very necessary practical help throughout the PhD; Dr. Karsten Tischer, for always having an answer for my questions and Dr. Armando Damiani, for fruitful discussions on qPCR and latin-american literature and his wife Patrícia for keep lab moral high up with her wonderful cakes.
To Dr. Susann Beetz and Dr. Martina Sick for the ZIBI Graduate School Berlin, a big acknowledgment for all the help and support provided throughout the years. They really did a great job and I feel privileged for having been a part of their project. I thank also Frau Angela Daberkow, the visible face of the Dahlem Reseach School, for her kindness and interest.
Also to thank for is the generous four-year finantial support provided by the Fundação para a Ciência e Tecnologia (FCT) from Portugal, which always worked perfecly and allowed me to dedicate myself to my PhD without caring too much about finances.
My postdoc colleagues come next. They have been great, particularly Dr. Walid Azab, who got me going again after a less good lab period, even if he had a lot on his plate already with his own project and his three kids. Thank you very much Walid! Also, I would like to thank Dr. Guangangg Ma, which started in this very lab as a PhD student and which is now back in China; Drs. Matthias Sieber and Dušan Kunec, also known as the “couple”, most of all for the laughs. If I ever end up being a postdoc, I want to be just like you, but without dressing in black everyday. Dr Najet Chbab would also fall into this category. Thank you so much for getting me started! In the beginning of 2008, I did not really have a clue of what I should do, both with my plasmids and with life in Berlin in general. Thanks a lot for the good moments we spent together discovering Berlin (and assembling IKEA furniture)!

Then I come to thank my all fellow doctoral students for all for the good moments, the nice music and the great jokes! From this big group I would like to highlight my bench mates Annachiara Greco (a.k.a. my Latin twin, so many things we did together, so many pictures we took, so many courses endured!), Timo Schippers (the coolest wisest scientist ever, who made me a bit cooler too hopefully and who superbly translated the abstract to German) and his super shy alter ego the waspman for the ocasional laugh, Nora Thormann (the sportiest vet that ever was, who showed me that people with tattoos are nice), Swaantje Roth (to whom I owe I lot, in several ways. Without your support, things would have been really different and most likely a lot harder), Annemarie T. Engel for constant support during the PhD, Sina Arndt for making us all speak in German in the lab, Nina Wallaschek, who is always nice and friendly, and Valdimir Public, for always lending us his buffers and antibodies. Also many thanks to my other colleagues Bart Spiesschaert (thanks for revising the introduction!), Zhiyong Xu (David), Dimitris Zickos (my personal IT guy), Imme Sakwa, Teng Huang (Thomas, who always got my samples out of the PCR termocycler)...and all the others i don´t mention here.

Also, I would like to thank our technicians: Ann Reum, for the essential help provided with the growth of all the MDV viral mutants; to Silke Feineis, for helping me out several times with her extensive proteomics knowledge; to Annett Neubert, for always being helpful and as happy as it can possibly be; to Rosita Romeis, for always providing me with freshly autoclaved Eppendorf tubes and LB medium. Also, a special thanks to Christine Leiskau, who was always friendly and encouraging regarding German-speaking progress, and to Katharina Malik, our secretary, without whom a lot of my bureaucratical problems would not be solved.

For my very international friends outside the lab, all of whom are doctors by now: Tim Mak, who is always on the search for interesting things; Christina Meissner, my Austrian friend, who helped me with my Y2H subcloning; Uwe Koppe, always friendly and eager to help (Thanks for the USP.CTAP try-outs); and last but not least the Barisons, Francesca and Nicola (because one without the other cannot be): thanks a lot to all of you for the karaoke sessions, great cooking/brunching and high-quality gossip!

Coming to an end, I would like to thank all my friends in Portugal for keeping in touch, for their support and for always listening to my constant lab complaining. That goes also to my family, particularly my parents and my stepfather, who never stopped believing that I would eventualy succeed and who always allowed me to really come home to Portugal and to have a good time away from the lab. Thanks a lot for all your trust and comprehension throughout the years, you always helped me a lot by believing that I could do everything, if i really wanted to. And last but not least, I would like to thank Leonardo Galvis, an unexpected very nice surprise from these years in Berlin. Thanks so much for listening, for supporting, for

being there. I actually thought you did not exist but you were there after all…I tell you, German classes can bring a lot more than der, die and das!

16 Selbständigkeitserklärung

Hiermit bestätige ich, dass ich die vorliegende Arbeit selbständig angefertigt habe. Ich versichere, dass ich ausschließlich die angegebenen Quellen und Hilfen Anspruch genommen habe.

Berlin, den 14. December 2012

Inês Margarida Berenguer Veiga